Università Ca'Foscari Venezia

Scuola Dottorale di Ateneo
Graduate School

Dottorato di ricerca
in Scienze Chimiche
Ciclo XXVI
Anno di discussione 2014

The influence of sizing and iron-gall inks on the kinetics and degradation mechanism of cellulose in sealed vessel.

SETTORE SCIENTIFICO DISCIPLINARE DI AFFERENZA: **CHIM/12**
Tesi di Dottorato di Sara Zaccaron, matricola 955841

Coordinatore del Dottorato	**Tutore del Dottorando**
Prof. Maurizio Selva	**Prof. Renzo Ganzerla**

TABLE OF CONTENTS

EXPERIMENTAL APPROACH

IRON-GALL INKS. A COMPUTATIONAL STUDY

TABLE OF CONTENTS

ABSTRACT

Ancient papers should be considered a multivariate system as characterized by several interacting components: cellulose, sizing materials and iron gall inks are the principals. Iron gall complexes have been the most used writing material since the 12th century; however, they are well-known degrading agents for cellulose compromising its integrity and stability ("ink corrosion" phenomenon). Conversely, sizing agents seem to have a protective effect on cellulose deterioration. Moreover, no studies have been by now dealt with the evaluation of the induced-degradation mechanism of these components on cellulose in confined conditions (e.g. archival holdings, bundles or stacks). This research study is based upon all these observations. It proposes to assess whether the presence of iron gall inks and sizing materials on paper can modify the mechanism and kinetics of cellulose degradation in closed systems. Model samples reproducing ancient papers have been prepared and subjected to artificial aging in sealed vessel.

Results obtained revealed a clear superposition of oxidation and hydrolysis for all inked and sized samples. Moreover, iron-gall inks most likely release degrading VOCs (volatile organic compounds) in a very short time, compared to the whole aging process, as well as they significantly causes an increase of paper degradation. They deform the autocatalytic mechanism of pure cellulose by adding acidity to the system and thus leading the autocatalytic curve to degenerate. Regarding sizing, its protective effect on cellulose breakdown has been confirmed by all analyses as well as by kinetic studies performed. The presence of the sizing layer over the fibres conceivably reduces the self-degradation of cellulose as well as limits the negative effect of additional degrading compounds emitted by inks eventually present.

Additionally, a supplementary theoretical study has been carried out on iron-gall inks in order to improve the knowledge in metallo-gallate inks chemistry. Despite the great importance of these writing media as well as several experimental investigations of their degrading effect on cellulose, scarce information are still present in the literature about their chemical structure and electronic features. This makes some degradation pathways still unclear. To this end, a computational study has been carried out to ascertain both the electronic configuration of the ground and the excited states of iron-gall complexes as well as their oxidizing power.

List of Abbreviations

α	Excess of produced acidity during the autocatalytic process
A	Rearranged product after cellulose hydrolysis
C	Cellulose (in general)
DP_v	Viscosity-average degree of polymerisation
DP_n	Number-average degree of polymerisation
DP_w	Weight-average degree of polymerisation
GPC	Gel-permeation Chromatography
H	Acidity
LODP	Levelling-off degree of polymerisation
n^0	Initial amount of overall scissile bonds in cellulose (suffixes a, c and w stand/hold for glycosidic bonds in the amorphous or crystalline regions and weak links, respectively)
S_v	Viscosity-average number of scissions suffered by each initial chain of cellulose
S_n	Number-average number of scissions suffered by each initial chain of cellulose
S_w	Weight-average number of scissions suffered by each initial chain of cellulose
SEC	Size-exlusion Chromatography
VOCs	Volatile organic compounds

1

INTRODUCTION

Cellulose in an important raw material in several technical, scientific as well as cultural contexts. It is used in high-voltage power cables and as insulator in power transformers. However, it has also a paramount importance in cultural heritage as it is the main component of paper in archival holdings. Thus, cellulose aging experiments are of great interest in many different field of studies in order to evaluate its long-term performance.

The literature on these topics is quite too voluminous for a detailed review. Thus, a brief analysis of peculiar aspects taken into consideration for the development of the present research work are reported below together with some critical observation of literature limits.

CELLULOSE as REFERENCE MATERIAL for PAPER

It is worth noting that cellulose is the basic substrate of paper. So that, almost all research works on archival holdings have considered cellulose as the modelling material to predict the aging behaviour of paper. Nonetheless, *paper* is a highly more complex system than pure cellulose, characterized by several components interacting each other. The papermaking process has been changed along with centuries and different materials have been used in the production. The first type of produced paper was principally characterised by a cotton-cellulose substrate, a protein sizing and inks. Among all, iron-gall inks could be surely considered as the most widely used since the Medieval times. Their great importance is also related to the so-called "ink corrosion" phenomenon frequently observed in archival collections and characterised by the loss of paper substrate owing to the degradation induced by the ink itself.

As conservation scientists, we aim to stop, or at least to slow down, the rate of paper degradation in order to prevent our Heritage from destruction. To this end, the exclusion of other components than cellulose could lead to an incomplete knowledge and inadeguate interventions. Thus, a valuable understanding of the degradation mechanism should necessarily involve the study of interactions among all elements. This could be provided by properly simulating the considered system, mainly because

its degradation usually results from a complex overlapping of reaction mechanisms synergistically related.

ACCELERATED AGING AND KINETICS

In order to evaluate the long-term behaviour of items in opportunely short times, accelerated artificial aging are usually performed. Normally, chemical and physical changes take place too slowly to be easily studied and aging tests can variously speed them up. Many different aging methods have been developed for the study of cellulose induced-degradation. The most widely accepted and exploited test for paper involves the use of ventilated oven at 80 °C and about 60% relative humidity. In such method, volatile compounds (VOCs) owing to degradation are removed as the internal atmosphere is constantly renovated. Nevertheless, some authors (Shahani 1995; Zou et al. 1996; ASTM D6819-02e2; Zervos and Moropoulou 2005; Strlic et al. 2010) have quite recently suggested that keeping released VOCs inside the reaction space could plausibly simulate the natural degradation of cellulose in closed environments (e.g. books, archival material in stacks and bundles). The sealed vessel aging method has been proposed and it has been stated (Zervos and Moropoulou 2005; Strlic et al. 2010, 2011) that volatile degradation products (mainly acidic) emitted by cellulose interact with cellulose itself causing further degradation according to a supposed autocatalytic mechanism (Shahani 1995) (see Cap. 5).

Though, the kinetic equation describing the degradation process in closed vessel is quite difficult to be modelled owing to the complexity of the system. Calvini et al. (2008) firstly suggested a modelling kinetic equation. However, very few reports of autocatalytic behaviour for cellulose aging in sealed system have been found in the body of literature studied and even fewer example are present about the application of the proposed autocatalytic equation. The most important research works on cellulose subjected to an artificial aging in closed system come from Zou et al. (1996) and Zervos and Moropoulou (2005), who characterized the degradation process by monitoring the degree of polymerisation and the mechanical properties of cellulose, respectively. Later re-elaborations and re-modelling of their data through the autocatalytic equation proposed by Calvini et al. (2008) have confirmed an autocatalytic trend of degradation of cellulose in such system. Moreover, it has been revealed that the shape of the autocatalytic degradation depends upon the system acidity (see Cap. 6):

- nearly neutral cellulose samples give rise to S-shaped kinetic plots (Zervos and Moropoulou study);

- acidic cellulose samples show an initial linear kinetic plots converging towards an asymptotic value corresponding to the consumption of the amorphous domains. This could be roughly considered a degenerated autocatalytic trend (Zou research).

DEGRADATION MONITORING PARAMETERS

Since the 1980s (Feller 1980) the importance of the degree of polymerisation in cellulose degradation studies has been underlined and it has become the principal parameter to evaluate kinetic mechanism and degradation rate of papers. Kinetic studies are commonly carried out in terms of DP values experimentally evaluated on different cellulosic subtrates using different technique. Moreover, the effective meaning of DP has been usually misunderstanding as several research works correlate it to e.g. the percentage of scissile bonds or the fraction of broken bonds, thus obtaining misleading conclusions. All these consideration entail several problems of comparison among studies performed until now. Nevertheless, by introducing the number of glycosidic bonds (C) and scissions (S) as chemical reagent and product of degradation reaction, respectively, deeper knowledge on specific mechanisms can be reached. Models based on the bond scissions concept more easily allow comparison between ideal kinetic laws and experimental results brought about by different research groups on different cellulosic substrates. However, few works are present in literature based on the number of scission kinetics, thus making difficult to compare and interpret kinetic data.

EXPERIMENTAL TIMES

Degradation of cellulose usually takes several time to be (almost) completed. It has been stated (Nelson and Tripp 1953; Yachi et al. 1983) that cellulose degradation substantially proceeds untill the consumption of the amorphous domains. The levelling-off degree of polymerisation, LODP (Calvini 2005), is the average length of (hard) chains in the crystalline regions and most likely represents the asymptotic value of degradation. Nontheless, few research works verified the degradation mechanisms and the proposed kinetic models in long-lasting experiments until the LODP has been reached. Short-aging-time experiments are the common practise in cellulose degradation studies where the whole pathway is generally deduced by the initial stage of degradation without determining the levelling-off degree of polymerisation nor verifiying the consistency of these deductions.

2

AIMS of THE STUDY

This project is intended to contribute to the ongoing research on paper degradation. The main purpose of the present work is to shed some light on the degrading processes occurring in closed systems. Moreover, this study aims to ascertain the influence of iron-gall inks and gelatine sizing on the kinetics and mechanism of cellulose degradation.

A new experimental concept has been developed. Problems already addressed by other researchers have been treated with a completely different insight on degradation phenomena and a novel approach to cellulose-based materials. Specifically, problems outlined in the introductive chapter has been faced as following described.

1. **Paper has been considered a multivariate system, thus constituted by synergistically interacting components.**
   Unlike previous researches, this project has considered cellulosic materials as interconnected multicomponent systems. Particularly, ancient paper has been chosen as reference model. It can be chronologically considered the first multivariate paper-system with the lower degree of complexity as characterised by the fewest number of interacting components. Gelatine sizing and iron-gall inks have been studied as they represent the most common constituents of ancient papers.

2. **Sealed vessel technique as artificial aging method has been exploited.**
   The main reason behind this choice is that it plausibly simulates degradation occurring in closed environments, such as books or archival material in stacks and bundles. There is no futher need to point out that this method closely reseamble the real condition of cellulose-based materials in archives and that it has been by now rarely performed on a multivariate cellulose-system. Even though some authors (Dupont 2002b; Potthast et al. 2008) have carried out artificial aging in ventilated oven on simplified "paper system", no study have been found in the body of literature on the evaluation of sizing- and iron-gall-ink-influenced mechanism of paper degradation in closed environments.

3. **Long-lasting aging experiments has been carried out.**

   Contrary to the vast majority of literature studies, a long-lasting approach has been chosen in order to have a reliable insight into the degradation pathway throughout the whole process. Moreover, some experimental consistencies of proposed kinetic models are intended to be verified. In fact, kinetic mechanism available in literature have not been already tested nor kinetic equations have been by now modelled on multivariate cellulose-system breakdown in confined conditions.

3

CELLULOSE: CHEMISTRY AND DEGRADATION

Cellulose is a biopolymer made of D-glucopyranosyl units linked by β-(1,4)-glycosidic linkages (Fig. 3.1). Each unit of anhydroglucose (AGU) has hydroxyl groups at C2, C3 and C6 position characterized by typical reaction of primary and secondary alcohols. Each polymer chain is provided with two chemically different ends: a reducing (with both an aliphatic structure and a carbonyl group) and a non-reducing end group (where a closed ring is present) with free hydroxyl groups at C1 and C4 position respectively. Cellulose is considered a polydisperse polymer as it is composed by several chains of different length. The number of glucopyranosyl units per chain defined the degree of polymerization (DP).

Glucose building units adopt a stable $^4C_1$ chair conformation and a linear arrangement is forced by hydrogen bonding between adjacent oxygen and hydrogen atoms.
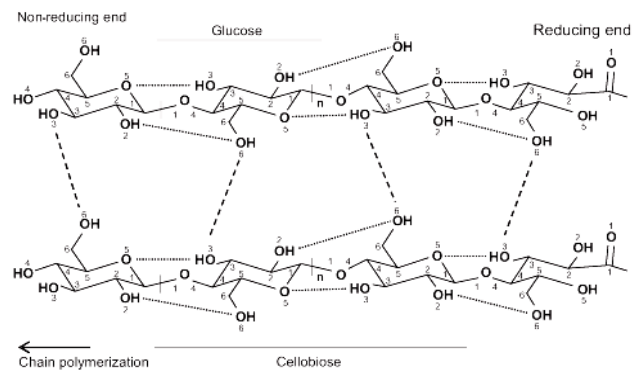
Fig. 3. 1 – The structure and hydrogen bonding pattern of cellulose polymer. Dashed lines: inter-chain hydrogen bonds. Dotted lines: intra-chain hydrogen bonds (Festucci-Buselli 2007).

Inter- and intra-molecular hydrogen linkages are likely to be also responsible for the supramolecular organisation of cellulose with different levels of structural arrangement (Pérez and Mazeau 2004; Chanzy, H. 1990; Sugiyama, J. et al. 1985; Lichtenegger, H. et al. 1999). The macromolecular structure of polymer is not uniform and cellulose is regarded as semi-crystalline; the coexistence of an organized

crystalline bulk (around 70 to 90%) together with less-ordered amorphous domains (about 30 to 10%) are generally accepted (Szczepanowska, 1986, O'Sullivan, 1997) (Fig. 3.2). Crystalline regions are more hardly degraded due to their lesser accessibility to reactive species. Conversely, chemical species can easily diffuse through amorphous domains due to the local chain disorder. Thus, degradation does not occur uniformly throughout the whole polymer but quickly and more easily in the amorphous regions (Erofeev et al., 1982). Moreover, some authors (Rowland and Roberts, 1972) underlined that non-uniformity rates of reaction have been found even within the amorphous domains.
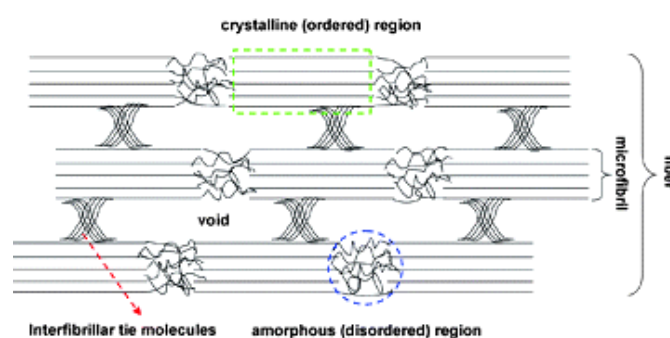
Fig. 3. 2 – Schematic model of cellulose showing crystalline stands (green squared frame) and amorphous regions (blue round frame) (Dufrasne et al. 2012).

3.1. DEGRADATION PHENOMENA

Cellulose is characterized by different degradation mechanisms occurring naturally. Nevertheless, degradation can be also induced by artificial aging. It has been established that hydrolysis represents the predominant degradation pathway at environmental conditions, with a potential synergism with oxidation and probable contribution of crosslinking. These three reactions have also been accounted for the breakdown of cellulose during thermal artificial aging (Graminski et al., 1979; Wilson and Parks, 1983). Among all evaluated parameters, acidity of paper has been identified as the most important intrinsic factor that promotes its degradation, together with elevated temperature and high relative humidity.

As the main degradation mechanisms affecting cellulosic materials, oxidation and both acid- and alkaline-catalyzed hydrolysis (McBurney 1954, Fellers et al. 1989) are briefly described below.

3.1.1 Oxidation

The oxidative degradation of cellulose can occur naturally (autoxidation, mainly through a free radical mechanism (Kolar 1997)) or can be artificially induced in presence of oxygen[1], light, transition metal ions[2] or specific chemical reagents (i.e. sodium hypochlorite, NaClO, or sodium metaperiodate, $NaIO_4$). Due to the presence of several hydroxyl groups along the chains, cellulose is very sensitive to oxidation. This phenomenon results in the formation of carbonyl (C=O, adehyde and ketone) and carboxyl groups (-COOH) at the primary and secondary hydroxyl groups of the pyranose ring. Carbonyl groups are chromophores, thus able to absorb visible radiation and their formation is mainly responsible for the yellowing of cellulose as a consequence of aging. As oxidation comes about, the opening of pyranose ring (Figg. 3.3 and 3.4) can occur though it does not necessarily take place.

Fig. 3. 3 – Principal oxidative reactions of hydroxyl groups of cellulose without pyranose ring opening (Margutti et al. 2001).

---

[1] The atmospheric oxygen is a non-specific oxidizing specie (Major, 1958) most likely acting by converting terminal or other carbonyl groups to peroxides (Strlič et al. 2005a). This produces new oxidized moieties togheter with a possible ring opening.

[2] Transition metals are involved in the so-called "Fenton reaction" (Shahani and Hengemihle, 1986, 1995; Bicchieri and Pepa, 1996) whit the formation of reactive radicals as oxidising species which rapidly induce the depolymerisation of cellulose (Calvini and Gorassini, 2002a; Calvini and Silveira, 2008; Potthast et al., 2008)
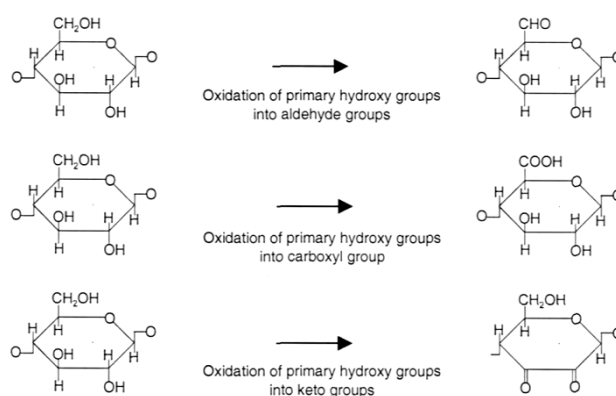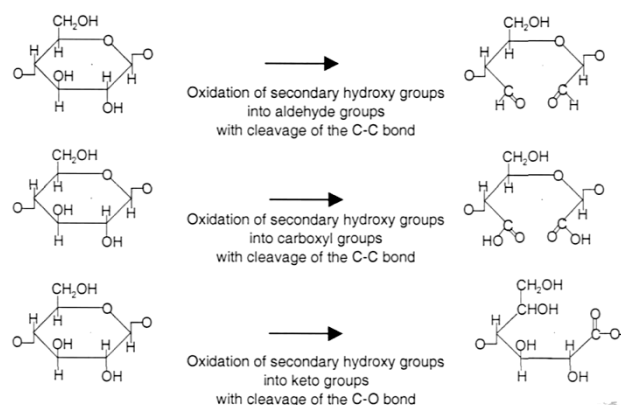
Fig. 3. 4 - Principal oxidative reactions of hydroxyl groups of cellulose with pyranose ring opening. (Margutti et al. 2001)

Carboxyl groups, instead, are non-chromoforic and acidic thus they increase the acidity of the whole system. Anyway, the glycosidic bond become weaker and depolymerisation together with changes in the polymeric structure can also occur, leading to a reduction in the physical and mechanical strength of the material.

In the early researches, the Russel effect[3] has been exploited to study cellulose and paper oxidation (Daniels, 1984; Daniels, 1986; Caverhill et al., 1999). Nevertheless, oxidative degradation has been mostly monitored by following the copper number (quantity of copper ions reduced by cellulose) (Graminski et al., 1979) and the methylene blue absorption (quantity of dye bonded by the carboxyl groups of cellulose)[4]. Recently, more valuable and promising techniques have been developed. Among all, chemiluminescence studies (Rychlý and Rychlá, 2005; Strlič et al., 2005a; Strlič et al., 2005b) and fluorescent labelling techniques (Potthast and al. 2006) are nowadays the most widely employed.

3.1.2   Hydrolysis

Hydrolytic degradation of cellulose can occur both in acid or in alkaline media and mainly causes the cleavage of β-glycosidic bonds with a decrease in the degree of polymerisation and the formation of new reducing free end groups (Fig. 3.5).

---

[3] The Russell effect (discovered in 1897) involves the formation of a developed image on photographic plates. This is most likely a consequence of either an emission of light or volatile hydrogen peroxide owing to the auto-oxidation of the objects under examination.

[4] Cellulosic materials with a high copper number or a high methylene blue absorption have been usually referred to as "reducing" ad "acidic" respectively.
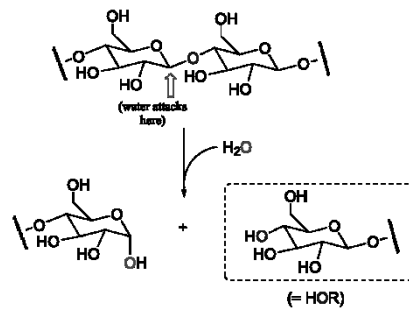
Fig. 3. 5 – Glicosidic bond cleavage in cellulose polymer due to hydrolysis (Soderberg 2012).

The chain cleavage can be quantitatively measured by viscometric analyses of cellulose solutions or by gel-permeation chromatography (GPC) (Emsley et al., 2000; Hill et al. 1995; Zou et al., 1994). The perceivable effects occurring due to such reactions are principally weakening and embrittlement phenomena of fibres .

Moreover, glycosidic bonds can be even more susceptibile to acid-catalysed hydrolysis if oxidized functionalities are present. In fact, the formation of carbonyl groups wherever in the cellulose chain, increases the adjacent glycosidic linkages susceptibility and the effect of an acidic environment.

Alkaline-catalysed hydrolysis has been widely investigated as it is involved in the *Kraft* delignification process of pulps. Alkali-induced cleavage of glycosidic bond only occurs temperatures around 160 to 180°C and with strong alkali media (Fig. 3.6).

Nevertheless, if β-alkoxy carbonyls are present along cellulose chains (*oxidized cellulose*), an alkaline medium can easily degrade them even in milder condition (room temperature and diluted alkali) (Malesic et al., 2002; Kolar 1997). A beta-alkoxy elimination reaction occurs by gradually shortening the chains through the so-called *peeling reaction* (Calvini et al., 2004; Dupont, 1996a; Bicchieri and Pepa, 1996) which spilts off the glucosidic units one by one (Fig. 3.7). Acidic and low molecular weight decomposition products are formed, such as b-isosaccharinic acid (Corbett and Kenner, 1953). Such reaction ends as a *stopping reaction* occurs (owing to the formation of metasaccharinic acid from isosaccharinic) or the consumption of amorphous domains is reached.
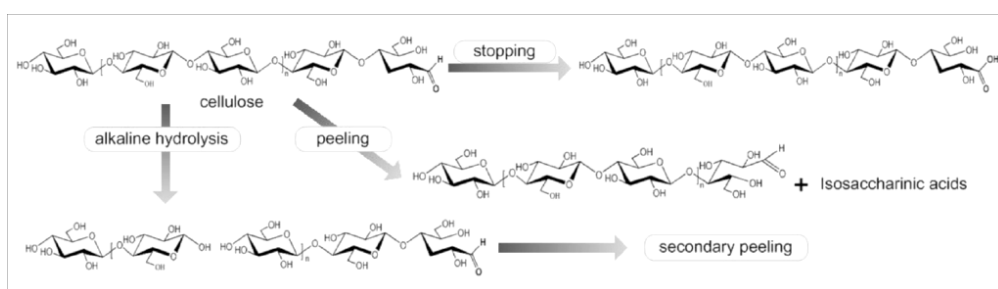
Fig. 3. 6 – Alkaline-catalysed hydrolysis of cellulose (Sixta 2012).
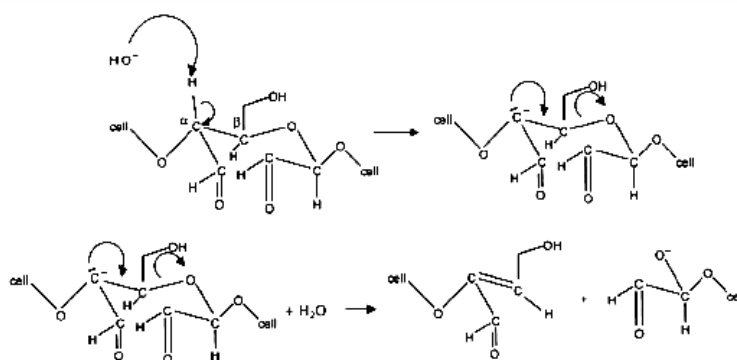
Fig. 3. 7 – Alkaline-catalysed hydrolisis of oxidized cellulose through a beta-alkoxy elimination reaction (Giorgi 2013).

All the above reactions must be considered when treating cellulosic materials with alkaline solutions for restoration purpose as well as when dissolving cellulose in strongly alkaline media for analytical evaluations (i.e. viscometric analysis using copper etylenediamine). Some researches have been recently focused on pre-treatments of oxidized samples with reducing agents (i.e. sodium borohydride) to convert carbonyl to hydroxyls groups. A decrease in their rate of alkali-induced degradation has, in fact, been observed (Block 1986; Tang 1986).

4

THE CHEMISTRY OF PAPER COMPONENTS

4.1. IRON-GALL INKS

Iron-gall ink has been the most important and widespread writing medium in western world since the Middle Ages and until the last century (Carvalho, 1904; Zerdoun and Yehouda 1983). A large variety of recipes have been developed (Neevel 2000; Daniels 2000; Stijnman, 2004; Budnar et al. 2004, 2006) even though the ancient procedure generally requires three or four main ingredients:

- *Iron(II) compound*, mainly derived from vitriol (an historic term commonly referred to the heptaydrated ferrous sulphate – $FeSO_4 \cdot 7H_2O$);

- *Gallotannins,* principally extracted from gall nuts (abnormal outgrowths of plant tissues produced as a protective defence towards insects stings, mainly Cynipidae family wasps);

- *Water* (or wine), as aqueous medium;

- *Arabic gum,* used as a binder to increase the solution viscosity.

Usually, the preparation firstly involved a cold or hot extraction of tannic compounds in water; ancient recipes sometimes required the usage of wine as it allowed an increase in gallotannins solubility and also improved extraction yield (Carme Sistach et al. 1999). Then, the iron(II) compound and eventually a binder were added, and the mixture became black. Some recent researches stated that the freshly prepared ink starts oxidising once exposed to air (Neevel 1995; Strlic et al. 2010), becoming insoluble and suitable to be used as writing medium.

4.1.1   Meaningful ink constituents

A great variety of parameters are involved in the ink preparation (e.g. raw materials, ratio of each ingredients, procedures), so that the quality of inks depend on several variables, barely controllable. For sake of simplicity, only the ink-system constituents relevant for the present study are briefly described below.

Iron/tannin ratio

Early studies on the molecular structure of iron-gall inks (Wunderlich 1991, 1994) stated as they can be represented by macromolecular 1:1 complexes of iron(II) and gallic acid. However researches carried on in the 1990s (Neevel 1995, and references therein) underlined as most of historical recipes contain much iron(II) than needed for the complex formation. Hence, some of the iron ions do not contribute to the formation of the ink complex and are thus available to participate in other reactions (e.g. iron(III) hydroxide formation by air-oxidation or radical oxidative degradation, see below).

On the bases of such studies, iron/tannin ratio is a meaningful parameter to be considered in inked paper degradation. Regarding iron to tannin content, iron-gall inks can be defined as

- *Balanced* (or "ideal"), with an equilibrated molar ratio between iron ions and tannic acid around 3:1 (3.7 mol/mol)

- *Unbalanced*, if the molar ratio between iron ions and tannic acid is higher than 3.7 mol/mol (excess of iron).

Arabic gum

The Arabic gum is the natural exudates of the acacia tree. Its chemical structure is quite complex even though it can be generally defined as a mixture of polysaccharides (hydrophilic) and heteropolysaccarides (hydrophobic) fractions. As iron-gall inks constituent, Arabic gum has been principally used as a binder: it both stabilizes the pigment in aqueous solution and sticks it onto the paper surface. Moreover, its thickening properties prevent a quick penetration of the ink into the fibres allowing sharper lines.

Some studies (Remazeilles et al. 2004; Rouchon Quillet et al. 2004) have suggested that the Arabic gum may have a protective role in inked paper degradation. In fact, it can act as a physical barrier limiting the diffusion of oxygen or free iron ions to the support below. Nevertheless, the protective effect is limited in time because the gum is itself very sensitive to degradation.

4.1.2   Ink-induced degradation

Despite technical details on its preparation variability, iron-gall inks are principally known as considerably paper degrading components (the so-called *iron-gall ink*

corrosion). Discolouration, embrittlement and perforation are the main damages occurring on cellulosic material due to the presence of iron-gall inks.

Since the beginning of the 20th century, a systematic scientific research has been carried out into this topic. The degradation pathway seems to be ascribed to a mixed mechanism (Margutti et al. 2001, Carme Sistach et al. 1998, Strlic and Kolar 2002;) involving both oxidative and hydrolytic reactions:

- *Acid-catalysed hydrolysis* (see Cap. 3.1.2) is most likely related to the low value of pH as well as the release of sulphuric acid that may migrate from inked areas to the surrounding paper (Neevel and Mensh 1999);

- *Autoxidation* is probable catalysed by transition metal ions (i.e. iron and copper) (Williams et al. 1977; Shahani and Hengemihle 1986; Messner et al. 1988; Banik 1988; Daniels 2002) as they can trigger redox reactions by easily changing their oxidation state.

For a description of the chemical structure of iron-gall inks see "Iron-gall inks. A computational study" at the end of the first part of this dissertation

4.2. GELATINE SIZING

Sizing materials have been using in paper production since antiquity. The purpose of such treatments is to prevent penetration or spreading of liquids (i.e. inks) through or on cellulose sheets thus allowing drawing or writing upon the surface. Several natural compounds have been used in the past and many synthetic polymers are still used nowadays.

Although a full dissertation on paper sizing would be interesting, this go beyond the aims of this thesis. Thus, only the gelatine sizing and related assessment are briefly discussed.

Gelatine sizing was first introduced in the Italian papermaking in the 13th century and it was widely used all over Europe until the 19th century (Garlick 1986). Some changes in additional materials used may have occurred over the time, but the method remained essentially the same. First of all, raw animal materials was boiled until the proper sizing solution was obtained. Then, each paper sheet was dipped in the warm

solution and finally lightly pressed to distribute the size and remove the exceeding material before being dried.

From a <u>chemical</u> point of view, gelatine is derived from the hydrolysis of collagen either in alkaline or acid medium. Collagen is the principal protein found in animal connective tissue, skin and bones and gelatine is obtained by boiling these materials in water. This procedure destroys the hydrogen bonding interactions among the protein strands so thus the partially degraded (denatured) collagen is obtained. Upon cooling, a strands' network will be partially reformed resulting in adhesive functions.

Formerly, some <u>additives</u> have been added to improve sizing properties. Among all, **alum** (at the beginning the natural double-sulphate of aluminium and potassium and later a synthetic aluminium sulphate) (Green 1992; Bruckle 1992, 1993) has been commonly used to improve gelatine adherence as well as to prevent microbial growth. However, today it is well-known that a great drawback in using alum is the increasing acidity of papers that could even seriously affects documents stability.

4.2.1   Gelatine degradation

As a consequence of aging (either natural or artificially-induced) gelatine may suffer losses of strength as well as a decrease in solubility due to cross-linking phenomena that lead to the formation of less-soluble polypeptides. Moreover, it has been demonstrated that gelatine undergoes hydrolysis upon aging and that alum contents higher than 10% accelerates hydrolysis reactions (Dupont 2002b).

Besides, even after short aging periods, gelatine-sized papers show remarkable yellowing phenomena owing to chromophores groups formed along protein chains.

Apart from gelatine degrading phenomena, recent researches suggested a protective effect of sizing toward cellulose degradation (Barret 1992; Barret and Mosier 1997; Dupont 2002c,d; Nguye et al. 2004) as it is most likely to have a buffer effect against acidity produced during degradation. Dupont and co-workers (2003), in fact, demonstrated a decrease in the rate of degradation of gelatine-sized paper in respect to non-sized ones.

5

ACCELERATED AGING

Accelerated aging is a testing method widely used in material science to study the long-term behaviour of items in conveniently short times. Normally, chemical and physical changes take place too slowly to be easily studied and accelerated-aging tests can variously speed them up in order to achieve different purposes:

- The evaluation of the stability and durability of materials;

- The prediction of the potential lifespan of items;

- The study of mechanisms and patterns of degradation involved and their physical consequences on the material.

In the field of conservation science, aging tests are also used so as to mainly evaluate the long-term efficacy of conservation treatments adopted to hinder the natural decay of cultural heritages.

5.1. NATURAL versus ARTIFICIAL AGING of PAPER: an OPEN DEBATE

Several questions have been raised in the past about the reliability of accelerated aging as a predictive tool on permanence of paper. As it represents a simulated test carried out by non-natural extreme conditions, thorough studies should be done and the compatibility of changes occurring during artificial and natural aging has to be carefully ascertained (Erhardt and Mecklenburg 1995). Moreover, a deep knowledge of the material and its degradation mechanisms is of paramount importance to obtain meaningful information about the potential credibility of aging tests in predicting the natural decay of paper.

Many *objections* come by in the literature on paper permanence tests (Porck 2000), mainly focused on:

- the effectiveness of artificial aging in producing same effects as natural one;

- the possible introduction of other reactions than naturally occurred;

- which should be the aging conditions in order to guarantee a trustworthy simulated approach;

- the reliability of using high temperature without undesired side reactions being introduced (Arney and Jacobs 1980; Bansa and Hofer 1989; Bansa 1992, 2000; Erhardt and Mecklenburg 1995; Shahani et al. 2001).

Nevertheless, even though it is barely possible to exactly reproduce the natural aging of paper in a laboratory, accelerated aging techniques are unluckily irreplaceable. Hence, one or more of the artificial aging techniques presently available should necessarily be employed bearing in mind that results from such tests have to be evaluated with caution.

5.2. PRINCIPLES AND MAIN TECHNIQUES OF ARTIFICIAL AGING OF PAPER

Natural aging on paper notoriously causes even serious damages to cellulosic materials. The study of these changes, naturally occurred during degradation, can take several years or even decades at ambient condition. Thus, extreme conditions are usually applied in order to reduce experimental times. Artificial accelerated aging bases on the well-known simple concept that temperature generally increases the rate of most chemical reactions. By measuring specific properties before and after the aging treatment, kinetics and effectiveness evaluation on degrading mechanisms can be done.

Many techniques are employed to artificially induced degradation and several parameters can be exploited. The main methods usually applied to cellulosic materials are:

- *Thermal aging in open oven*, both by static heating or thermal cycling;

- *Thermal aging in closed system* (sealed vessel method), by sealing the material into a closed vial and subjecting it to elevated temperature;

- *Climatic chamber aging*, by varying both temperature and moisture;

- *Chemical aging*, including acids, alkalis or oxygen usage;

- *Photo-degradation,* by using radiations at different wavelength;

- *Microbiological degradation*, by using specific microorganisms ;

Among all these methods, thermal aging is the most widely employed in cellulose research. It refers to the chemical and physical processes that occur at elevated temperatures as it is well-known that increased temperature accelerates most of the degradation processes that occur in polymers.

As far as this thesis work is concerned, only the **sealed-system technique** has been exploited in order to simulate degradation occurring in closed books and paper stacks. Nevertheless, a brief description of the most widely used open-system thermal method will be firstly supplied in order to understand the reasons that lie behind the chosen technique.

5.2.1. Humid or dry oven aging

Oven aging is an extensively employed method since the 1950s (Major 1958; Roberson 1976; Arney and Novak 1982; Fellers et al. 1989), consisting in exposing samples to a thermal degradation in air-circulating heating systems. Deterioration products are continuously removed and further degradation induced by released volatile compounds is avoided.

Research works by Whitmore and Bogaard (1994) as well as by Zou and co-workers (1994) indicate a primarily hydrolytic mechanism of thermal degradation of cellulosic materials in such systems. Whitmore demonstrated that no significant oxidation is generally produced during thermal aging as the ratio of the scissions to the produced carbonyl groups remains unvaried and approximately equal to 1.

5.2.2. Sealed systems aging

The sealed vessel technique refers to enclosing a properly pre-conditioned material in an air-tight container before subjecting it to an elevated temperature. The method has been firstly exploited to compare humidified and dry papers as it allowed to retain the paper moisture whitin the system (Richter, 1954; Czepiel, 1960). Nevertheless, further studies (Kaminska et al. 2001; Shahani et al. 2001; ASTM D6819-02e3 2002) have revealed a positive feedback of the trapped degradation products on the rate of aging. Volatile organic compounds (VOCs) owing to cellulose degradation are most likely re-absorbed in the structure of paper along with aging time thus gradually causing further increase of degradation rate (Zervos and Moropoulou 2005; Dupont 2006; Zervos 2007; Sawoszczuk 2008).

Moisture importance

Moisture seems a key parameter in closed-system aging of paper. Shahani (1995) first and Zou (1996a) later, have confirmed that high moisture contents may increase the observed degradation rate of cellulose as a consequence of an increased relative humidity level inside the enclosures.

Volatile organic compounds emitted during closed-vessels aging

Volatile organic compounds (VOCs) emitted by paper during its degradation have been investigated by several research groups using different analytical techniques. Gas chromatographic-spectroscopic (GC-FID and GC-MS) and gas chromatographic-olfactory (GC sniffing technique) techniques were used by Buchbauer et al. (1995), while high performance liquid chromatography (HPLC) or head-space solid-phase microextraction (HS-SPME) coupled with gas chromatography and mass-spectrometry (GC/MS) were used by Levchik (1998) and Lattuati-Derieux et al. (2004; 2006) respectively. The main identified species include: furanic compounds (e.g. furfural and furoic acid), hydrocarbons (both aliphatic and polycyclic aromatic), alcohols, aldehydes (e.g. vanillin and 4-hydroxybenzaldehyde) and acids (acetic, formic, butanoic and hydroxybenzoic acid) (Emsley and Stevens, 1994, Lattuati-Derieux et al., 2006; Gibson et al. 2012).

06

KINETIC MODELS OF CELLULOSE DEGRADATION

6.1. MEANINGFUL PARAMETERS

6.1.1   Scissions per chain

Kinetic studies on paper degradation have been firstly carried out using the viscometric degree of polymerisation (Santucci 1963, 1972; Santucci and Plossi Zappalà 1975; Calvini et al. 1988; Plossi Zappalà 1997). Further emphasis on the importance of this parameter to assess the rate of cellulose degradation has been provided by Feller et al. (1985). Thus, the degree of polymerisation has become the most significant parameter in such studies and the majority of published kinetic researches bases on it. Nevertheless, as frequently restated, frequent misleading statements could be derived from such approach and the usage of scission per chains has been proposed (Calvini and Gorassini 2006; Calvini 2008b; Calvini 2010; Calvini 2012; Whitmore and Bogaard 1994).

Sharples (1954a, 1971) has suggested the kinetics of degradation depending upon the number of broken bonds which is reciprocally related to the degree of polymerisation. Taking into consideration the moments of distributions (Montroll 1941; Herdan 1953), the zero-order moment (M0) can be defined as the number of cellulose chains in the system, while the first-order moment (M1) as the number of anhydroglucose monomers. By thus, considering the definition of the molecular mass averages for a given polymer (Mw, Mn, Mv, Mz) (see Attachment III), for cellulose the number of scission (S) can be either defined as:

- the number of *scissions per anhydroglucose unit*

$$S = 1/DP^t - 1/DP^0 \qquad\qquad 6.1$$

- the number of *scissions per initial cellulose chain*

$$S = DP^0/DP^t - 1 \qquad\qquad 6.2$$

It is worth noting that the DP in equations (6.1) and (6.2) is referred to the number-average degree of polymerisation. In fact, the number-average DP[5] (DP_n) can be expressed by

$$DP_n^0 = M1/M0 \qquad\qquad 6.3$$

During degradation scissions of inter-monomer bonds occur increasing M0 by S while M1 does not change. The relationship (6.3) thus becomes

$$DP_n^t = M1/(M0 + S) \qquad\qquad 6.4$$

It can be easily shown that the number of broken bonds per initial chain is

$$S/M0 = DP^0/DP^t - 1 \qquad\qquad 6.5$$

whereas the number of scissions per anhydroglucose unit is

$$S/M1 = 1/DP^t - 1/DP^0 \qquad\qquad 6.6$$

as stated above.

Unfortunately, DP_n cannot be easily evaluated as advanced (and not easily available) techniques are required (e.g. size-exclusion chromatography). More frequently, the degree of polymerisation is simpler measured by viscometry and the viscosity-average degree of polymerisation (DP_v) is obtained. It is widely assumed (Whitmore and Bogaard 1994) that $DP_v = 2DP_n$ so the equation (6.1) becomes

$$S_v = 2/DP_v^t - 2/DP_v^o \qquad\qquad 6.7$$

However, some consideration should be made at this point

- DPv is calculated from the intrinsic viscosity through the Mark-Houwink constants, *K* and *a* (see Attachment II);

- several standard methods (i.e. TAPPI, ASTM, ISO, AFNOR) are available and different *K* and *a* values are used.

Thus, different values of DPv can be calculated from the same intrinsic viscosity. Considering equation (6.7), experimental uncertaintie are even amplified as a difference between two reciprocal values of DP_v is used. Besides, different DP values

---

[5] Generally, the degree of polymerisation can be expressed as $DP = M_{polymer}/M_{monomer}$. Thus, the number-average DP of cellulose is defined as $DP_n = M_n/162$, where M_n can be evaluated trough SEC analyses and 162 is the molecular mass of the anhydroglucose unit (g/mol) (Kačík et al. 2009; Halajová and Kačík 2011).

(DP_v, DP_n, DP_w) can be obtained with different techniques (viscometry, SEC, osmometry) (Lauriol et al. 1987; Evans and Wallis 1989; Dupont et al. 2002a; Dupont and Mortha 2004; Lojewski et al. 2011) leading to different S values for the same sample. Consequently, the equation (6.2) should be preferably used (Calvini, 2008b) as the ratio between two DP values allows minimisation of errors as well as a meaningful comparison between degrees of polymerisation evaluated with different methodologies.

Millimoles of scissions

In order to quantitatively correlate the kinetic parameter S with data from other chemical analyses, equation (6.1) should be rather expressed in terms of millimoles of scissions per 100 grams of cellulose (Whitmore and Bogaard 1994) as

$$S_{mmol/100g} = 617 \cdot (1/DP_n^t - 1/DP_n^o)$$
6.8

or

$$S_{mmol/100g} = 617 \cdot (DP_n^0/DP_n^t - 1)$$
6.9

where DP refers to the number-average degree of polymerisation while 617 is the reciprocal value of the anyhdroglucose molecular weight (AGU, M=162.15 g/mol). This approach allows coherent comparison between the kinetics of degradation and other quantitative data, such as the carbonyl or carboxyl groups content[6] (Potthast et al. 2006), the emission of volatile organic compounds (Gilbert et al. 2009), the decrease of pH in acidic or alkaline hydrolysis or even the weight loss.

Bearing in mind that the scissions per chain S converge towards the LODP (see below, Cap. 6.1.2), Calvini (2005) proposed a correction factor (n°) corresponding to the initial amount of scissile units:

$$n°_{mmol/100g} = 617 \cdot (1/LODP - 1/DP_n^o)$$
6.10

---

[6] Both the concentration of carbonyl groups [CO] and the number of scissions (S) are proportional to the reciprocal DP (Whitmore and Bogaard 1994).

6.1.2 The levelling-off degree of polymerisation (LODP)

As previously asserted (see Cap. 3), the cellulose macromolecule is composed by both crystalline and amorphous regions; moreover, glycosidic bonds available for degradation just belong to the amorphous domain as crystalline bulk is highly stable. Hence, as stated by some authors (Nelson and Tripp 1953; Yachi et al. 1983), the levelling-off degree of polymerisation (LODP) should be considered. Calvini et al. (2005) endorsed this statement introducing n° as the asymptotic limit of cellulose degradation and defined it by

$$S_{LODP} = n° = DP°/LODP - 1 \qquad\qquad 6.11$$

or

$$S_{LODP} = n° = 1/LODP - 1/DP^0 \qquad\qquad 6.12$$

coherently with equations (6.1) and (6.2). Thus, the levelling-off degree of polymerisation corresponds to the extent of cellulose crystalline regions and n° represents the initial number of available scissile glycosidic bonds. Obviously, the LODP should be separately evaluated, for instance by using strong chemicals to induce the complete degradation of the amorphous domains (e.g. prolonged exposure to highly acidic vapours, Withmore and Bogaard 1994).

6.2. KINETIC MODELS of DEGRADATION

6.2.1 The linear kinetic model

Customarily, the kinetics of cellulose degradation has been followed using the linear *Ekenstam equation* (Ekenstam 1936; Emsley and Stevens 1994; Zou et al. 1996a)

$$1/DP^t - 1/DP^0 = kt \qqquad\qquad 6.13$$

where DP° and DP^t are the number-average degree of polymerisation before and after degradation, respectively. The equation has been developed from the empirical kinetic law

$$DP = DP^0 \cdot e^{-kt} \qquad\qquad 6.14$$

assuming that the polymer is monodisperse (with narrow distribution of DP) and bonds between monomers are equal (i.e. with the same probability of being broken).

Nevertheless, a deviation from linearity has been experimentally observed by several authors (e.g. Feller et al. 1986; Emsley and Stevens 1994; Bicchieri and Pepa 1996; Heywood et al. 1999; Whitmore and Bogaard 2001). An upward or downward curvature in the kinetic plots at long aging times (corresponding to low values of DP but still in the range of applicability of the kinetic law) has been detected and different hypotheses have been suggested:

- The presence of the the so-called *"weak links"*(Marx-Figini 1983; Feller et al. 1986; Emsley and Stevens 1994). They have been considered to be for some (not fully ascertained) reasons more sensitive than "normal" β-1,4 bonds. Probabaly, their weakness could be ascribed either to mechanical stress (Sharples 1954a, b; Michie et al. 1961) or to the presence of different functional groups along the chain (e.g. oxidized groups) which could inductively destabilize the neighbouring glycosidic bonds (Golova and Nosova 1973; Bicchieri and Pepa 1996; Whitmore and Bogaard 1995; Dupont 1996; Margutti et al. 2001).

- The presence of a diffusion-driven mechanism (Emsley et al. 1997).

6.2.2 Kinetic models of hydrolytic degradation in open systems

The hydrolytic mechanism of degradation can be generally written as

$$C + H \ \overset{k}{\to} \ P + H \qquad\qquad 6.15$$

where C and P represent cellulose chains before and after degradation, respectively. H can be considered an acidic degrading agent which catalyse the hydrolytic reaction and *k* the hydrolysis rate constant. By developing eq. 6.15 and just considering the time dependence of C

$$C = C° \, e^{- \, k \, t} \qquad\qquad 6.16$$

The introduction of the number of scissions (S) and the initial amount of cellulose linkages available for degradation (n°) (see Cap. 6.1.2)

$$C = n° - S \quad \text{and} \quad C° = n°$$

leads to the ***first-order kinetic law*** (eq. 6.17) already suggested in the 1940s as the theory of polymer degradation (Montroll, 1941) has been developed

$$S = n° \, (1 - \, e^{-kt})$$ 6.17

Equation 6.17 resembles an autoretardant degradation regime typically characterising open-system aging of cellulosic materials (i.e. oven aging) and where all bonds (n°) react at the same rate until only monomers remains.

Nevertheless, at this point some important consideration should be done.

1. **Ekenstam equation describes the initial stage of degradation**.
    It can be easily demonstrated that the Ekenstam equation (6.13) is the simplified zero-order approximation of the more general first-order kinetics (6.17). In fact, if n°>>S, then

$$S = n° \, k \, t$$ 6.18

otherwise (6.17) is obtained. By remembering that S can be either expressed as the number of scission per chain (DP°/DP - 1) or per monomer (1/DP-1/DP°), the Ekenstam equation (6.13) is achieved. That being so, some important consideration has to be done:

*   Ekenstam equation holds for the *initial stage of degradation* when $k \cdot t \approx 0$;

*   the correct form of the right-side of the Ekenstam equation should consider n°. Unluckily, the equation has been frequently mistaken as *n° has been usually implied*. Just a few studies considers that the rate constant *k* in equation (6.13) should include the n° value, as evident from the comparison with equation (6.18). This "unintentional" oversight has often led to misleading interpretation of kinetic analyses of aging data as well as incorrect kinetic models of cellulose degradation.

2. **n° represents the asymptotic value of cellulose breakdown as only amorphous regions are affected by degradation**.
    The first-order kinetics has been developed for soluble polymers degrading in homogeneous systems and where all bonds are available for the degradation (Krassig 1985). However, as far as cellulose is concerned, degradation occurs in heterogeneous conditions and affects the glycosidic bonds most likely in the

amorphous domain without a monomeric stage being reached. Thus, the n°
parameter in equation (6.17) represents the number of linkages available for
degradation as defined by the equation (6.11) and asserted by Calvini et al.
(2005). Unfortunately, very rarely LODP is reported in literature and usually not
even evaluated in the kinetic studies of cellulose. Even though this should have
hindered the application of equation (6.14) as the asymptotic value of n° was
unknown, this has not been the case among several kinetics researches in the
field of paper studies.

However, in cases n° has been not evaluated, the **Emsley equation** (6.19)
(Emsley et al. 1997) should be preferably applied. The equation is defined as

$$1/DP^t - 1/DP^0 = \frac{k_{1,0}}{k_2} (1 - e^{-k_2 t})$$

6.19

were $k_{1,0}$ is the (initial) rate constant of hydrolysis and k_2 is a free parameter
without a physical meaning and useful to assure a reasonable curve fitting
exercise (i.e. the rate constant of decrease of k_1). It is worth noting that even
the Emsley equation is simply an Ekenstam approximation useful to evaluate
just the initial fastest mechanism of degradation (Calvini 2014) as evincible by
mean of a linear MacLaurin serie approximation.

3. **Cellulose bonds are not identical throughout all the polymeric structure and
can degrade with different rate**.
As previously stated (Cap. 3), cellulose is characterised by amorphous and
crystalline domains, so that amorphous (a) and crystalline (c) glycosidic linkages
are present. Moreover, some weak links (w) could be also present.
Consequently, the general first-order kinetic law (eq. 6.17) should be better
defined as a sum of parallel process, thus becoming

$$S = n_w^0 \left(1 - e^{-h^\circ k_w t}\right) + n_a^0 \left(1 - e^{-h^\circ k_a t}\right) + n_c^0 \left(1 - e^{-h^\circ k_c t}\right)$$

6.20

where $n_w°$, $n_a°$ and $n_c°$ are the initial amount of weak links and of glycosidic
bonds in the amorphous and crystalline regions, respectively. A constant
degradation rate for each type of bond is assumed.

Equation 6.20 should be applied when deviations from eq. 6.17 are evident, as
clearly depicted in figure 6.1. Re-elaborated data by Daruwalla and Narsian
(1966) show that two simoultaneous mechanism of reaction occur as confirmed
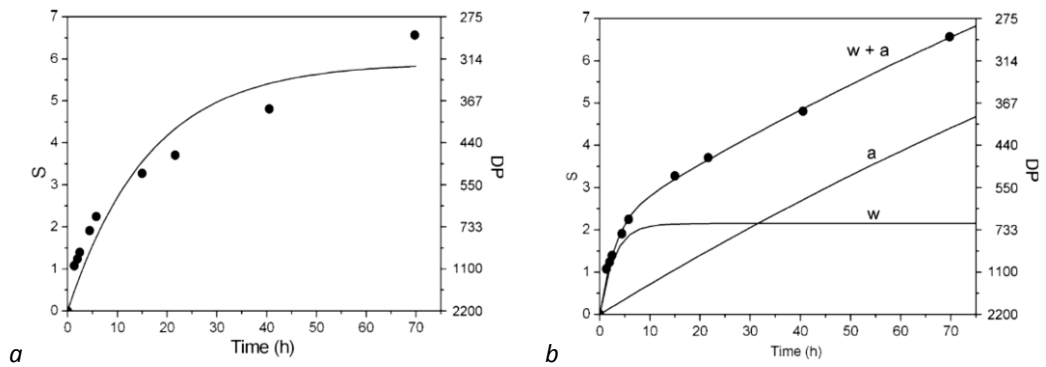by the good fit of data with eq. 6.20 (Fig. 6.1b) (Calvini et al. 2008b).

Fig. 6. 1 – Re-elaborated data after Daruwalla and Narsian (1966). Circles: experimental data by Daruwalla and Narsian. Lines: best fit with equation 6.17 (a) and 6.20 (weak links plus amorphous bonds) (b). (Calvini et al. 2008b)

6.2.3 Kinetics in sealed enclosures

The hydrolytic degradation occurring in sealed enclosures has been ascribed by a positive feedback of acid production from the degraded cellulose. Acidic compounds produced by the aging process are retained by the paper matrix and an increasing rate of acid hydrolysis is observed as the concentration of these acidic species increases with aging time. This process is considered to be *autocatalytic* (Shahani 1995).

Recently, working under these assumptions, Calvini et al. (2007, 2008b) have introduced a kinetic equation that considers the autocatalysis and explains most of the experimental data in literature. Considering the hydrolytic mechanism of degradation (eq. 6.15), a positive feedback may imply further degradation of the already degraded cellulose (P) leading to a rearranged degraded cellulose (A) and an additional production of acidity ($\alpha \cdot H$)

$$P \;\; \xrightarrow{k_A} \;\; A \;+\; \alpha H \tag{6.21}$$

By developing 6.15 and 6.21, the following equations are obtained:

$$dC/dt = -k\,C\,H \tag{6.22a}$$

$$dP/dt = k\,C\,H - k_A\,P \tag{6.22b}$$

$$dA/dt = -k_A\,P \tag{6.22c}$$

29

$$dH/dt = \alpha\, k_A\, P \qquad\qquad 6.22d$$

The above system represents the autocatalytic mechanism of reaction and it is clearly not linear which implies no analytical solution. To overcome such difficulty, two widely applied strategies are usually carried out by:

- starting with an excess of acidity H so that dH/dt ≈ 0 (hydrolysis in acidic environment);

- removing the excess of acidity H from the system, so that dH/dt = 0 (ventilated oven aging).

So that, the kinetic model of degradation resembles an autoretardant regime as described by the first-order kinetics in eq. 6.17 (or in eq. 6.20 if different kind of glycosidic linkages are supposed to exist).

Nontheless, aging in sealed enclosure must take into consideration all system equations 6.22 a-d. In order to obtain an analytical solution, an approximate approach has been proposed by Calvini and co-workers (2008b) by applying a finite differences algorithm to the system of equations 6.22. To this end, the reaction mechanism could be approximated to

$$C\ +\ H\ \overset{k}{\rightarrow}\ A\ +\ \alpha H \qquad\qquad 6.23$$

By introducing the number of scissions (S) and the initial amount of cellulose linkages available for degradation (n°) (see Cap. 6.1.2)

$$C = n° - S\ ;\ \ A = S\ \ ;\ \ \ H = h° + \alpha S$$

the following expression is obtained

$$dS/dt = k\,(n° - S)(h° + \alpha S) \qquad\qquad 6.24$$

The integration of eq. 6.24 yields to the **autocatalysis kinetic model** of degradation as:

$$\boldsymbol{S = \frac{h°\, n°\, (\, 1 - e^{-\,k\,(h° +\, \alpha\, n°)\, t}\,)}{h° +\, \alpha\, n°\, e^{-\,k\,(h° +\, \alpha\, n°)\, t}}} \qquad\qquad 6.25$$

where n°, h°, α and k are unknown values which can be evaluated by a curve fitting exercise of kinetic data.

Additionally to the autocatalysis equation, Calvini and co-workers were able to verify that the kinetic curve depends on the initial amount of acidity (h°/n°) (Fig. 6.2):

- *neutral samples* (low values of h°/n°) show a sigmoidal S-shaped curve (Zervos and Moropoulou, 2005);

- *acidic samples* (high values of h°/n°) show an initial linear shape followed by a curvature toward the asymptotic n° value as the levelling-off degree of polymerisation is approached (Zou et al 1996a).
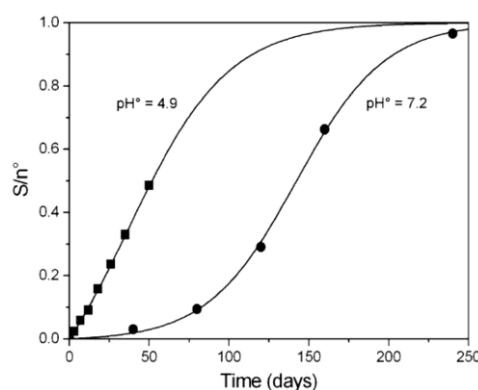

Fig. 6. 2 – Autocatalytic kinetic curves depending on the initial amount of sample acidity. Circles: re-elaborated experimental data after Zervos and Moropoulou (2005). Squares: re-elaborated data after Zou et al. (1996a). Lines: best fit with eq. 6.25. (Calvini et al. 2008b)

It has to be highlighted that deviations from this generalized model have been observed, even though a limited application of such a model has been performed since now. However, among all exceptions, the simoultaneous occurrence of an oxidative mechanism of degradation seems particularly interesting. Santucci and Plossi (1975) have artificially oxidized some cellulose samples before subjecting them to accelerated aging in closed vessels. Figure 6.3 depicts the kinetic plot of their re-elaborated data and a clear superposition of an autoretardant and an autocatalytic mechanism is evident (Calvini et al., 2008b). The kinetic trend may be probably ascribed to a faster degradation rate of glycosidic bonds influenced by the presence of oxidized moieties along the chains.
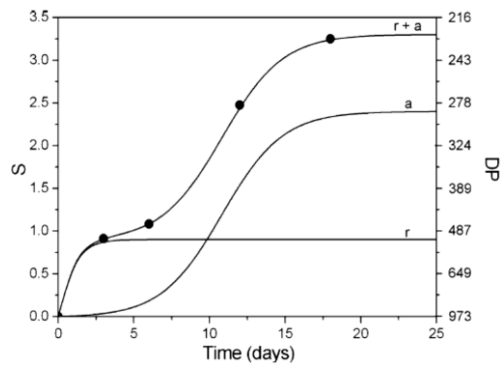
Fig. 6. 3 – Autocatalytic kinetic curve of oxidized cellulose. Circles: re-elaborated experimental data after Santucci and Plossi (1975). Lines: best fit with the sum of eq. 6.17 (r, autoretardant) and 6.25 (a, autocatalysis). (Calvini et al. 2008b

Summarising all the above statements:

- Kinetics evaluation should take into account the **number of scissions S** to allow comparison between different techniques;

- Kinetic data should be evaluated by plotting the **number of scissions per initial chain (S = DP°/DP – 1)** against aging time, in order to minimize experimental errors (eq. 6.2);

- To coherently compare the kinetics of degradation to other "quantitative" data, S should be expressed in mmol/100g of cellulose (eq. 6.9);

- Cellulose degradation drifts towards the **levelling-off degree of polymerisation** (LODP) and n° represents the kinetics asymptotic limit (eq. 6.11, 6.12);

- The most suitable **kinetic equation** should be used to fit the experimental data in order to obtain reliable rate constant and mechanism of degradation (Table 6.1):

Equation name	Equation expression	Applicability
Ekenstam	$1/DP^t - 1/DP^0 = k't$	• First steps of degradation
Emsley	$1/DP^t - 1/DP^0 = \dfrac{k_{1,0}}{k_2}\left(1 - e^{-k_2 t}\right)$	• kinetic data with a downward curvature • LODP *NOT* evaluated, thus n° (i.e. kinetics asymptote) *UN*known
Autoretardant *(first-order)*	$S = n°\left(1 - e^{-h°\,k\,t}\right)$ where $n° = DP°/LODP - 1$	• Kinetic data with a downward curvature • LODP evaluated, thus n° (i.e. kinetics asymptote) known
Autoretardant (w + a + c)	$S = n_w^0\left(1 - e^{-h°\,k_w\,t}\right)$ $+\ n_a^0\left(1 - e^{-h°\,k_a\,t}\right)$ $+\ n_c^0\left(1 - e^{-h°\,k_c\,t}\right)$	• Kinetic data deviate from a simple first-order eq. • LODP evaluated, thus n° (i.e. kinetics asymptote) known
Autocatalysis	$S = \dfrac{h°\,n°\left(1 - e^{-k\,(h°+\,\alpha\,n°)\,t}\right)}{h° +\, \alpha\,n°\,e^{-k\,(h°+\,\alpha\,n°)\,t}}$	• Sealed vessels aging
Autorestardant + Autocatalysis	$S = n°\left(1 - e^{-h°kt}\right) +$ $+\ \dfrac{h°\,n°\left(1 - e^{-k\,(h°+\,\alpha\,n°)\,t}\right)}{h° +\, \alpha\,n°\,e^{-k\,(h°+\,\alpha\,n°)\,t}}$	• Data deviate from a simple S-shaped curve

Table 6. 1 – Summarising table of kinetic models for cellulose degradation.

7

MATERIALS AND METHODS

7.1. SAMPLE PREPARATION

Reference cellulose

Samples have been prepared using Whatman® Grade No. 1 qualitative filter paper (Sigma Aldrich); this type of paper is obtained from cotton linters and it is considered to be mostly composed by pure alpha cellulose without sizing or fillers. Grammage was equal to 87 g/m^2 and the ash content lower than 0.06%. More technical data are reported in the table below (Tab. 7.1).

Whatman® Grade No. 1 qualitative filter paper	
article No	28413938
limit	0.25 psi wet burst
	150 sec/100 mL speed (Herzberg)
W × L	460 mm × 570 mm
thickness	180 μm
ash	≤0.06%
pore size	11 μm (Particle retention)
basis weight	87 g/m^2

Table 7.1 – Technical data of Whatman paper used in this thesis.
(http://www.sigmaaldrich.com/catalog/product/aldrich/z695122?lang=it&region=IT)

Although this material does not completely reflect historic rag papers and the current decision could be considered as a senseless simplification as generally papers do not consist of just pure cellulose (see cap. XX) several reasons support this choice. Whatman paper has been firstly chosen in order to compare our results with literature data as it is widely used in simulated studies on cellulose degradation. Secondly, its chemical compatibility with cotton-based papers allows a good simulation of ancient writing supports. Thirdly, undesired interaction between cellulose and other naturally occurring components such as hemicelluloses or residual lignin have been avoided.

Gelatine sizing

A sizing aqueous suspension has been prepared by first letting 25 g of rabbit skin glue (*Kremer Pigmente*) soak overnight in about 1 L of cold deionised water. After complete swelling the solution was heated in a water bath at 50°C and 1.25 g of alum ($KAl(SO_4)_2 \cdot 12H_2O$) (*Sigma Aldrich*) was then added and mixed slowly.

Some authors (Barret and Mosier, 1995; Spitzmueller 1992) have earlier tested historical paper recommending lower range of glue concentration than used here. However, quantities chosen in these experimentats have been established after some trials with different concentration of glue in water (from 2 to 100 g of glue per litre). On the basis of the simultaneous evaluation of the increase in samples' weight and of FT-IT ATR signals, 25 g/L has been chosen as the most suitable for the purpose. In fact, the sample has showed a mild weight increase (6%) and signals related to peptide bonds at 1520 and 160cm^{-1} have been well identifiable without interference with the analysis of cellulose typical ones.

In the course of the thesis it will be referred to sizing with either the terms of sizing, gelatine or animal glue.

Iron-gall inks (IGIs)

Three different writing ink samples have been prepared using recipes available in the literature and referred as traditional method of preparation (Senvaitiene et al., 2006; Thompson, 1996; Wunderlich, 1994; Krekel, 1999a,b). The choice of using traditional prescription is due to evaluate the effect of some intrinsic compounds historically used in iron-gall inks preparation. Particularly, iron/tannin ratio and arabic gum were taken into consideration, as stated in Cap. 4.1.1.

Analytical grade reagents and distilled water have been used for the preparation of all inks.

Iron-gall ink 3

About 160 ml of cold distilled water and 10 ml of 10% acetic acid (Carlo Erba) have been added to 10 g of powdered oak galls (*Kremer Pigmente*), 5.3 g of iron(II) sulphate ($FeSO_4 \cdot 7H_2O$) (*Sigma Aldrich*) and 5.3 g of arabic gum (*Kremer Pigmente*). As soon as reagents have been mixed a deep blue-black colour has been obtained. The mixture has been stored for 8 weeks in a covered becher with intermediate blending before being filtered. The pH of the final ink solution was equal to 1.63.

IGI3 can be defined as an iron-exceeding iron-gall ink as the molar ratio iron/tannin was equal to 5.9 mol/mol (see Cap. 4.1.1).

Fig. 7. 1 – Preparation of iron-gall ink 3. Left: ingredients used. Right: ready-prepared ink.

Iron-gall ink 4

About 200 ml of distilled cold water has been mixed with 23.064 g of powdered oak galls (*Kremer Pigmente*) and mixture has been stored for 3 days. To this, 7.584 g of iron(II) sulphate ($FeSO_4 \cdot 7H_2O$) (*Sigma Aldrich*), 0.6 g of sodium chloride (*Sigma Aldrich*), 6 ml of 10% acetic acid (*Carlo Erba*) and 0.954 g of alum ($KAl(SO_4)_2 \cdot 12H_2O$) (*Sigma Aldrich*) have been added and a deep black colour has been obtained. The mixture has been stored covered for 2 weeks with intermediate mixing and then filtered. The pH of the final ink solution has been equal to 1.69.

IGI4 can be defined as a balanced iron-gall ink as the molar ratio iron/tannin was equal to 3.7 mol/mol (see Cap. 4.1.1).

Iron-gall ink N

93.3105 g of powdered oak galls (*Kremer Pigmente*) have been added to about 190 ml of warm commercially available white wine. 58.13 g of arabic gum (*Kremer Pigmente*) and 46.8 g of iron(II) sulphate ($FeSO_4 \cdot 7H_2O$) (*Sigma Aldrich*) have been gently added and the mixture stored covered for 1 day. The ink has been then filtered with a sieve due to its high viscosity. The pH of the final solution was equal to 2.17.

IGIN can be defined as an iron-exceeding iron-gall ink as the molar ratio iron/tannin was equal to about 5.6 mol/mol (see Cap. 4.1.1).
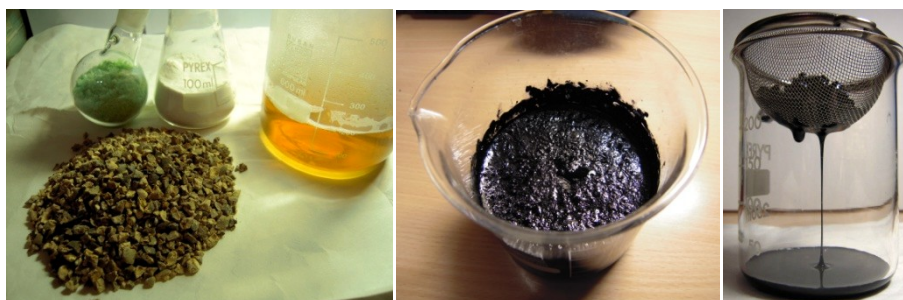
Fig. 7. 2 – Preparation of iron-gall ink N. Left: ingredients used. Centre: the prepared ink after 1 day of rest and before filtration. Right: ink during sieve filtration.

Paper samples preparation

Cellulose sheets have been cut into pieces of suitable dimensions (see below "Artificial aging method. Paper/Volume ratio") and properly prepared in order to simulate single and multiple interactions between considered components.

Purification

First of all, to avoid the possible influence of already existing oxidised groups, all Whatman sheets have been purified by 1 day immersion in 0.1 M NaOH, followed by washing with distilled water and 1 day immersion in 0.1 M HCl. The withdrawn samples have been then firstly washed with tap water and then with distilled water to the neutrality. Purified sample with no ink and no sizing application is referred to as *reference paper* (W).

Sizing

In order to simulate ancient writing supports and evaluate the influence of sizing on the degradation mechanism of cellulose, some purified Whatman sheets have been soaked with the animal glue solution. About 500 mL of gelatine solution have been poured into a Pyrex tray resting on a hot plate at 30°C. Each paper sample has been placed in the size bath for 20 minutes then individually removed and vertically air-dried overnight. Samples with sizing application are referred to as *sized papers* (S).

Inks application

Moreover, the effect of iron-gall inks have been investigated by the application of a constant volume (5 ml) of each ink solution to the paper samples. A third of both sized

and non-sized papers' surface have been brushed with the prepared inks (Figure 7.3). The surface has been intentionally not fully covered with ink in order to measure the "indirect" effect of emitted VOCs on cellulose even not directly in contact with the inked area. Moreover, possible interfering effects of applied ink has been avoided. Samples with ink application are referred to as *inked papers*.

Thus, each aging-time *set* of samples under investigation has been composed by 8 pieces and all sets have been prepared at the same time and conditions. Examples of prepared samples (Tab. 7.2) and a summarising table of meaningful parameter evaluated (Tab. 7.3) are reported below.

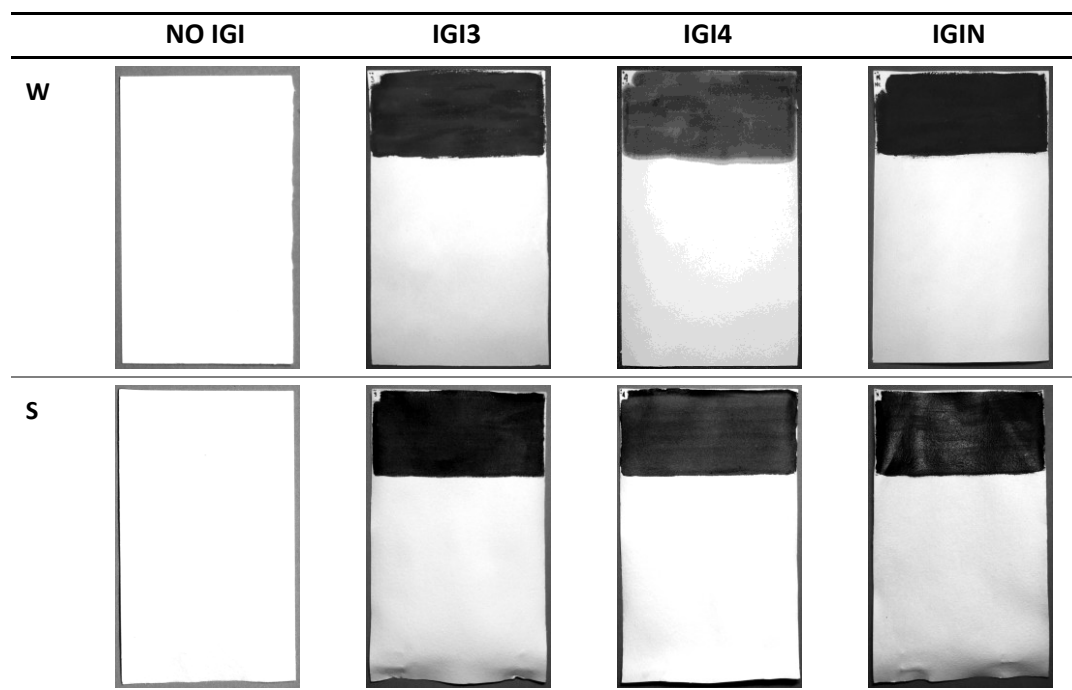|	NO IGI	IGI3	IGI4	IGIN
W				
S				

Table 7. 2 – Non-degraded samples under investigation. First line: non-sized samples (W). Second line: sized samples (S).

Samples	Gelatine Sizing	Iron Gall Inks		
		pH	Fe/Tan (mol/mol)	Arabic gum (g/L)
Unsized				
W	-	-	-	-
WN	-	2.2	5.6	300
W3	-	1.6	5.9	30
W4	-	1.7	3.7	-

Sized				
S		-	-	-
SN	2.5 g/L lapin glue	2.2	5.6	300
S3	5%w alum	1.6	5.9	30
S4		1.7	3.7	-

Table 7. 3 – Summarising table of samples characteristic parameters. IGI3 and IGIN are iron-exceeding inks whereas IGI4 has an ideal ratio between iron and tannin.

7.2. ARTIFICIAL AGING METHOD

Sealed vessel aging parameters used in the present work are reported in table 7.4.

Artificial aging parameters	
Temperature	80 °C
Sealed system	Heat-sealed glass tube
Paper/Volume$_{vial}$ ratio	1g / 15ml
Conditioning before aging	25°C, 50% R.H.

Table 7. 4. Aging parameters used in the present study.

All the samples have been pre-conditioned to 25 °C and 50% relative humidity (RH) for at least 24 hours prior to the aging experiment.

As far as the aging method is concerned, ASTM D6819-02e3 standard (2002) has been taken as guideline for the present study although some parameters have been changed as described below.

1. ***Temperature.*** The ASTM recommended temperature equal to 100°C. Nevertheless, the temperature of 80°C has been preferably chosen, firstly to compare the obtained results with literature data. Moreover, the observation of contributions from all considered components would have been allowed by the relatively low temperature and undesired side-effects avoided.

2. ***Sealed enclosures***. Identical vials as recommended by ASTM have intended to be used. However, their difficult commercial availability as well as already underlined problems of tightness (Kaminska et al. 2001) have driven the choice elsewhere. As the basic assumption of this aging method is valid only when the vials employed are perfectly leak-proof, heat-sealed glass tubes specifically prepare for this purpose have been used instead of glass vials with polypropylene caps and TFE gaskets prescribed by the ASTM method. Technical specifications of adopted enclosures are reported in table 7.5.

Sealed enclosures	
Height (mm)	270
Internal diameter (mm)	13
Internal volume (ml)	36
Glass thickness (mm)	1

Table 7. 5. Technical specifications of heat-sealed glass tubes used in the present study.

3. ***Paper/volume ratio***. Oxygen and humidity are of paramount importance in cellulose degradation and their careful control is essential to predict a reliable reaction pathway. ASTM standard recommends to use 1 g of dry cellulose per 36 ml of reactor volume. Differently, in this study a higher ratio has been used (2.4 g/36 ml). In fact, by considering both the initial conditioning (25°C, 50% RH) and the aging temperature, an increased internal relative humidity near to 65% at 80°C has been roughly estimated[7] (Calvini, a). This percentage allows reliable comparison with literature data on analogous aging studies

All the conditioned samples have been properly folded and placed inside a vial afterwards subjected to the artificial aging test in a Memmert dry heat oven. Tubes have been subsequently withdrawn after 6, 22, 36, 60, 70, 82, 169 and 417 days of accelerated aging (Fig 7.3). This approach has allowed the evaluation of a coherent degrading process as undesired differences in samples preparation and aging have been avoided.

---

[7] It is worth noting that water-absorbing materials (such as cellulosics) in a confined system change the internal humidity due to temperature variations. If temperature raises, the material releases its absorbed water increasing the relative humidity of the system.

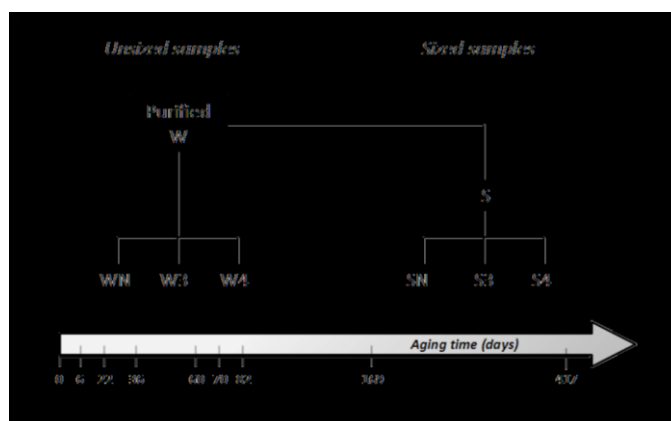Once out of the oven, all vials have been left to cool for 24 h and afterwards opened by breaking the glass.

Fig. 7. 3 – Summarising scheme of samples and aging times exploited.

7.3. EXPERIMENTAL EQUIPMENT

Multi-detector size-exclusion chromatography (SEC) associated with fluorescent labelling techniques and viscometry have been the main methods used in this study. Viscometric analyses has allowed the evaluation of the viscosity-average degree of polymerisation (DPv). The SEC (or Gel Permeation Chromatography, GPC) system has provided the molecular mass distributions together with the number- and the weight-average molar masses. Moreover, labelling procedures have supplied quantitative information on carbonyl and carboxyl groups. Technical specifications, measurement conditions and materials used are described below. For a theoretical description of techniques used, referred to attachments [1] and [2].

Colorimetric analyses have been also exploited, but less widely. For the determination of the optical properties of samples, a portable Konica Minolta spectrophotometer CM-2600d has been used. L*, a* and b* coordinates of CIEL*a*b* color system have been determined and ΔE values calculated by the well-known equation

$$\Delta E = \sqrt{(\Delta L^*)^2 + (\Delta a^*)^2 + (\Delta b^*)^2}$$

7.3.1. VISCOMETRY

The viscosity-average degree of polymerisation (DPv) of all samples has been measured by viscometric analyses, according to the ASTM Standard D 1795–90.

Sample preparation

Each paper under investigation has been sampled in the most distant part to the inked area. The collected samples have been cut into small pieces of 2 mm x 2 mm and weighted. Then, conditioning at 23°C and R.H. 50% has been performed before dissolving pulps in a 0.5 M aqueous solution of cupriethylenediamine hydroxide (CED) at ambient condition under magnetic stirring.

Prior to these steps all sized samples have been gently boiled in water at 90-100°C for 1 hour to avoid the interference of gelatine on solutions' viscosity; also all unsized samples have been treated as such for experimental coherence.

It is well known that degradation can cause a cleavage of cellulose chains, consequently reducing the viscosity of a diluted polymer solution. In order for the viscosity of the analysed solutions to fall within the measurable range of the viscometer even for the highly degraded cellulose (long-time aging), increasing amount of sample has been dissolved ranging from 10 mg (unaged cellulose) to 90 mg (417-day-aged samples) per 20 ml of CED.

Additionally, it is worth noting that CED is strongly alkaline (pH = 12) and causes degrading phenomena on aged cellulose (Cap. 3.1.2). In order to limit damages induced by the solvent, the stirring time has been the least necessary to guarantee a proper dissolution.

Levelling-off DP

In order to evaluate the levelling-off degree of polymerisation value (LODP) of cellulose under investigation, a purified Whatman sample has been prepared by three day exposure to concentrated HCl vapours in order to degrade cellulose amorphous domains (Whitmore and Bogaard, 1994) and analysed as described below.

Equipment

Viscosity measurements have been done in a water bath at 25 ± 0.1 °C using a Ostwald-type capillary glass viscometer. For each sample solution the analyses has been repeated three consecutive times and the efflux time values averaged.

The viscometric degree of polymerisation

The average DPv values have been calculated from the intrinsic viscosity $[\eta]$[8] expressed in ml/g by means of the empirical relationship known as the Mark-Houwink-Sakurada equation (see Attachment [2]), using K=1.5 and a=1 as indicated in the UNITEX CH33:

$$DP_v = 1.5 \cdot [\eta]^1$$

The degree of polymerisation and the LODP values of both sized and unsized unaged samples (DP°) are reported in table 7.6 and they have been used to evaluate the number of scissions per initial cellulose chain by applying eq. 6.2 (Cap. 6.1.1) and 6.11 (Cap. 6.1.2)

Viscometric degrees of polymerisation	
DP° (W)	1369
LODP (W)	172
DP° (S)	1306
LODP (S)	171

Table 7. 6. Viscosity-average degrees of polymerisation for unsized (W) and sized (S) whatman paper.

---

[8] The reduced viscosity (η_r) value necessary to extrapolate $[\eta]$ was calculated in previous viscometric experiments of given cellulose sample at three different concentrations.

7.3.2. SIZE EXCLUSION CHROMATOGRAPHY

Size exclusion chromatography analyses have been performed during the doctoral internship period at the Biopolymer and Paper Analytics laboratory (Boku Universität) in Vienna. Analyses have been performed on some of the samples under investigation, according to the standard procedure (Röhrling et al. 2002a, b, c; Potthast et al. 2003; Bohrn et al. 2006a, c) described below. Refer to attachment [2] fo more theoretical details on these methods.

Sample preparation

Unlabelled samples

About 10 mg of sample have been defibrillated in a two-blade cutting mill using bidistilled water. The solution has been then filtered, cellulose fibres dried with ethanol 96% under vacuum and transferred into a 4 mL vial (Fig. 7.4). In the case of long-term aged samples, to avoid low mass injection due to an extent sample degradation, about 30 mg of dry sample have been disintegrated.
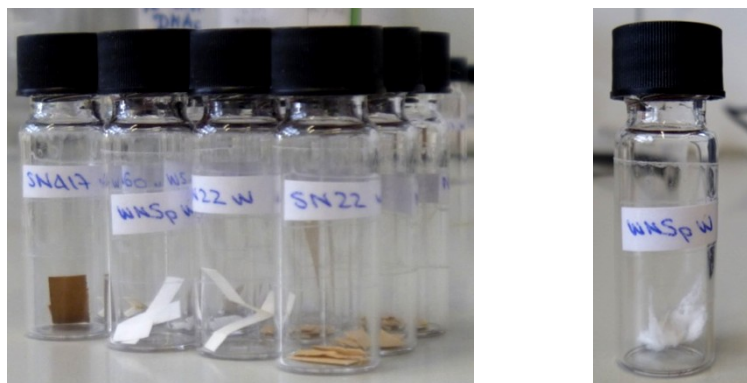

Fig. 7. 4 – Samples under preparation for GPC analyses. Right: cut papers. Left: pulp fibres after disintegration and drying.

Labelled samples

In the case of labelling procedure, the same sample preparation described above has been used. However, 0.1 M HCl solution instead of pure water has been used in the mill defibrillation. Acid sample disintegration would have been not necessary for CCOA labelling. Nevertheless, a coherent defibrillation procedure has been carried out in the present study for all labelled samples.

Moreover, to avoid low mass injection due to the sample degradation, about 50 mg of dry sample have been disintegrated and about 25 mg of wet sample have been used for each labelling procedure.

Fluorescent labelling procedure

CCOA method

An heterogeneous carbazole-9-carbonyloxyamine (CCOA) labelling of carbonyl groups have been performed accordingly to published works (Röhrling et al. 2002 b, c; Potthast et al. 2003).

About 20 - 25 mg of dry pulp (both sample and standards, separately) have been suspended in 2 mL of CCOA stock solution prepared by dissolving 60 mg of label in 50 mL of zinc acetate buffer (20 mM, pH 4.0).

Fig. 7. 5 – CCOA labelling method. Suspended pulps in CCOA-Zn(CH$_3$COO)$_2$ solution.

The suspension has been agitated in a water bath for 7 days at 40 °C. The pulp has been then removed by filtration and transferred into a dry vial for the activation procedures (see below).

FDAM method

Fluorenyl diazomethane (FDAM) labelling of carboxyl groups have been performed accordingly to protocols (Bohrn et al. 2006a, b).

The preparation of 40 ml of FDAM labelling solution has required several steps

- *Solubilisation*. In a three-neck round-bottomed flask 110 mL of absolute ethanol have been mixed to 1.046 g of 9H-Fluoren-2-yl-carboxaldehyde and stirred under mild heating for 5 minutes;
- *Hydrazone synthesis*. After the solution has cooled down, 11 mL of Hydrazin in tetrahydrofuran (1 mL/L, already prepared and stored at 4°C) have been added. The flask has been equipped with a reflux condenser and filled with argon from a balloon. The system has been maintained under stirring for 30 minutes;
- *Ethanol removal*. Through a rotary evaporation (water bath at 40°C) ethanol has been removed and a light yellow milky product has remained at the bottom of the flask
- *Hydrazone oxidation*. 20 ml of N,N-dimethylacetamide (DMAc) has been added together with about 5 mg of MnO_2. Stirring has been maintained for about 1 hour.
- *Filtration*. The mixture has been filtrated using a Buchner filter half-filled with celite and MgSO4 and DMAc has been added till 40 mL of the final red filtrate solution have been obtained (approximately 0.125 mol/L in DMAc).

About 20 – 25 mg of dry pulp has been suspended in 3 mL of DMAc and 1 mL of FDAM solution has been added.
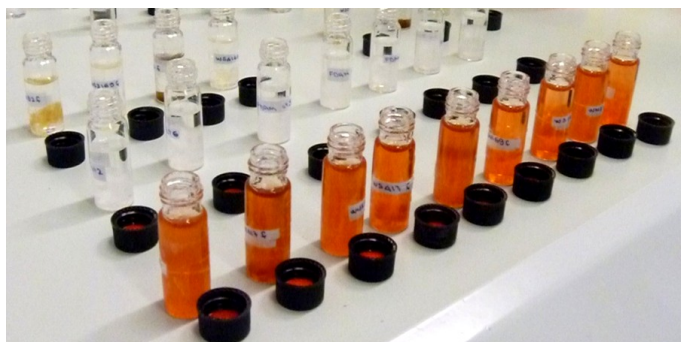

Fig. 7. 6 – FDAM labelling procedure. Addition of the label solution to the pulp fibres.

The suspension has been agitated in a shaking bath at 40 °C for 7 days and the pulp subsequently filtered off, washed with DMAc and transferred into a dry vial.

Activation

To achieve a good molecular disperse dissolution in N,N-dimethylacetamide/lithium chloride (DMAc/LiCl) (9%, w/v) used as cellulose solvent, both labelled and unlabelled cellulose samples had to be activated by solvent exchange (water to DMAc). The activation treatment has consisted in adding anhydrous DMAc to the prepared pulp fibres and leaving them overnight under mechanical shacking. A subsequent filtration under vacuum has produced efficiently activated and readily soluble samples.

Dissolution

After activation, dissolution of pulps in 2 ml of freshly prepared[9] N,N-dimethylacetamide/lithium chloride 9 %(w/v) (DMAc/LiCl) has been carried out at room temperature. Each solution has been stirred at room temperature until complete dissolution[10] (about 2 to 7 days has been usually necessary).

GPC sample preparation

300 µL of dissolved samples have been filtered through a 0.45 μm pore polytetrafluoroethylene (PTFE) filter and diluted with 900 µL of fresh DMAc/LiCl 9%w/v prior to injection. Then GPC analyses have been performed according to the available GPC system setup (see below).

General analytics and GPC method

Measurements have been performed with a GPC-Fluorescence-MALLS-RI system providing the average molecular mass values (Mn, Mw and Mz) and the molecular weight distribution (MWD). Additionally, the content of oxidized groups in relation to the molecular mass (MM) has been obtained.

GPC instrumentation

A schematic instrumental setup is provided in attachment [3]. Samples have been automatically injected using an autosampler (HP 1100) and then chromatographic analyses have been performed on thermostated (column oven Gynkotek STH 585) four-serial GPC columns.

---

[9] Freshly prepared solution of DMAc/LiCl are preferable in order to avoid moisture contamination which would affect cellulose dissolution.
[10] The dissolution has been considered complete when the solution had a clear appearance with no visible solid residues.

The signal has been monitored by a multiple-angle laser light scattering detector (Wyatt Dawn DSP) with an Ar ion laser (λ_0 = 488 nm); a refractive index (RI) detector (Shodex RI-71); a fluorescence detector (TSP FL2000) for CCOA and FDAM labelled samples. The analytical system has included also an online degasser (Dionex DG-2410), a Kontron 420 pump and a pulse damper.

GPC measurement parameters

The following parameters have been used in the GPC measurements

- mobile phase: N,N-dimethylacetamide/lithium chloride (DMAc/LiCl) (0.9% w/v), filtered through a 0.02 µm filter;
- flow rate 1.00 mL/min;
- injection volume: 100 µL;
- columns: four PLgel MIXED A LS, 20 µm, 7.5 x 300 mm (Agilent);
- fluorescence detection: λ_{ex} = 286 nm, λ_{em} = 330 nm (CCOA); λ_{ex} = 252 nm, λ_{em} = 323 nm (FDAM).

Data evaluation

Chromeleon, Astra and GRAMS/32 software have been used for molecular weight distributions and polymer-relevant parameters calculation. A specific refractive index increment (*dn/dc*) of cellulose in 0.9% w/v DMAc/LiCl at 25 °C and 488 nm has been considered to be 0.136 mL/g. As far as labelled samples are concerned, a calibration of oxidized groups content has been carried out using reference pulps[11] (Röhrling et al. 2002b) coherently prepared as samples under investigation.

The *standard deviation* has been evaluated on the basis of previous long-term determinations of standard pulps (Röhrling et al 2002b): for the average molecular masses DS has been around 5-10% while around 5% for carboxyls and carbonyls determination.

GPC degree of polymerisation evaluation

Number- and weight-average degrees of polymerization (DPn and DPw respectively) have been obtained by dividing Mn and Mw values (in kg/mol) by 0.162 kg/mol corresponding to the molecular weight of anhydroglucose (cellulose repeat unit).

---

[11] Standard pulp for the CCOA method: Cl HCE BI 223; Solucell 108/99; Saiccor Jumbo 25/99C; Modo Z1 366/97; Modo 366/97; KZO3 14/00. Standard pulp for the FDAM method: Ray_Sulf FEZ1089; Bacell FEZ1095; KZ03 FEZ1085; Weyerh FEZ1090; Sappi FEZ1078; Atisholz FEZ1086; Cellunieu FEZ1084.

Polydispersity index (PDI) has been calculated by dividing Mw by Mn. The calculated DP_{GPC} values has been used to evaluate the number of scissions per initial cellulose chain by applying the eq. 6.2 (Cap. 6.1.1).

8

RESULTS AND DISCUSSION

Experiments have been set up in order to determine the influence on cellulose of the various components characterising ancient papers during artificial accelerated aging tests: sizing and iron-gall inks.

In the present section, the characterisation of samples firstly takes into account the influence of sizing thus results of unsized and sized papers is separately considered. Within each group, the effect of the iron-gall inks studied is evaluated and a comprehensive comparison between all components of the ancient-paper-system is finally summarised.

As previously stated, characterisation of degradation have been principally carried out on the basis of viscosity-, number- and weight-average degrees of polymerisation (*DPv*, *DPn* and *DPw*, respectively). Moreover, changes in the molecular weight distribution patterns (MWD) of all analysed samples along with aging time have been explored. The oxidized groups evaluated through labelling methods coupled to SEC technique have been also considered in order to ascertain if oxidative degradation had been occurred during aging.

8.1. CHARACTERISATION OF DEGRADATION

First of all, it is worth noting that differences in DP values from SEC and viscometry are evident for all sized and unsized samples (cf. Table 8.1 and 8.5) but they are most likely related to different Mark-Houwink α parameter used as calibration value. Despite such differences, all data show a meaningful decrease of all DP values with increasing aging time, resulting in a overall greater degradation of inked samples than non-inked ones.

It is generally agreed that hydrolysis as well as oxidation could be responsible for changes occurring on cellulose in the presence of iron-gall inks. However, viscosity alone (*DPv*) does not allow to establish if DP decrease could be ascribed just to

hydrolytic or even to oxidative degradation. Moreover, if oxidation takes place and oxidized functionalities (such as a keto or aldehyde groups) are formed along the chains, β-alkoxy elimination reaction could be induced by the viscometry alkaline medium resulting in the cleavage of glycosidic bonds and thus chain scissions. Hence, Sv values higher than the corresponding S_{GPC}'s might indicate that a solvent-induced degradation affected viscometric determinations.

As far as samples under investigation are concerned, the correlation between Sv and Sw gives an insight into such a problem. The plot of the weight-average against the viscometric scissions per chain are presented in figure 8.1. Slopes evaluated from linear regression of experimental data are higher than 1, thus confirming that different calibration setup has been used to calculate DPv and DP_{GPC} values.
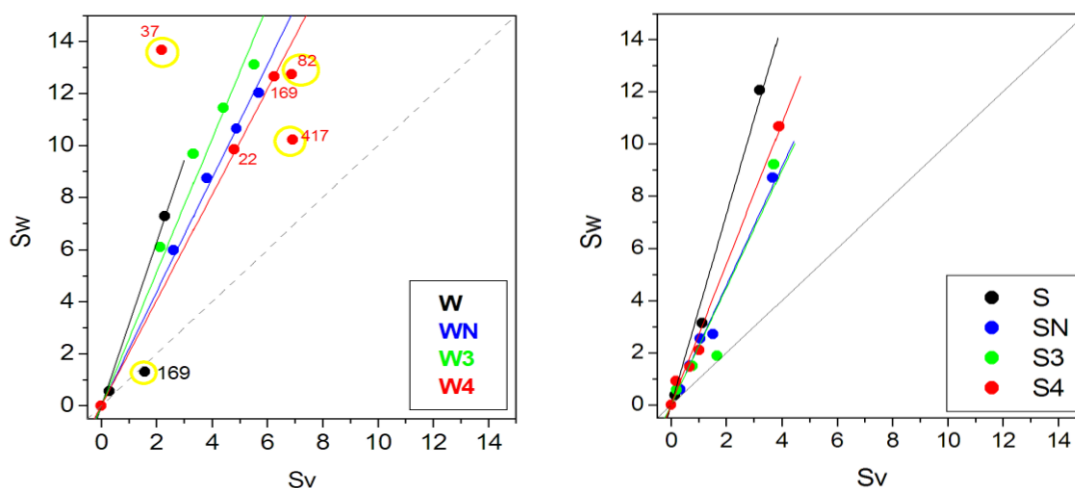

Fig. 8. 1 – Plot of the weight-average (Sw) vs. the viscometric scissions per chain (Sv). Left: unsized samples plot. Slopes obtained by linear regression are (W) 3.14±0.01, (WN) 2.19±0.04, (W3) 2.57±0.11, (W4) 2.03±0.09. Right: sized samples plot. Slopes obtained by linear regression are (S) 3.65±0.18, (SN) 2.29±0.09, (S3) 2.25±0.25, (S4) 2.69±0.11.

Data trends depicted in figure 8.1 suggest that there is likely no reason to think that appreciable amounts of β-alkoxy-susceptible carbonyl groups have been formed neither in unsized nor in sized samples. Hence, unreliability of viscometric data is conceivably ruled out.

Further characterisation of degradation will be hereafter presented by separately considering unsized (Cap. 8.1.1) and sized (Cap. 8.1.2) samples.
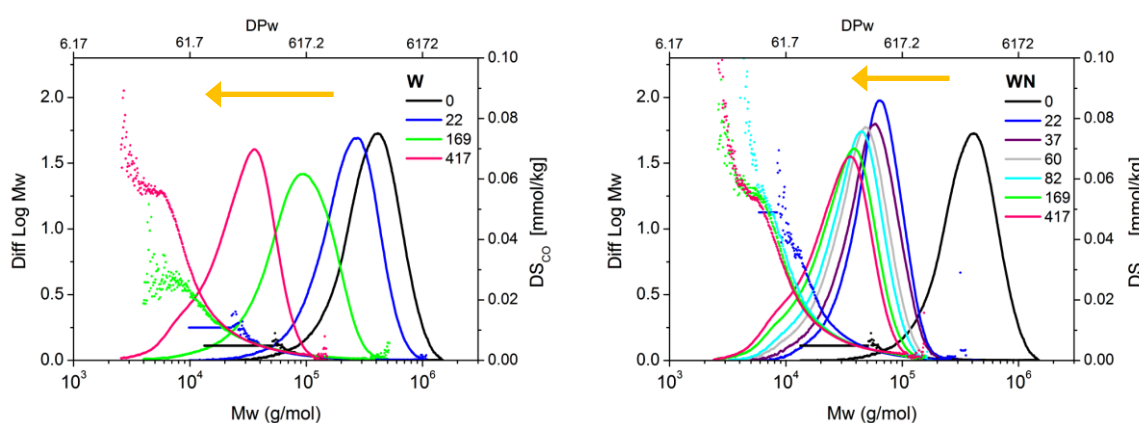
8.1.1 Unsized samples

The degree of polymerisation as well as the scissions per chain values of all unsized samples calculated from viscometry and SEC are reported in table 8.1. They evidently suggest that the artificial aging in closed vials of unsized papers caused the expected degradation of the cellulosic substrate (i.e. an increase in the number of chain scissions S corresponding to a decrease in the DP values).

Ageing time (days)	Size-Exclusion Chromatography					Viscometry	
	DPn	DPw	Sn	Sw	pDI	DPv	Sv
W							
0	1794	2527	0	0	1.41	1369	0
6	-	-	-	-	-	1116	0.12
22	1120	1613	0.55	0.57	1.44	1067	0.28
37	-	-	-	-	-	891	0.54
169	700	1093	1.56	1.93	1.56	531	1.42
417	203	305	7.84	8.95	1.51	414	5.62
LODP	540	541	2.32	3.67	1.00	172	6.96
WN							
0	1794	2527	0	0	1.41	1369	0
6	-	-	-	-	-	661	1.07
22	306	404	4.86	5.25	1.32	-	-
37	258	361	5.96	5.99	1.39	378	2.62
60	189	278	8.48	8.09	1.47	342	3.01
82	180	259	8.97	8.91	1.44	285	3.81
169	141	217	11.76	10.35	1.54	245	4.25
417	124	194	13.46	11.84	1.56	205	5.62
W3							
0	1794	2527	0	0	1.41	1369	0
6	-	-	-	-	-	736	0.86
37	260	356	5.89	6.11	1.37	436	2.14
60	-	-	-	-	-	362	2.78

82	157	237	10.43	9.76	1.51	304	3.51
169	131	203	12.73	11.31	1.55	270	3.76
417	114	179	14.81	12.54	1.57	210	5.47
W4							
0	1794	2527	0	0	1.41	1369	0
6	-	-	-	-	-	784	0.75
22	179	233	9.01	9.85	1.31	-	-
37	115	172	14.61	13.67	1.49	429	2.19
169	109	185	15.41	12.66	1.69	184	5.63
417	147	225	11.18	10.22	1.53	173	6.85

Tab. 8. 1 – Viscosity-, number- and weight-average degrees of polymerisation (DPv, DPn and DPw, respectively) and corresponding scissions per chain values of all unsized samples at different aging times (in days). Degrees of polymerisation and corresponding scissions per chains values related to SEC analyses (DPn and DPw, Sn and Sw) have been calculated as stated in Cap. 7.3.2.7. All values are presented according to samples acronyms defined: W, pure cellulose without sizing nor iron-gall inks; WN, W3 and W4, pure cellulose without sizing treated with inkN, ink3 and ink4, respectively.

In order to ascertain the effect of the aging process, changes in the degradation pattern are evaluated. Figure 8.2. depicts the MWD (continuous lines) and the $DS_{C=O}$, the degree of substitution of carbonyl groups profiles (dots), of all unsized samples during accelerated aging.
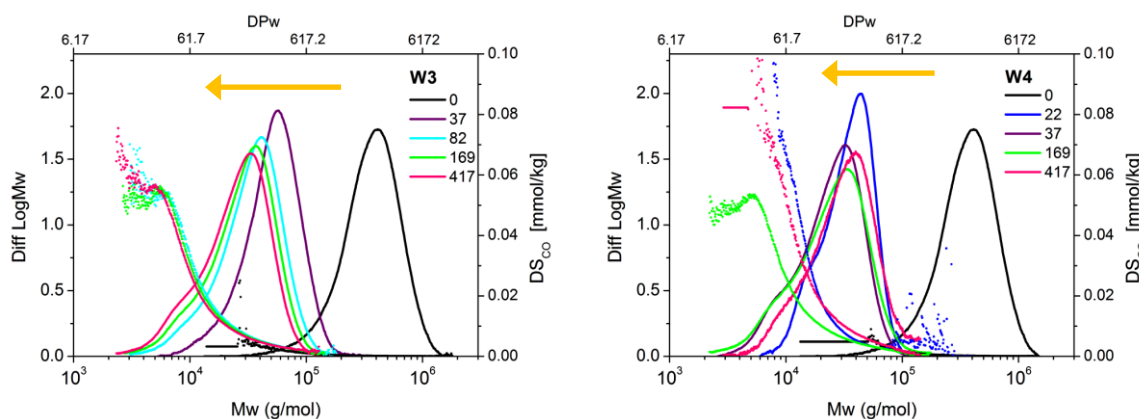
Fig. 8. 2 – The molecular weight distribution (MWD) and the degree of carbonyl groups substitution (DS$_{CO}$) of unsized samples depending on the time of accelerated aging. Top left: reference sample of pure cellulose (W).

The molecular weight distribution. The left shifting of the MWD curves (Fig. 8.2, yellow arrows) of all unsized samples towards lower MM values indicates that changes due to degradation in closed system have occurred. Noticeable differences characterized the inked papers and the reference sample (W).

Pure cellulose (W, fig. 8.2, top left) exhibits a gradual left-shift with increasing aging time. In fact, after 22 days of aging (blue curve) the distribution slightly shifts with a negligible decrease in height and width (no substantial variation of polydispersity). Conversely, inked samples display a greater reduction of cellulose chains length as a significant shift of MWD is evident even after 22 days of treatment. When the severity of the conditions is taken into account a broadening of distributions of all samples are evident (increased values of polydispersity, Fig. 8.3) and some signs of accumulation appear as indicated by the arising shoulder on the low-Mw side (left side of distributions). This probably indicates the presence of cellulose oligomers owing to degradation, as was suggested by Stephens et al. (2008). Moreover, the amount of such oligomers increases with aging time as shown by the higher intensity of the shoulder of long-aged samples. Consequently, the main peak undergoes a decrease in height as the amount of related molecules is reduced.

However, samples influenced by the presence of ink 4 (W4, fig. 8.2, below right) shows a slighter MWD decrease compared to other iron-gall-ink-treated samples. Ink 4 probably early on produces a greater amount of degrading species which severely degrade the substrate within few days of artificial treatment. Regarding the longest-time aged W4 (the pink curve in Fig. 8.2, below right), its out-of-trend behaviour could be related to probable aggregation phenomena of highly degraded fragments.
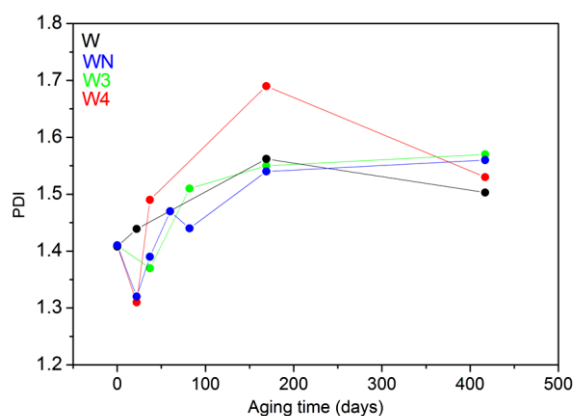
Fig. 8. 3 – The polydispersity index (PDI) of unsized samples depending on the time of accelerated aging. Black dots and line: the reference sample of pure cellulose (W); blue, green and red dots and lines: unsized cellulose treated with ink N, 3 and 4, respectively.

The degree of substitution of carbonyl groups profiles. SEC analyses coupled to the CCOA labelling technique, have been used even to ascertain if oxidative degradation had occurred. The carbonyl groups profiles (Figure 8.2, dotted distributions) indicate a clear superposition of oxidation and hydrolysis for all unsized samples. Prolonged degradation times lead to greater degrees of C=O substitution (fig. 8.2, green and pink DS_{CO} profiles, corresponding to 169 and 417 days of artificial aging). Moreover, the carbonyl-functionalities content is mainly detected in the low-Mw fragments (low molecular weight region on the left side of distributions), as a consequence of cellulose degradation.

Moreover, the total amount of carbonyl as well as carboxyl groups have been obtained through GPC investigations. Data of oxidized functionalities for all unsized samples are reported in table 8.2.

Oxidized groups (mmol/100g)*	Aging time (days)	UNSIZED SAMPLES			
		W	WN	W3	W4
CO	0	0.188	0.188	0.188	0.188
	22	0.48	3.329	*n.a.*	9.554
	82	*n.a.*	5.575	6.483	8.343
	169	1.125	7.057	7.531	8.219
	417	2.55	7.9	8.381	9.827

COOH	82	n.a.	0.463	0.472	0.422
	169	0.421	0.253	0.485	0.455
	417	0.482	0.589	0.517	0.589

Tab. 8. 2 – Total amount of oxidized groups for unsized samples at different aging times (in days). n.a, data not available.

FDAM-GPC analyses had been performed just to some of the available samples and they revealed a negligible amount of carboxyl moieties. Thus, no further FDAM labelling have been carried out and contribution of carboxyl groups is hereafter excluded in the evaluation of the oxidative process. Conversely, an overall increase of carbonyl moieties along with aging time for all samples is evident. Pure cellulose (W) exhibits a mild raise in C=O groups whereas if iron-gall inks were applied, the total number of carbonyl groups increased more drastically. However, such results alone does not allow to state if an oxidative mechanism have occurred. As stated by Whitmore and Bogaard (1995), hydrolysis of cellulose should produce one new carbonyl per scission as the aldehyde group at the new reducing end formed due to the chain cleavage. Thus, correlating chain scissions to the amount of carbonyl groups a best-fit slope of data around 1 should suggest a pure hydrolytic mechanism. Conversely, higher values imply that oxidative reactions occured and carbonyl groups formed also along the cellulose chains.

Figure 8.4. reports this correlation plot for unsized samples under investigation. Slopes of the best-fit lines to the data were determined by linear regression and the reported dashed line on the graph represents one carbonyl produced per chain scission.
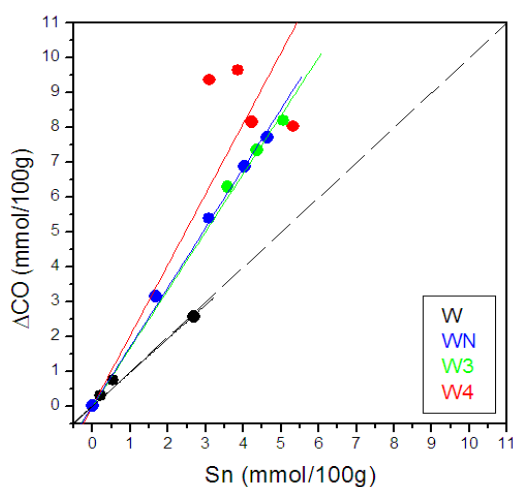
Among all available scissions per chain values (Sn, Sw and Sv), the number-averages S has been chosen in order to assure a methodological coherence. Slopes of the best-fit lines to the experimental data indicate the production of

- 0.97 ± 0.05 (W)
- 1.71 ± 0.03 (WN)
- 1.67 ± 0.03 (W3)
- 2.03 ± 0.27 (W4)

carbonyls per chain scission. This suggests pure whatman (W) has substantially undergone an hydrolytic degradation whereas inked samples have been affected both by hydrolysis and oxidation. Moreover, despite the scattering data, W4 seems having suffered a greater oxidation than W3 and WN.

In order to clarify the oxidation pathway along with aging time, a kinetic description of the process have been carried out. According to data trends, some assumption should firstly be made

- for pure cellulose, few data are available thus limiting a proper kinetic study.
- the formation of oxidized groups follows a first order rate law
- for inked samples two reaction mechanisms probably occurred, a faster and a slower one.

Thus, oxidative degradation of reference samples (W) has been modelled with the following pseudo-zero order equation

$$[\Delta CO] = k_{app} \cdot t \qquad \qquad 8.1$$

where $k_{app} = [CO]_\infty \cdot k_o$.

On the other hand, inked samples oxidation kinetics has been modelled according to the first-order equation 8.2

$$[\Delta CO] = [CO]_\infty \,(1 - e^{-\,k_o\, t}) + J_o \cdot k_{jo} \cdot t \qquad \qquad 8.2$$

where $[CO]_1$ is the asymptotic value of the first reaction and represents the amount of carbonyl groups formed during the faster oxidation according to k_o rate constant.

The slower mechanism (represented by the second term of eq. 8.2) is unknown and should be approximated. As a first order kinetics has been previously supposed, the linear term of MacLaurin series development should be consider a good estimation of the first stage of the unknown reaction. J remains undefined but kinetic parameters of unsized samples can be compared in terms of $[CO]_1$, k_1 and J (for inked samples). The kinetic study of the carbonyl content of unsized samples according to equations 8.1 and 8.2 is presented in figure 8.5.
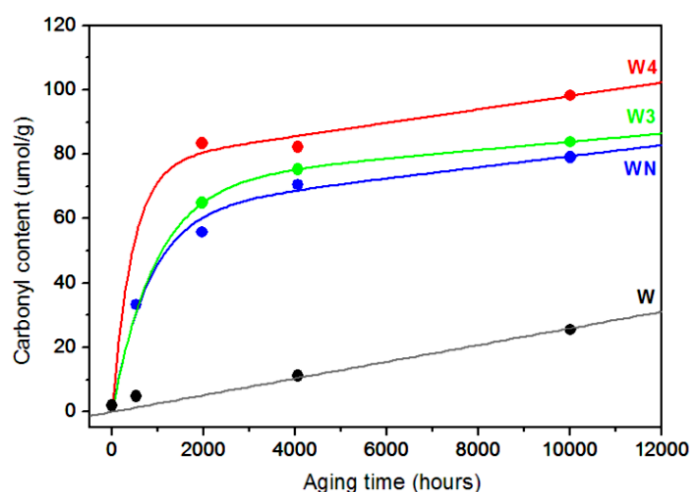

Fig. 8. 5 – Kinetic models defined in equations 8.1 (pure cellulose, W) and 8.2 (inked samples WN, W3 and W4) applied to the carbonyl content data of unsized samples. Circles: experimental data; Lines: best fit.

Kinetic parameters of carbonyl groups formation upon artificial aging of unsized samples in closed vessels are summarised in table 8.3.

CO Kinetic parameters	UNSIZED SAMPLES			
	W	WN	W3	W4
$[CO]_1$ *(umol/g)*	-	62.16	71.12	77.2
k_o *(days^{-1})*	-	3.00 E-02	2.53 E-02	5.47 E-02
$k_{app} = [CO]_1 \cdot k_1$ *(days^{-1})*	1 E-04	1.86	1.80	4.22
J_o *(umol/g)*	-	1.61	1.38	1.82
k_{jo} *(days^{-1})*	-	2.53 E-02	2.19 E-02	2.76 E-02

Tab. 8. 3 – Kinetic parameters of carbonyl groups formation during artificial aging of all unsized samples, as determined by Eq. 8.1 and 8.2.

The comparison between the kinetic parameters obtained, reveals that the presence of iron-gall inks sensibly increases the total amount of carbonyl groups from the first steps of degradation (cf. [CO]1). The apparent rate constant (k_{app}) of carbonyl formation owing to the fastest oxidative reaction is thirty times faster for W3 and WN that compared to the reference paper W. Ink 4, indeed, exhibits an even stronger induced-oxidation as the estimated rate of W4 degradation is more than seventy times higher than pure cellulose and slightly higher than other inks.

Regarding the slowest reaction, analogous contribution is shown for all inked samples considering both the amount and the rate of carbonyl formation.

Additional considerations upon oxidation can be given by also considering changes in optical properties of papers owing to the aging process. It has been shown (Calvini et al. 1996) that carbonyl moieties formation generally leads to yellowing and browning phenomena. Thus, kinetic studies of C=O development and colour changes along with aging time are hereafter compared in order to evaluate possible correlation. The kinetic of yellowing has been modelled on ΔE parameter according to assumptions and kinetics of carbonyl contents described above.

Thus, the following equations have been used:

- pure cellulose reference paper (W)

$$[\Delta E] = k'_{app} \cdot t \qquad\qquad 8.3$$

where $k'_{app} = [\Delta E]_\infty \cdot k_e$.

- inked samples

$$[\Delta E] = [\Delta E]_\infty (1 - e^{-k_e t}) + J_e \cdot k_{je} \cdot t \qquad\qquad 8.4$$

where $[\Delta E]_1$ and k_e are the kinetic parameters describing the fastest reaction whereas the slower mechanism is unknown, thus approximated (MacLaurin developments linear term) , and characterised by J_e and k_{je} parameters.

ΔE has been chosen as monitoring parameter as it includes the contribution of all significant colour variables (L*, a*, b*) that sensibly changed during the performed aging process. The kinetic trends and parameters evaluated according to equations 8.3 and 8.4 is presented in figure 8.6 and table 8.4, respectively.
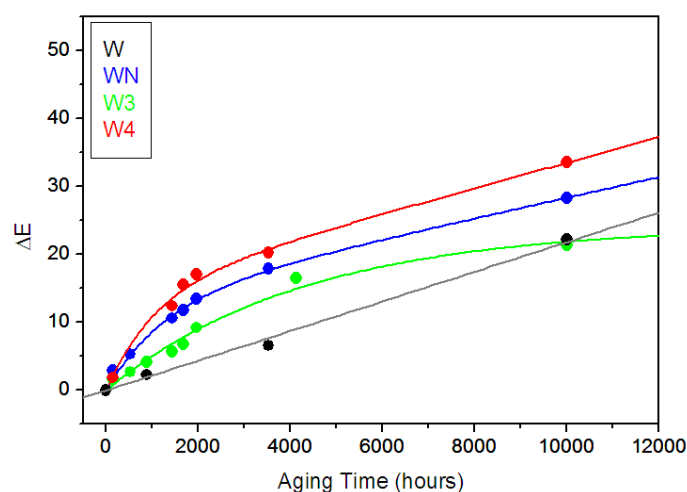
Fig. 8. 6 – Kinetic models defined in equations 8.3 (pure cellulose, W) and 8.4 (inked samples WN, W3 and W4) applied to the study of yellowing of unsized samples (colorimetric data not reported).

Kinetic parameters of colour changing of unsized samples are summarised in table 8.4.

ΔE Kinetic parameters	UNSIZED SAMPLES			
	W	WN	W3	W4
$[ΔE]_1$	-	13.11	24.16	14.66
k_e *(days^{-1})*	-	1.84 E-02	5.76 E-03	2.25 E-02
$k'_{app} = [ΔE]_1 \cdot k_e$ *(days^{-1})*	9.0 E-05	0.24	0.14	0.33
J_e *(umol/g)*	-	1.65	3.9 E-07	3.1
k_{je} *(days^{-1})*	-	2.19 E-02	5.30 E-09	1.44 E-02

Tab. 8. 4 – Kinetic parameters of discoloration process occurred during artificial aging of all unsized samples, as determined by Eq. 8.3 and 8.4.

As far as the aging time increases, the yellowing of samples likewise increases even though an overall mild colour change occurred owing to artificial aging. ΔE kinetic parameters shows just a strong positive feedback of iron-gall inks on cellulosic substrate. In fact, regarding ink samples, the apparent rate constant (k'_{app}) owing to the fastest oxidative reaction is several order of magnitude greater than compared to the pure cellulose.

Nevertheless, a cross comparison of the apparent rate constants owing to browning and oxidation reveals that no considerable difference is detected for pure cellulose ($k_{app} \approx k'_{app}$). Conversely, ink-induced oxidation is more significant and proceeds about

ten times faster than corresponding sample yellowing. Hence, this most likely indicates that not all formed carbonyls functionalities contribute to the yellowing of samples which seems having a minor effect on cellulose related to oxidation.
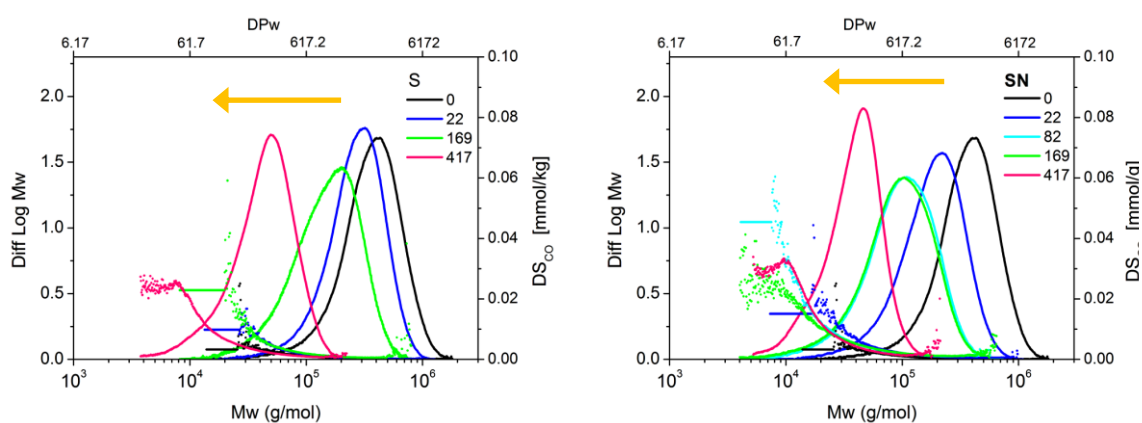
8.1.2 Sized samples

The degree of polymerisation and the scissions per chain values of all sized samples calculated from viscometry and SEC are reported in table 8.5. They reveal the expected degradation of the cellulosic substrate with a decrease in the DP values and a consequent increase in the number of chain scissions S, in agreement with unsized samples behaviour.

Ageing time (days)	Size-Exclusion Chromatography					Viscometry	
	DPn	DPw	Sn	Sw	pDI	DPv	Sv
S							
0	2564	1306	0.00	0.00	1.47	1306	0.00
22	1860	1138	0.31	0.38	1.40	1143	0.15
169	620	614	3.67	3.13	1.66	614	1.13
417	196	310	12.70	12.06	1.54	310	3.21
LODP	-	-	-	-	-	172	6.59
SN							
0	1748	2564	0.00	0.00	1.47	1306	0.00
22	1120	1613	0.56	0.59	1.44	986	0.32
37	662	1018	1.64	1.52	1.54	776	0.68
82	447	724	2.91	2.54	1.62	637	1.05
169	398	690	3.39	2.72	1.73	593	1.52
417	191	264	8.17	8.70	1.39	244	3.68

S3							
0	1748	2564	0.00	0.00	1.47	1306	0.00
22	1131	1615	0.55	0.59	1.43	1094	0.19
82	676	1025	1.59	1.50	1.52	738	0.77
169	514	888	2.40	1.89	1.73	689	1.67
417	196	251	7.91	9.21	1.28	277	3.71
S4							
0	1748	2564	0.00	0.00	1.47	1306	0.00
22	872	1339	1.01	0.92	1.54	1109	0.18
82	667	1041	1.62	1.46	1.56	782	0.67
169	415	825	3.21	2.11	1.99	712	1.01
417	129	220	12.52	10.68	1.70	267	3.89

Tab. 8. 5 – Viscosity-, number- and weight-average degrees of polymerisation (DPv, DPn and DPw, respectively) and corresponding scissions per chain values of all sized samples at different aging times (in days). Degrees of polymerisation and corresponding scissions per chains values related to SEC analyses (DPn and DPw, Sn and Sw) have been calculated as stated in Cap. 7.3.2.7. All values are presented according to samples acronyms defined: S, Whatman paper treated with gelatine sizing; SN, S3 and S4, Whatman papers treated with gelatine sizing and inkN, ink3 and ink4, respectively.

The molecular weight distribution MWD (continuous lines) and the $DS_{C=O}$, the degree of substitution of carbonyl groups profiles (dots) of all sized samples during accelerated aging are reported in figure 8.7.
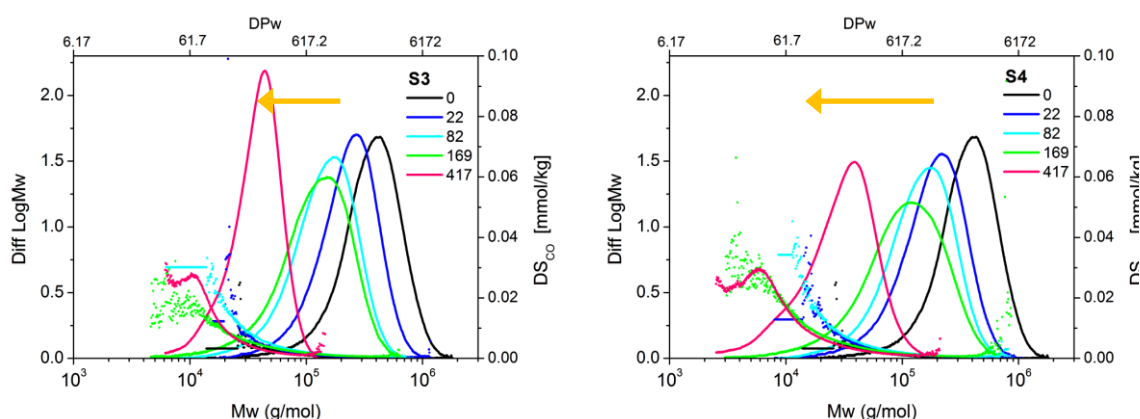
Fig. 8. 7 − The molecular weight distribution (MWD) and the degree of carbonyl groups substitution (DS$_{CO}$) of sized samples depending on the time of accelerated aging.

The molecular weight distribution. The increased aging time weakly affects the MWD of sized samples as a gradual shifts to lower Mw (fig. 8.7, yellow arrows) is observed together with a reduction in peaks' height. The broadening of distributions with increasing degradation gives evidence of a greater polydispersity of all samples as confirmed by raising values of PDI (fig. 8.8). These observations suggest a modest loss of high Mw components of cellulose as a consequence of induced degradation. Moreover, signs of accumulation of lower Mw products (revealed by the shoulder on the left side of distributions, fig. 8.7) are barely visible just for the longest-aged samples (pink curves).

On the whole, sized samples have been subjected to significantly lower degradation than unsized one's. This could be suggestive of a protecting effect of gelatine sizing against degradation.
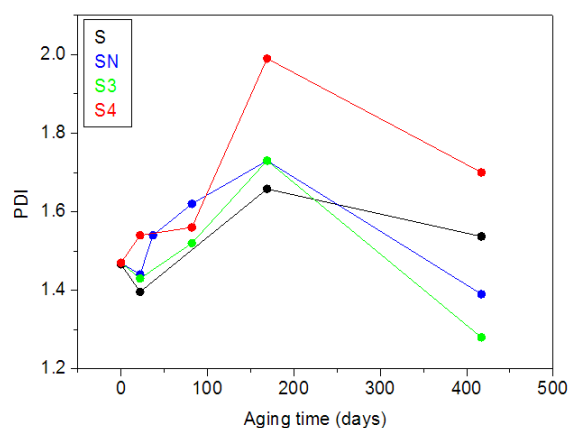

Fig. 8. 8 − The polydispersity index (PDI) of sized samples depending on the time of accelerated aging. Black dots and line: sized Whatman paper (S); blue, green and red dots and lines: sized cellulose treated with ink N, 3 and 4, respectively.

The degree of substitution of carbonyl groups profiles. Carbonyl profiles analysis shows that oxidized groups affected the low molecular weight fractions (left side of distributions) and their amount just slightly increases with aging. Generally, a visible growth of oxidized moieties are detectable after just 22 (blue profiles) and 82 (cyan profiles) days of aging, even though no considerable further changes occur after almost 420 (pink profiles).

The total amount of carbonyl as well as carboxyl groups have been also evaluated. Data of oxidized functionalities for all sized samples are reported in table 8.6.

Oxidized groups (mmol/100g)	Aging time (days)	SIZED SAMPLES			
		S	SN	S3	S4
CO	0	0.180	0.180	0.180	0.180
	22	0.406	0.488	0.498	0.687
	82	*n.a.*	2.021	1.193	1.216
	169	2.071	2.071	1.347	1.632
	417	7.772	4.503	3.384	4.195
COOH	82	*n.a.*	0.934	0.761	1.219
	169	0.844	1.833	1.153	0.859
	417	1.122	1.355	1.541	1.517

Tab. 8. 6 – *Total amount of oxidized groups for sized samples at different aging times (in days). n.a, data not available.*

As previously underlined for unsized samples, reported data show just a slight increase of carboxyl groups, thus being considered negligible in the evaluation of the oxidative process. On the other hand, an overall increase of carbonyl moieties along with aging time for all sized samples is evident.

Similarly to previously reported studies on the oxidative processes occurred to unsized samples, even sized papers have been further investigated through

- the correlation between the number-average chain scissions and the amount of carbonyl groups

- the kinetic analysis of both oxidized functionalities and the discoloration development with time.

The correlation plot between Sn and the carbonyl content (fig. 8.9) exhibits unexpected data trends.
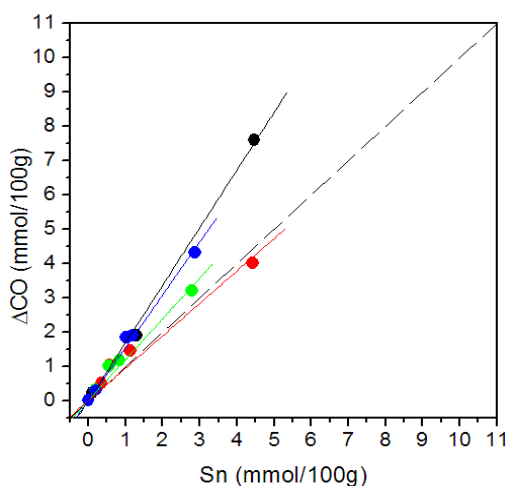

Fig. 8. 9 – The correlation plot of carbonyl groups to the number-average chain scissions (both expressed in the same units of measure, mmol/100g of cellulose) for all sized samples along with aging time. The dashed line represents one carbonyl produced per scission.

According to the best-fit lines, obtained slope values indicate the production of
- 1.68 ± 0.04 (S)
- 1.54 ± 0.04 (SN)
- 1.19 ± 0.07 (S3)
- 0.95 ± 0.07 (S4)

carbonyls per chain scission.

These data might suggest that sized Whatman without inks (S) and sized samples with ink N (SN) and 3 (S3) have been affected both by hydrolysis and some oxidation whereas sized samples with ink4 (S4) has mainly being subjected to an hydrolytic degradation. However, this could be seen as an anomalous behaviour. There is no reason to think that S trend should be different from W one, as none of these samples should be subjected to the degrading influence of oxidizing agents. Moreover, iron-gall inks should even increase oxidation, as stated for unsized papers. Something went wrong with sized papers analyses and merits further studies.

Nevertheless, it could be possible that gelatine sizing has to some unknown extent interfered during the labelling procedure thus being functionalised. Additionally, if

VOCs emitted by inks during aging degraded the gelatine oxidized moieties, a reduction of interference would occur, thus resulting in lower carbonyl contents with increasing degrading power of ink-emitted species.

The kinetic analysis of both oxidized functionalities and discoloration development with time is following reported.

As far as oxidation is concerned, all data have been modelled according to eq. 8.1 and 8.2. Modelled kinetic curves of the carbonyl content of sized samples is presented in figure 8.10 whereas the kinetic parameters obatined are summarised in table 8.7.
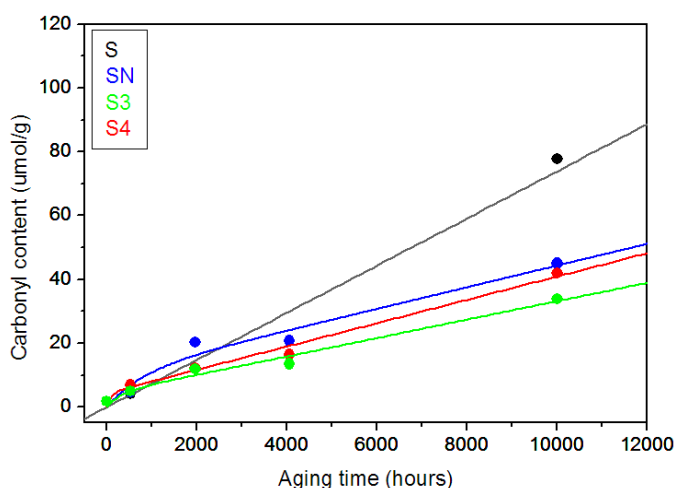
Fig. 8. 10 - Kinetic models defined in equations 8.1 and 8.2 applied to the carbonyl content data of sized samples.

CO kinetic parameters	SIZED SAMPLES			
	S	SN	S3	S4
$[CO]_1$ (umol/g)	-	10.35	4.31	4.36
k_o (days^{-1})	-	3.1 E-02	7.5 E-02	0.25
$k_{app} = [CO]_1 \cdot k_1$ (days^{-1})	3.1 E-04	0.31	0.32	1.6
J_o (umol/g)	-	1.22	1.12	3.82
k_{jo} (days^{-1})	-	6.7 E-02	6.3 E-02	0.23

Tab. 8. 7 - Kinetic parameters of carbonyl groups formation during artificial aging of sized samples, as determined by Eq. 8.1 and 8.2.

Accordingly to what was observed for unsized samples, sized paper without inks (S) exhibits lower apparent rate constant (k_{app}) than samples where inks. Among all, ink4 induces a faster oxidation as its estimated rate constant is several times higher than sized cellulose.

Regarding the slowest reaction, an analogous slight contribution to the overall oxidation process is shown for ink N and 3.

With regard to the optical properties of sized papers, the kinetic trends and the related parameters have been evaluated according to equations 8.3 and 8.4, thus presented in figure 8.11 and table 8.8, respectively.
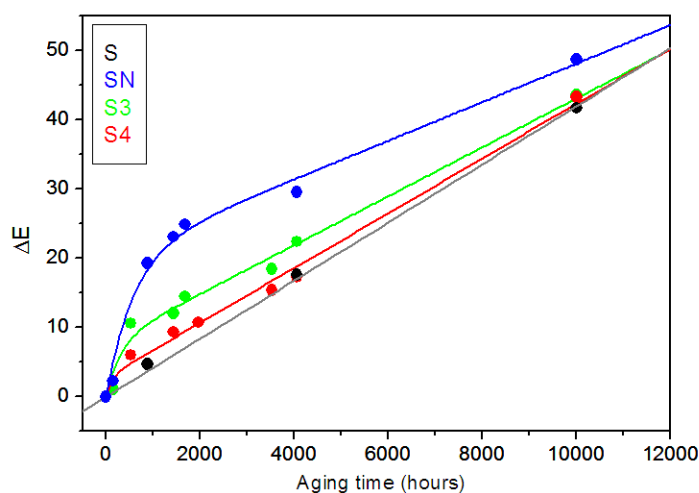
Fig. 8. 11 - Kinetic models defined in equations 8.3 and 8.4 applied to the study of ΔE data of sized samples (colorimetric data not reported).

ΔE kinetic parameters	SIZED SAMPLES			
	S	SN	S3	S4
$[\Delta E]_1$	-	20.26	7.78	2.78
k_e *(days^{-1})*	-	0.04	0.08	0.19
$k'_{app} = [\Delta E]_1 \cdot k_e$ *(days^{-1})*	1.7 E-04	0.83	0.62	0.51
J_e *(umol/g)*	-	3.73	4.21	4.44
k_{je} *(days^{-1})*	-	0.02	0.02	0.02

Tab. 8. 8 - Kinetic parameters of colour changes occurred during artificial aging to sized samples, as determined by Eq. 8.3 and 8.4.

Sized samples display a strong variation in colour even within the first steps of degradation. However, this could be probably attributed to yellowing phenomena occurred to the sizing layer. Colorimetric analyses are substantially related to a surface property of the material and it is worth knowing that gelatine become strongly yellow due to degradation. ΔE kinetic parameters shows just a considerable positive feedback of iron-gall inks on cellulosic substrate darkening. In fact, regarding ink samples, the apparent rate constant (k'_{app}) owing to the fastest oxidative reaction is significantly higher than sized sample without inks.

Nevertheless, a cross comparison of apparent rate constants owing to colour changes and oxidation reveals that a slight difference is detected for pure cellulose ($k_{app} \approx k'_{app}$). Conversely, ink-induced yellowing of the support is more significant than oxidation, in disagreement with observation done for unsized papers. This is presumably related to a side-effect of surface sizing coating.

8.2. KINETICS OF DEGRADATION

In order to shed some light on the degradation mechanism of iron-gall-ink-induced degradation on cellulose in closed systems, a long-lasting kinetic studies has been carried out. The kinetic model here presented has been chosen after several kinetic approaches had been applied to the experimental data.

The proposed model combines an autocatalytic sigmoidal equation and a first order expression, and it is represented by the equation

$$S = n_v \left(1 - e^{-k_v t} \right) + \frac{h° \, n \, \left(1 - e^{-k \, (h° + \, \alpha \, n) \, t} \right)}{h° + \, \alpha \, n \, e^{-k \, (h° + \, \alpha \, n) \, t}} \qquad \qquad 8.5$$

n_v and k_v define the contribution of the first order kinetic representing the degradation of cellulose induced by the emission of volatile compounds from inks. $h°$, n, k and α are the autocatalytic mechanism parameters, where $h°$ represents the initial acidity of the system, n the amount of scissile units affected by autocatalytic degradation, k the rate constant of the autocatalysis (hydrolysis) and α the excess of produced acidity.

The results (lines) of the curve fitting exercise based on the kinetic model defined by equation 8.5 are shown in figure 8.12 and 8.13 for unsized and sized samples, respectively.
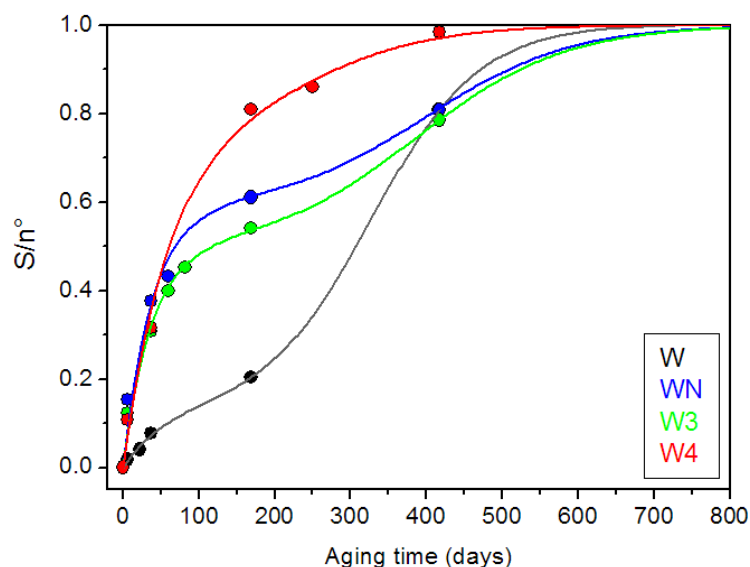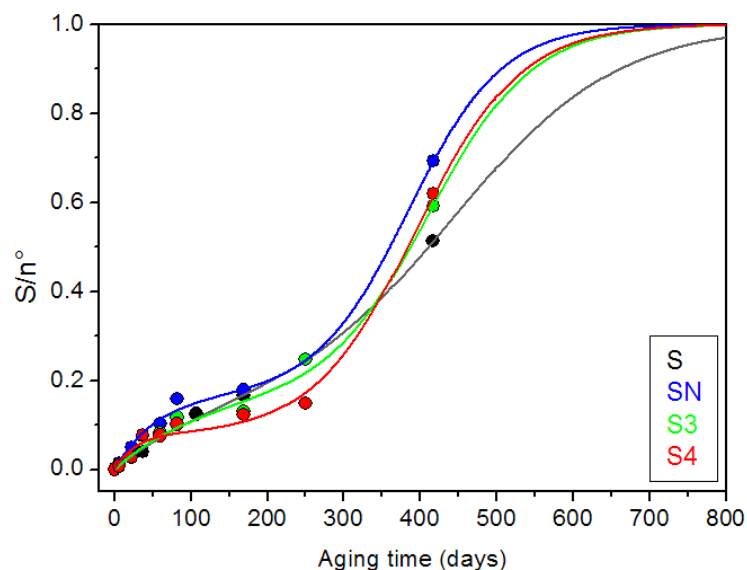

Fig. 8. 12 - Unsized samples. Normalised plot (S/n°) of the proposed model according to eq. 8.5. S: scissions per chain (DP°/DP − 1); n°: glycosidic bonds per chain in the amorphous regions (n° = DP°/LODP − 1). Circles: experimental data; lines: best fit with Eq.8.5.

Fig. 8. 13 - Sized samples. Normalised plot (S/n°) of the proposed model according to eq. 8.5. S: scissions per chain (DP°/DP − 1); n°: glycosidic bonds per chain in the amorphous regions (n° = DP°/LODP − 1). Circles: experimental data; lines: best fit with Eq.8.5.

The application of this model to the samples under investigation on the present study has been based on some considerations upon obtained viscometric data. It is worth noting that the autocatalysis is a positive feedback reaction of cellulose as such and is not due to ink-emitted VOCs. The volatile species released by iron-gall inks deform the autocatalytic shape by adding more acidity than the self-produced by cellulose. Thus, the autocatalytic curve degenerate resulting in an apparently autoretardant or even linear shape.

In fact, data plot suggests that iron gall inks release degrading VOCs (both acids and oxidizing species) in a very short time, compared to the whole aging process. In particular, the emission might be better described by two simultaneous emissive processes: a fast release of acidic species (that consequently leads to high values of h°) and a slower release of oxidizing compounds. These conceivably mask the autocatalysis of cellulose during the initial steps of degradation.

Bearing in mind what stated above, the kinetic model for the first steps of degradation should therefore correspond to the sum of two first-order equations with significant differences in the rate constant in order to model the fastest as well as the slowest process. Unfortunately, the complexity of the proposed kinetics is hardly modelling. A first approximation to describe the additive contribution of the released

VOCs (both acidic and oxidant) can be done by considering just a first order reaction, thus using a first order equation added to the autocatalytic one of cellulose[12].

However, the emission of VOCs seems to decrease after almost 80 days and the autocatalytic S-shaped degradation of cellulose becomes evident. The noticeable slowdown of volatile species release after 4000 hours of aging could be ascribed to some kind of "deactivation" or degradation phenomena of emitted compounds. However, VOCs-catalysed reactions could even be hypothesized as the degradation mechanism induced by iron-gall inks, thus supposing a decrease in their catalysing power upon with time.

Anyway, without specific analyses of emitted species in the investigated systems along with degradation, no definitive explanation can be given and further investigation should be necessary.

As far as sized samples are concerned, it is hypothesised that gelatine sizing should prevent cellulosic fibres from degradation induced by inks. Thus, a sigmoid-shaped autocatalytic mechanism of degradation is expected for all sized samples, eventually slightly modified if inked samples are considered.

The proposed mechanism has been tested through viscometric analyses and kinetic parameters obtained are reported in table 8.9 and 8.10 for unsized and sized samples, respectively. As previously stated (Cap. 6.1.1), in order to minimise the effect of polydispersity, the number of scissions per chain (i.e., $S=DP_v°/DP_v-1$: Calvini et al. 2008) has been utilised.

---

[12] A preliminary test using two first-order equations to describe the initial stage of degradation shows a substantially negligible contribution of the slowest process (k1=2000 e k2=0.02). Hence, in first instance the approximation with a single first order kinetic equation could be accepted

UNSIZED SAMPLES.

	Kinetic Parameters	W	WN	W3	W4
Ac	k_a *(days^{-1})*	0.0036	0.0037	0.0031	0.009
	$h°$	0.0051	0.043	0.065	0.075
	n_a	5.41	2.84	3.47	1.23
Fo	n_v	1.55	4.12	3.49	5.73
	k_v *(days^{-1})*	0.011	0.026	0.026	0.015
	$n_a + n_v = n°$	6.96	6.96	6.96	6.96
	$h°/ (n_a + n_v)$	7.3 E-04	6.2 E-03	9.3 E-03	1.1 E-02
	ratio $h°$	1	8.4	12.7	14.7

Tab. 8. 9 - Kinetic parameters of unsized samples determined through eq. 8.5. Ac: autocatalytic kinetic parameters; k_a: autocatalytic hydrolysis rate constant; $h°$: the initial acidity; n_a: contribution of the autocatalytic reaction. Fo: first-order kinetic parameters; n_v: contribution of the first order reaction; k_v: first order reaction rate constant.

Kinetic parameters obtained through the best fits with eq. 8.5 are following discussed in order to understand the degradation mechanism of sized samples.

- **n_v , contribution of ink-emitted VOCs on cellulose degradation**. Iron-gall inks show a greater contribution of the first order reaction process than pure cellulose (W). This confirms that inks release degrading volatile species in a very short aging time. Among all, ink 4 exhibits the highest n_v value, nearly equal to the calculated asymptotic value of the amorphous phase degradation ($n°$, corresponding to the levelling-off DP). This suggests that ink 4 emits great amount of degrading species thus leading to a strong acidity of the system.

- **k_v , paper degradation rate due to the presence of VOCs.** The presence of iro-gall inks significantly causes an increase of paper degradation as inked papers show higher k_v values than reference sample. Particularly, emitted VOCs from ink N and 3 barely doubled the degradation rate of pure cellulose (W). Regarding ink 4, it reveals an anomalous behaviour as released volatiles does not substantially influenced cellulose rate degradation.

- **n_a , contribution of autocatalysis.** Pure cellulose (W) quite obviously shows a greater amount of bond subjected to an autocatalytic degradation as no degrading species are present in the system. On the contrary, lower n_a values for inked samples suggest a slighter autocatalytic contribution. In particular, as far as ink4 is concerned, the autocatalysis of cellulose seems to be almost masked by the first-order-emission reaction or better, it is most likely that the autocatalysis strongly degenerate due to the high acidity introduced by ink4. This hypothesis might be corroborated by the highest ka values exhibits by W4 compared to all other samples.

- **ratio h°, surplus of degrading species emitted by the inks from the early stages of aging compared with the intrinsic amount of VOCs produced by cellulose itself.** Inked papers produce about 10 times higher amount of degrading compounds than pure cellulose. Among all, ink 4 shows the greatest surplus of emitted VOCs compared to the other inks.

SIZED SAMPLES.

	Kinetic Parameters	S	SN	S3	S4
A **c**	k_a *(days^{-1})*	1.5 E-03	2.9 E-03	2.7 E-03	2.4 E-03
	h°	0.098	0.01	0.012	0.018
	n_a	5.63	5.50	5.48	6.08
F **o**	n_v	0.96	1.09	1.11	0.51
	k_v *(days^{-1})*	9.5 E-03	1.9 E-02	9.2 E-03	3.7 E-02
	$n_a + n_v = n°$	6.59	6.59	6.59	6.59
	$h°/ (n_a + n_v)$	1.49E-02	1.52E-03	1.82E-03	2.73E-03
	ratio h°	1	2.1	2.5	3.7

Tab 8. 10 - Kinetic parameters of sized samples determined through eq. 8.5. Ac: autocatalytic kinetic parameters; k_a: autocatalytic hydrolysis rate constant; h°: the initial acidity; n_a: contribution of the autocatalytic reaction. Fo: first-order kinetic parameters; n_v: contribution of the first order reaction; k_v: first order reaction rate constant.

Kinetic parameters obtained through the best fits with eq. 8.5 of sized samples substantially confirm the limiting effect of sizing on cellulose degradation. In fact, the presence of the sizing layer over the fibres conceivably reduces the interaction of degrading species with the above cellulose (cf. n_v), thus having a tiny influence on degradation rate of the support (cf. k_v). Moreover, h° ratio of sized samples are sensibly lower than corresponding unsized paper corroborating the hypothesis that the negative effect of additional degrading compounds emitted by inks is strongly limited by sizing. Finally, the n_a value are close to the amount of overall scissile units present (n°). This is suggestive of the fact that the autocatalysis is quite the dominant degradation mechanism of sized samples, even if iron-gall inks are present.

9

CONCLUDING REMARKS

The aim of the study was to ascertain the degrading mechanism occurring in real paper, considered as a complex multivariate system. The possibility to carried out a long-lasting aging experiment, never attempted before, allowed a valuable insight on degradation kinetics of cellulose. Moreover, the influence of gelatine sizing and iron-gall inks in a closed environment has been for the first time studied in order to characterized the induced degradation of sized and unsized samples, treated with tree different iron gall inks.

To this end, all samples have been mainly characterized through viscometry and size-exclusion chromatography.

Both methods confirm the expected depolymerisation of cellulose occurred due to the aging treatment in sealed vessels. In fact, a decrease in the degrees of polymerisation values (either viscometric- and GPC-averages DP) was observed as well as a broadening and a left-shift of the molecular weight distributions along with aging time. Additionally, the formation of cellulose oligomers owing to long-lasting degradation conceivably reveals a chain-cleavage mechanism affecting all samples.

Nevertheless, unsized samples clearly showed a greater degradation than sized ones, either considering inked and non-inked papers. This confirms a protecting effect of gelatine sizing against degradation thus corroborating the initial hypothesis which has driven the present work.

As far as iron-gall inks effect is concerned, their presence strongly affected samples stability as a intense breakdown of cellulose was evident. Among all inks under investigation, ink 4 induced the most intense degrading effect which could be most likely related to the absence of Arabic gum. The binder, in fact, can act as a degradation-limiting component, in agreement with data found in literature regarding this issue.

GPC analyses proved to be very useful even to explore oxidation processes. In fact, with the exception of pure cellulose, a clear superposition of oxidation and hydrolysis for the all investigated samples was detected, with carbonyl-functionalities mainly affecting the low molecular weight fragments. Kinetic analyses of the oxidation mechanism revealed that for unsized inked samples carbonyl formation owing to aging

is more significant and proceeds about ten times faster than corresponding yellowing. This most likely indicates that not all carbonyl groups contribute to the colour changing. Conversely, sized papers analyses seemed probably being affected by a gelatine interference during labelling procedures and further studies are necessary to unveil the oxidation mechanism.

A further purpose of this research work was to carry out a kinetic study in order to fill the gap of knowledge about the degradation of a multicomponent cellulose-system in closed environments. In fact, no study have been found in literature on the evaluation of sizing- and ink-influenced mechanism of degradation on paper in sealed vessels. Moreover, defined kinetics available in literature have not been already tested nor kinetic equations have been by now modelled on inked-induced breakdown in confined conditions. To this end, a kinetic model has been proposed bearing in mind that the autocatalysis is the most probable mechanism responsible for cellulose degradation in closed vessels. It is worth noting that the autocatalysis is a positive feedback reaction of cellulose as such. However, the results obtained revealed that volatile species released by iron-gall inks during aging deform the autocatalytic shape by adding more acidity than the self-produced by cellulose and thus leading the autocatalytic curve to degenerate.

Moreover, it is most likely that iron gall inks release degrading VOCs (both acids and oxidizing species) in a very short time, compared to the whole aging process, as well as they significantly causes an increase of paper degradation. Pure cellulose (W) quite obviously shows an autocatalytic degradation as no additional degrading species are present in the system. Nevertheless, if iron-gall inks are added (unsized inked samples), kinetics slightly resemble an autocatalysis and the influence of a first order reaction owing to emitted VOCs is predominant.

The investigation of sized samples substantially confirm the preventive effect of sizing on cellulose degradation. In fact, the presence of the sizing layer over the fibres conceivably reduces the self-degradation of cellulose as well as limits the negative effect of additional degrading compounds emitted by inks eventually present. Concluding, the autocatalysis is quite the dominant degradation mechanism of sized samples, even if iron-gall inks are present.

Regarding iron gall inks, it has not been possible to distinguish the degradation effect on the basis of their composition. Further work are necessary in order to properly elucidate this issue.

Nonetheless, the proposed kinetic model conceivably well explained degradation phenomena observed and some of these conclusions can be also confidently applied to other cellulose-based materials.

10

REFERENCES

Adeshives in *Paper Conservation Catalog*, 6th Edition, The Book and Paper Group of the American Institute for Conservation of Historic and Artistic Works. Editorial Board Liaison: Maynor, C., van der Reyden, D., **1989**

Arney, J. S., Jacobs, A. J., Accelerated *aging of paper: the relative importance of atmospheric oxidation*, Tappi 62 (7), 89-91, **1979**

Arney, J. S., Jacobs, A. J., *Newsprint deterioration. The influence of temperature on the relative contribution of oxygen-independent and oxygen-depended processes in the total rate* Tappi 63, 75-77, **1980**

Arney, J. S., Novak, C. L*., Accelerated aging of paper*, TAPPI 65 (3), 113-115, **1982**

ASTM D6819-02e3, *Standard Test Method for Accelerated Temperature Ageing of Printing and Writing Paper by Dry Oven Exposure Apparatus*, **2002**

Atherton, J. B., Hudson, F. L., Hockey, J. A., *The effect of temperature, light and some transitional metal ions on the sorption of sulphur dioxide by paper*, Appl Chem Biotechnol 23, 407-414, **1973**

Auerbach, A. B., El-Kafrawy, A., Snyder, F. W., Turbak, A. F., *Solvent system for cellulose,* US patent No. 4302252, **1981**

Baer, N. S., Indictor, N., *Use of the Arrhenius Equation in Multicomponent Systems* in *Preservation of paper and textiles of historic and artistic value*, Ed. Williams, J. C., Advances in Chemistry Series 164, American Chemical Society, Washington DC, 336-351, **1977**

Banik, G., Stachelberger, H., Messner, K., *Untersuchung der destruktiven Wirkung von Tinten aufSchrifttrdgermaterialie,.* Restauro 94, 302-308, **1988**

Bansa, H., *Accelerated aging of paper: Some ideas on its practical benefit*, Restaurator 23, 106-117, **2002**

Bansa, H., *Accelerated Aging Tests in Conservation Research: Some Ideas for a Future Method*, Restaurator 13 (3), 114-137, **1992**

Bansa, H., Hofer, H.H., *Artificial Aging as a Predictor of Paper's Future Useful Life* Abbey Newsletter Monograph Supplement 1 **1989**

Barański, A., Dziembaj, R., Konieczna–Molenda, A., Łagan, J.M., Walas, S., *On the applicability of Arrhenius equation to accelerated aging tests. The case of alum-impregnated cellulose*, Pol J Chem Technol 6, 1-8, **2004**

Baranski, A., Lagan, J.M., Lojewski, T*., The concept of mixed-control mechanisms and its applicability to paper degradation studies*, e-Preservation Science 3, 1-4, **2006**

Barret, T., *Evaluating the effect of gelatin sizing with regard to the permanence of paper* - Conference Papers Manchester, Institute of Paper Conservation, **1992**

Barrett, T., Mosier, C., *The role of gelatin in paper permanence*, *J Am Inst Cons* 34, No. 3, 173-186, **1995**

Begin, P. L., Kaminska, E., *Thermal Accelerated Ageing Test Method Development,* Restaurator 23, 89-105, **2002**

Berek, D. *Coupled liquid chromatographic techniques for the separation of complex polymers*, Prog Polym Sci 25, 873-908, **2000**

Bicchieri, M., Pepa, S., *The degradation of cellulose with ferric and cupric ions in a low-acid medium*, Restaurator 17, 165–183, **1996**

Billingham, N.C., Molar *Mass Measurements in Polymer Science*, John Wiley/Halsted, New York, **1977**

Block, I., Kim, H. K., *Accelerated Aging of Cellulosic Textiles at Different Temperatures. The Effect of Tetrahydridoborate Reduction* In *Historic textile and paper materials. Conservation and characterization*, Eds. Needles, H. L., Zeronian, S. H., Advances in Chemistry Series 212, American Chemical Society Washington DC, 411-425, **1986**

Block, I., *Temperature and humidity in the accelerated aging of cellulosic textile,*. ICOM Committee for Conservation Preprints, 7" triennial Meeting, Copenhagen, **1984**

Bogaard. J., Whitmore, P.M., *Effects of dilute calcium washing treatments on paper*. J Am Inst Conserv 40, 105–123, **2001**

Bohrn, B., Potthast, A., Schiehser, S., Rosenau, T., Sixta, H., Kosma, P., *A novel method for the determination of carboxyl profiles in cellulosics by fluorescence labeling. Part I: Method development*, Biomacromolecules 7, 1743-1750, **2006a**

Bohrn, R., Potthast, A., Rosenau, T., Kosma, P., Sixta, H., *A novel diazo reagent for fluorescence labelling of carboxyl groups in pulp*, Lenzinger Ber 83, 84-91, **2004**

Bohrn, R., Potthast, A., Rosenau, T., Kosma, P., Sixta, H., *Synthesis and testing of a novel fluorescence label for carboxyls in carbohydrates and cellulosics*, Synlett 20, 3087-3090, **2005**

Bohrn, R., Potthast, A., Rosenau, T., Sixta, H., Kosma, P., *Synthesis and Testing of a Novel Fluorescence Label for Carboxyls in Carbohydrates and Cellulosics* Synlett 20. 3087-3090, **2006b**

Bohrn, R., Potthast, A., Schiehser, S., Rosenau, T., Sixta, H., Kosma, P., *The FDAM method: determination of carboxyl profiles in cellulosic materials by combining group-selective fluorescence labelling with GPC*, Biomacromolecules 7, 1743–1750, **2006c**

Boyd, R. H., Lin, T.P., *Theoretical Depolymerization Kinetics. III. The Effect of Molecular-Weight Distribution in Degrading Polymers Undergoing Random-Scission Initiation*, J Chem Phys 45, 778-781, **1966**

Brannahl, C., Cramse, M., *Untersuchungen an Tinten*, Archivalische Zeitschrift 70, 79-98, **1974**

Bruckle, I., *Aspects of the use of alum in historical papermaking* IPC Conference Papers Manchester 1st - 4th April, 201-206, **1992**

Bruckle, I., *The Role of Alum in Historical Papermaking*, Abbey News, 17, 53-57, **1993**

Buchbauer, G., Jirovetz, L., Wasicky, M., Nikiforov, A., *On the Odor of Old Books,* J Pulp Pap Sci 21, J398-J400, **1995**

Budnar, M., Simčič, J., Rupnik, Z., Uršič, M., Pelicon, P., Kolar, J., Strlič, M.*, In-air PIXE set-up for automatic analysis of historical document inks,* Nucl Instrum Meth B 41, 219-220, **2004**

Budnar, M., Uršič, M., Simčič, J., Pelicon, P., Kolar, J., Šelih, V.S., Strlič, M., *Analysis of iron gall inks by PIXE* Nucl Instrum Meth B 243, 407-416, **2006**

Bülow, A., Begin, P., Carter, H., Burns, T., *Migration of volatile compounds through stacked sheets of paper during accelerated ageing. Part II: variable temperature studies*, Restaurator 21, 187–203, **2000**

Calvini, P., *Variation of relative humidity in a sealed showcase*, http://www.paolocalvini.it/ (a)

Calvini, P., Franceschi, E., Palazzi, D., *Artificially induced slow-fire in sized papers: FTIR, TG, DTA and SEM analyses*, Science and technology for cultural heritages 5 (1), 1-11, **1996**

Calvini, P., Conio, G., Lorenzoni, M., Pedemonte, E., *Viscometric determination of dialdehyde content in periodate oxycellulose. Part I. Methodology*, Cellulose 11, 99–107, **2004**

Calvini, P., Gorassini, A., Merlani, A. L., *On the kinetics of cellulose degradation: looking beyond the pseudo zero order rate equation*, Cellulose 15, 193-203, **2008b**

Calvini, P., Gorassini, A., Merlani, A.L., *Autocatalytic degradation of cellulose paper in sealed vessels*, Restaurator 28, 47–54, **2007**

Calvini, P., Gorassini, A., *On the Rate of Paper Degradation: Lessons From the Past*, Resturator 27, 275-290, **2006**

Calvini, P., Gorassini, A., *The Degrading Action of Iron and Copper on Paper. A FTIR-Deconvolution Analysis*, Restaurator 23 (4), 205-221, **2002**

Calvini, P., Grosso, V., Hey, M., Rossi, L., Santucci, L*., Deacidification of paper: A more fundamental approach*, Paper Conservator 12, 35–39, **1988**

Calvini, P., Silveira, M., *FTIR analysis of naturally aged FeCl3 and CuCl2-doped cellulose papers*, E-Preservation Science 5, 1-6, **2008a**

Calvini, P., *The influence of levelling-off degree of polymerisation on the kinetics of cellulose degradation*, Cellulose 12, 445–447 **2005**

Calvini, P., *The role of the Ekenstam equation on the kinetics of cellulose hydrolytic degradation*, Cellulose 19, 313-318, **2012**

Calvini, P., *What went wrong with the kinetics of cellulose degradation?* In *Cellulose: Structure and Properties, Derivatives and Industrial Uses*, Eds. Lejeune, A., Deprez, T., Nova Science Publishers Inc. New York, 417-426, **2010**

Calvini, P., *On the meaning of the Emsley, Ding & Wang and Calvini equations applied to the degradation of cellulose,* Cellulose, in press, 1-8, March **2014**

Carme Sistach, M., Gibert, J. P., Areal*, R., Ageing of Laboratory Irongall Inks Studied by Reflectance Spectrometry*, Restaurator 20, 151-166, **1999**

Carme Sistach, M.C., Ferrer, N., Romeo, M.T., *Fourier Transform Infrared Spectroscopy Applied to the Analysis of Ancient Manuscripts* Restaurator 19(4), 173–186, **1998**

Carvalho, D., N., *Forty Centuries of Ink*, The Banks Law Publishing Co Ed., London, **1904**

Caverhill, J., Stanley, J., Singer, B., Latimer, I., *The Effect of Ageing, on Paper Irradiated by Laser as a Conservation Technique* Restaurator 20, 57-76, **1999**

Celina, M., Gillen, K.T., Assink, R. A., *Accelerated aging and lifetime prediction: Review of non-Arrhenius behaviour due to two competing processes*, Polym Degrad Stab 90, 395-404, **2005**

Chanzy, H., *Aspects of Cellulose Structure* in *Cellulose Sources and Exploitation*, Eds. Kennedy, J.F., Phillips, G.O., Williams, P.A. Ellis Horwood Ltd., New York, 3–12, **1990**

Churms, S.C.J., *Recent progress in carbohydrate separation by high-performance liquid chromatography based on size exclusion*, Chromatogr. A 720, 151-166, **1996**

Corbett, W. M., Kenner, J., *The degradation of carbohydrates by alkali. Part II. Lactose*, J Chem Soc, 3572-3575, **1953**

Czepiel, T. P., *The Influence of Selected Metal Traces on the Color and Color Stability of Purified Cotton Linters*, Tappi 43 (4), 289-299, **1960**

Daniels, V. D., *Aging of paper and pigments containing iron and copper: a review* in *The Broad Spectrum. Studies in the Materials, Techniques, and Conservation of Color on Paper,* Eds. Stratis H. K., Salvesen, B., Archetype Publications Ltd. London, **2002**

Daniels, V. D., *The Russell Effect–a review of its possible uses in conservation and the scientific examination of materials*, Stud Conserv 29 (2), 57-62, **1984**

Daniels, V. D., *Monitoring the Autoxidation of Paper Using Photographic Materials* in *Historic textile and paper materials. Conservation and characterization*, Eds. Needles, H. L., Zeronian, S. H., Advances in Chemistry Series 212, American Chemical Society Washington, 317-327, **1986**

Daniels, V., *The Chemistry of Iron Gall inks* in *The Iron Gall Ink Meeting Postprints*, Ed. Brown, J.E., University of Northumbria Newcastle upon Tyne, **2000**

Danilov, S. N, Samsonova T. I., Bolotnikov, L. S., *Investigation of Solutions of Cellulose*, Russ Chem Rev 39, 156-168, **1970**

Daruwalla, E.H., Narsian, M.G., *Detection and identification of acid-sensitive linkages in cellulose fiber substances*, TAPPI 49(3), 106–111, **1966**

Dawsey, T. R., McCormick, C. L. *The lithium chloride/dimethylacetamide solvent for cellulose: a literature review*, J Macromol Sci -Rev Macromol Chem Phys C30, 405-440, **1990**

Debye, P., *Molecular Weight Determination by Light Scattering*, J. Phys. Coll. Chem. 51, 18, **1947**

Dupont, A. L., Barthez, J., Jerosch, H., Lavédrine, B., *Testing CSC Book Saver®, a commercial deacidification spray*, Restaurator 23, 39-47, **2002a**

Dupont, A. L., Egasse, C., Morin, A., Vasseur, F., *Comprehensive characterisation of cellulose- and lignocellulose-degradation products in aged papers: capillary zone electrophoresis of low-molar mass organic acids, carbohydrates, and aromatic lignin derivatives,* Carbohydr Polym 68 (1), 1-16, **2007**

Dupont, A. L., *Gelatine sizing of paper and its impact on the degradation of cellulose during aging: a study using size-exclusion chromatography* (Ph.D. thesis)   Universiteit van Amsterdam Faculteit der Natuurwetenschappen, Wiskunde en Informatica, **2003**

Dupont, A. L., Mortha, G., *Comparative evaluation of size exclusion chromatography and viscometry for the characterisation of cellulose*, J Chromatogr A 1026, 129–141, **2004**

Dupont, A. L., *Study of the degradation of gelatin in paper upon aging using aqueous size-exclusion chromatography*, J Chrom A 950, 113–124, **2002b**

Dupont, A. L., *The role of gelatine/alum sizing in the degradation of paper: a study by size exclusion chromatography in lithium chloride/N,N-dimethyllacetamide using multiangle light scattering detection* in Works of art on paper books, documents and photographs – techniques and conservation, Eds. Vincent, D., Alan, D., Smith, P. , International Institute for Conservation, Baltimore, 59–64, **2002c**

Dupont, A.L., *Degradation of Cellulose at the Wet/Dry Interface. II. An Approach to the Identification of the Oxidation Compounds,* Restaurator 17, 145-164, **1996**

Dupont, A.L., *Gelatine/alum sizing of paper and its impact on the degradation of cellulose: a study using size-exclusion chromatography with multiangle light scattering detection*. Actes du Congrès Art et Chimie "Les Polymères", Paris, France, 15-16 Oct, 69-74, **2002d**

Ekenstam, A., *Über das Verhalten der Cellulose in Mineralsäure-Lösungen, II. Mitteil.: Kinetisches Studium des Abbaus der Cellulose in Säure-Lösungen*, Ber. Dtsch. Chem. Ges. A/B 69, 553-559, **1936**

Ekmanis, J.L., *Gel permeation chromatographic analyses of* cellulose, Am Lab News Jan-Feb 10-11, **1987**

Ekmanis, J.L., Turbak, A.F., *GPC analysis of cellulose*, Lab highlights an internal communication of application and techniques 251, Waters Chromatography Division, Millipore, Milford, **1986**

Emsley, A. M., Stevens, G.C., *Kinetics and mechanism of the low-temperature degradation of cellulose*, Cellulose 1, 26–56, **1994**

Emsley, A.M., Ali, M., Heywood, R.J., *A size exclusion chromatography study of cellulose degradation*, Polymer 41, 8513–8521, **2000**

Emsley, A.M., Heywood, R.J., Ali, M., Eley, C.M., *On the kinetics of degradation of cellulose*, Cellulose 4, 1–5, **1997**

Erhardt, D., Endt, D. V., Hopwood, W., *The Comparison of Artificial Aging Conditions through the Analysis of Extracts of Artificially Aged Paper* in *Preprints 15th Annual Meeting of AIC*, Vancouver, British Columbia, Canada, 43-55, **1987**

Erhardt, D., Mecklenburg, M. F., *Accelerated VS Natural Aging: Effect of Aging Conditions on the Aging Process of Cellulose,* MRS Proceedings 352 **1995**

Erofeev, B. V., Shishko, A. M., Volkovich, S. M., Pesnyakevich, L. G., Matskevich, D. V. *Reactivity of the amorphous regions of cellulose,* Reports of the Academy of Sciences of the Byelorussian SSR, Vestsi Akd. Navuk Ussr, Ser, Khim, Navuk 1, 12–16. **1982**

Evans, R., Wallis, A.F.A., *Cellulose molecular weights determined by viscometry*, J Appl Polym Sci 37, 2331–2340, **1989**

Feller, R. L., Lee, S. B., Curran, M., *Three Fundamental Aspects Of Cellulose Deterioration*, Art And Archaeology Technical Abstracts Supplement 22, N.1, 277-358, **1985**

Feller, R. L., Lee, S. B.;, Bogaard, J., *The Kinetics of Cellulose Deterioration* In *Historic textile and paper materials. Conservation and characterization*, Eds. Needles, H. L., Zeronian, S. H., Advances in Chemistry Series 212, American Chemical Society Washington DC, 329-347, **1986**

Fellers, C., Iversen, T., Lindstrom, T., Nilsson, T., Rigdahl, M., *Ageing/Degradation of Paper, A Literature Survey*, FoU-projektet for papperskonservering, Report No. 1, Stockholm, **1989**

Gagnaire, D., Saint-Germain, J,. Vincendon, M., *NMR evidence of hydrogen bonds in cellulose solutions*, J Appl Polym Sci Appl Polym Symp 37, 261-275, **1983**

Garlick, K., *A Brief Review of the History of Sizing and Resizing Practices*, The Book and Paper Group Annual 5, The American Institute for Conservation, 94-107, **1986**

Gilbert, R., Jalbert, J., Tetreault, P., Morin, B., Denos, Y., *Kinetics of the production of chain-end groups and methanol from the depolymerization of cellulose during the ageing of paper/oil systems. Part 1: Standard wood kraft insulation*. Cellulose 16, 327–338, **2009**

Golova, O. P., Nosova, N. I., *Degradation of Cellulose by Alkaline Oxidation*, Russ Chem Rev 42, 327-337, **1973**

Graminski, E. L., Parks, E. J., Toth, E. E., *The Effects of Temperature and Moisture on the Accelerated Aging of Paper* In *Durability of macromolecular materials,* Ed. Eby, R. K. ACS Symposium Series 95, American Chemical Society Washington DC, 341-355, **1979**

Green, S., *The historical development of sizing agent,* IPC Conference Papers Manchester 1st - 4th April, 197-200, **1992**

Gurnagul, N., Howard, R. C., Zou, X., Uesaka, T., Page, D. H. J., *The Mechanical Permanence of Paper - a Literature-Review*, Pulp Pap Sci, 19, j160- j166, **1993**

Haerting, K., *Eisenoxyd-Zellulose*, Kolloid Zeitschrift 25, 74 – 79, **1919**

Halajová, L., Kačík, F., *Vplyv urýchleného starnutia na degradáciu recyklovaných buničín: časť 1: Teplota sušenia 100 °C (Influence of accelerated ageing on degradation of the recycled pulps: part 1: Temperature of dying 100 °C),* Acta Facultatis Xylologiae Zvolen 53 (1), 63—67, **2011**

Henniges, U., Reibke, R., Banik, G., Huhsmann, E., Hahner, U., Prohaska, T., Potthast, A., *Iron gall ink-induced corrosion of cellulose: aging, degradation and stabilization. Part 2: application on historic sample material*, Cellulose 15 (6), 861-870, **2008**

Herdan, G., *Fitting of polymer distributions of molecular weight by the method of moments*, J Polym Sci 10 (1), 1–18, **1953**

Herzberg, W., *Einfluss höherer Wärmegrade auf die Festigkeitseigenschaften von Papier*. Papier-Zeitung 24 (61), 23-43, **1899**

Herzberg, W., *Zerstörungen von Papier durch Tinte, Mitteilungen aus dem Staatlichen Materialprüfungsamt Berlin*, Wochenblatt für Papierfabrikation 55, 90 – 95, **1924**

Heywood, R.J., Stevens, G.C., Ferguson, C., Emsley, A.M., *Life assessment of cable paper using slow thermal ramp method*, Thermochim Acta 332, 189–195, **1999**

Hill, D. J. T., Le, T. T., Darveniza, M., Saha, T.K., *A study of degradation of cellulosic insulation materials in a power transformer. Part 1: molecular weight study of cellulose insulation paper*, Polym Degrad Stab 48, 79–87, **1995**

Houdier, S., Legrand, M., Boturyn, D., Croze, S., Defrancq, E., Lhomme, J., *A new fluorescent probe for sensitive detection of carbonyl compounds*, Anal Chim Act 382, 253-263, **1999**

Huglin, M. B., Light Scattering from Polymer Solutions, Academic Press New York, **1972**

Ivanov, V.I., Lenshina, N.Y.A., Ivanova, V.S., *Oxidative transformations in cellulose molecule,* J Polym Sci 53, 93–97, **1969**

Jerosch, H., Lavedrine, B., Cherton, J.C., *Study on the correlation between SEC and mechanical tests of different paper types for degradation stale evaluation,* Restaurator 23, 222-239, **2002**

Kačík, F., Geffertová, J., Kačíková, D., *Charakterizácia celulózy a buničín metódou gélovej permeačnej chroma tografie a viskozimetrie (Characterization of cellulose and pulps by the methods of gel permeation chromatography and viscometry)*, Acta Facultatis Xylologiae Zvolen 51 (2), 93—103, **2009**

Kaminska, E., Bégin, P. L., Grattan, D., Woods, D., Bulow, A., *Research Program on the Effects of Ageing on Printing and Writing Papers: Accelerated Ageing Test Method Development''* ASTM/ISR, Conservation Process and Materials Research Division, November, 30, 37-39, **2001**

Klages, F., Jung, H.A., Hegenberg, P*., Determination of acidity by means of aliphatic diazo compounds. III. Dynamic acidity of very strong acids*, Chem Ber 9, 1704–1711, **1966**

Kolar, J., *Mechanism of Autoxidative Degradation of Cellulose*, Restaurator 18, 163-176, **1997**

Kolbe, G., *Gelatine in Historical Paper Production and as Inhibiting Agent for Iron-Gall Ink Corrosion on Paper*, Restaurator 25, 26–39, **2008**

Kowalik, R., *Microbiodeteroration of Library Materials*, Restaurator 4, 99 - 114 & 135-219, **1980**

Krässig, H. A., *Cellulose structure, accessibility and reactivity*, Gordon and Beach Science Publishers Yverdon Switzerland, **1993**

Krassig, H., *Structure of cellulose and its relation to properties of cellulose fibers* in *Cellulose and its Derivatives: Chemistry, Biochemistry and Applications* Eds. Kennedy, J.F., Phillips, G.O., Wedlock, D.J., Williams, P.A., Ellis Horwood Limited Publishers Chichester UK, 3–25, **1985**

Krekel, C., *Chemische Struktur historischer Eisengallustinten* In *Tintenfrassschäden und ihre Behandlung*, Eds. Banik, G., Weber, H., Kohlhammer Stuttgart, 25-36, **1999a**

Krekel, C., *The chemistry of historical iron gall inks,* Int Journal Forensic Docum Exam 5, 54-58, **1999b**

Lattuati-Derieux, A., Bonnassies-Termes, S., Lavédrine, B., *Identification of volatile organic compounds emitted by a naturally aged book using solid-phase microextraction/gas chromatography/mass spectrometry*, J Chromatogr A 1026, 9–18, **2004**

Lattuati-Derieux, A., Bonnassies-Termes, S., Lavédrine, B., *Characterisation of compounds emitted during natural and artificial ageing of a book. Use of headspace-solid-phase microextraction/gas chromatography/mass spectrometry*, J Cult Herit 7 (2), 123–133, **2006**

Lauriol, J. M., Comtat, J., Froment, P., Pla, F., Robert, A., *Molecular Weight Distribution of Cellulose by On-Line Size Exclusion Chromatography - Low Angle Laser Light Scattering Part. II. Acid and Enzymatic Hydrolysis*, Holzforschung, 41(3), 165-169, **1987**

Lehtaru, J., Ilomets, T., *Use of Chelating Agent EDTA with Sodium Thiosulphate and Sodium Borohydride in Bleaching Treatment*, Restaurator 18, 191-200, **1997**

Levchik, S., Scheirs, J., Camino, G., Tumiatti, W., Avidano, M., *Depolymerization processes in the thermal degradation of cellulosic paper insulation in electrical transformers*, Polymer Degradation and Stability 61 (3), 507-511, **1998**

Lichtenegger, H., Müller, M., Paris, O., Riekel, C., Fratzl, P., *Imaging of the helical arrangement of cellulose fibrils in wood by synchrotron X-ray microdiffraction* J. Appl. Cryst 32, 1127–1133, **1999**

Łojewski, T., Zieba, K., Kołodziej, A., Łojewska, J., *Following cellulose depolymerization in paper: comparison of size exclusion chromatography techniques*, Cellulose 18, 1349–1363, **2011**

Luner, P., *Evaluation of Paper Permanence*, Wood Sci Technol 22, 81-97, **1988**

Major, W. D., *The degradation of cellulose in oxygen and nitrogen at high temperatures* Tappi J. 41, 530-537, **1958**

Malesic, J., Kolar, J., Strlic, M., *Effect of pH and Carbonyls on the Degradation of Alkaline Paper Factors Affecting Ageing of Alkaline Paper*, Restaurator 23, 145-153, **2002**

Margutti, S., Conio, G., Calvini, P., Pedemonte, E., *Hydrolytic and Oxidative Degradation of Paper,* Restaurator 22, 67-83, **2001**

Mark, H. F., *Encyclopedia of Polymer Science and Engineering*, Wiley, **1987** (2nd ed.)

Marx-Figini, M., *Newer structural and biosynthetic aspects of native cellulose as revealed by the kinetics of its hydrolytic degradation*, J Appl Polym Sci, Appl Polym Symp 37, 157–164, **1983**

McBurney, L. F., *Degradation of Cellulose*, in *Cellulose and Cellulose Derivatives,* Eds. E. Ott, E., Spurlin, H. M., Grafflin, U. W., Interscience Publisher Inc New York, 99-176, **1954**

McCormick, C.L., *Novel cellulose solutions,* US patent No. 4278790, **1981**

Melander, M., Vuorinen, T., *Determination of the degree of polymerisation of carboxymethyl cellulose by size exclusion chromatography*, Carbohydr Polym 46, 227-233. **2001**

Messner, K., Alberighi, L., Banik, G., Srebotnik, E., Sobotka, W., Mairinger, F., *Comparison of Possible Chemical and Microbial Factors Influencing Paper Decay by Iron-Gall Inks* Biodeterioration 7, 449-454, **1988**

Michie, R. I. C., Sharples, A., Walter, A. A., *The nature of acid-sensitive linkages in cellulose* J Polym Sci 51, 131-140, **1961**

Montroll, E*., Molecular size distributions and depolymerisation reactions in polydisperse systems*, J Am Chem Soc 63, 1215–1220, **1941**

Morgenstern, B., Kammer H-W., *Solvation in cellulose-LiCl-DMAc solutions*, Trends Polym Sci 4 (3), 87-92, **1996**

Neevel, J. G., Mensch, C. T. J., *The behaviour of iron and sulphuric acid during iron-gall ink corrosion*, Triennial meeting (12th), Lyon, 29 August - 3 September preprints. Vol. 2, **1999**

Neevel, J. G., *Phytate based treatment of ink corrosion – an updated review* in *Postprints of the Iron Gall Ink Meeting*, Ed. Brown, J. E., 4–5 September, Universityof Northumbria, Newcastle upon Tyne UK, **2000**

Neevel, J.G., *Phytate als chemische Inhibitoren von Tintenfraß auf Papier* in Tintenfraßschäden und Ihre Behandlung, Eds. Banik, G., Weber, H., Stuttgart, Kohlhammer 87-111, **1999**

Neevel, J.G., *The development of a new conservation treatment for ink corrosion, based on the natural antioxidant phytate In Preprints of the 8th International Congress of IADA Tübingen*, Eds. Koch, M.S., Palm, K.J., Copenhagen: The Royal Danish Academy of Fine Arts, School of Conservation, 93-100, **1995**

Nelson, M.L., Tripp, V.W., *Determination of the leveling-off degree of polymerization of cotton and rayon,* J Polym Sci 10(6), 577–586, **1953**

O'Sullivan, A. C., *Cellulose: the structure slowly unravels*, Cellulose, 4, 173-207, **1997**

Oye, R., Okayama, T., Matsubara, H., Hanamura, K., *Studies on degradation of paper and conservation II: Degradation of mechanical pulp-containing paper*, Japan Tappi J. 45, 277-284, **1991**

Pérez, S., Mazeau. K., *Conformations, Structures, and Morphologies of Celluloses* in *Polysaccharides. Structural Diversity and Functional Versatility*, (2th Ed). Ed. Dumitriu, S., CRC Press London **2004**

Philipp, H.J., Nelson, M.L., Ziifle, H.M., *Crystallinity of cellulose fibers as determined by acid hydrolysis,* Text Res J 17(11), 585–596, **1947**

Pionteck, H. and Berger, W., *Changes in cellulose structure during dissolution in LiCl:N,N-dimethylacetamide and in the alkaline iron tartrate system EWNN*, Cellulose 3, 127-139, **1996**

Plossi Zappalà, M., *Conservation of Acid Paper: Studies Carried out in the Chemistry Laboratory of the Istituto Centrale per la Patologia del Libro*, Restaurato 18, 12-24, **1997**

Porck, H., Rate *of paper degradation. The predictive value of artificial aging tests*, European Commission on Preservation and Access, Amsterdam **2000**

Potthast, A., Rosenau, T., Buchner, R., Röder, T., Ebner, G., Bruglacher, H., Sixta, H., Kosma, P., *The cellulose solvent system N,N-dimethylacetamide/lithium chloride revisited: The effect of water on physicochemical properties and chemical stability*, Cellulose 9, 41-53, **2002a**

Potthast, A., Rosenau, T., Sixta, H., Kosma, P., *Degradation of cellulosic materials by heating in DMAc / LiCl*, Tetrahedron 43, 7757-7759, **2002b**

Potthast, A., Röhrling, J., Rosenau, T., Borgards, A., Sixta, H,, Kosma, P., *A novel method for the determination of carbonyl groups in cellulosics by fluorescence labeling. 3. Monitoring oxidative processe*, Biomacromolecules 4, 743–749, **2003**

Potthast, A., Rosenau, T., Kosma, P., *Analysis of oxidized functionalities in cellulose* in *Polysaccharides II*, Ed. Klemm, D., Adv Polym Sci 205, Springer Berlin, 1–48, **2006**

Potthast, A., Henniges, U., Banik, G., *Iron gall ink-induced corrosion of cellulose: aging, degradation and stabilization. Part 1: model paper studies*, Cellulose 15, 849–859, **2008**

Rasch, R. H., *A Study of Purified Wood Fibers as a Paper-Making Material*, B.S. Jour. Research, 3 (RP107), p. 469 – 506, **1929**

Rémazeilles, C., Rouchon-Quillet, V., Bernard, J., *Influence of arabic gum on iron gall ink corrosion - Part I : A Laboratory Sample Study*, Restaurator 25, 220-232, **2004**

Richter, G. A., Wells, F. L., *Influence of Moisture in Accelerated Aging of Cellulose*, Tappi 39 (8), 603-608, **1956**

Roberson, D. D., *The evaluation of paper permanence and durability* Tappi J. 59, 63-69, **1976**

Röhrling, J., Potthast, A., Rosenau, T., Lange, T., Borgards, A., Sixta, H. and Kosma, P., *Synthesis and Testing of a Novel Fluorescence Label for Carbonyls in Carbohydrates and Cellulosics*, Synlett 5, 682-684, **2001**

Röhrling, J., Potthast, A., Rosenau, T., Sixta, H., Kosma, P., *Determination of carbonyl functions in cellulosic substrates*. Lenzinger Ber 81, 89-97, **2002a**

Röhrling, J., Potthast, A., Rosenau, T., Lange, T., Borgards, A., Sixta, H., Kosma, P., *A novel method for the determination of carbonyl groups in cellulosics by fluorescence labelling. 2. Validation and application*. Biomacromolecules 3, 969–975, **2002b**

Röhrling, J., Potthast, A., Rosenau, T., Lange, T., Ebner, G., Sixta, H., Kosma, P., *A novel method for the determination of carbonyl groups in cellulosics by fluorescence labeling. 1. Method development*, Biomacromolecules 3, 959–968, **2002c**

Rouchon Quillet, V., Remazeilles, C., Nguyen, T.P., Bleton, J., Tchapla, A., *The impact of gum arabic on iron gall ink corrosion*, Proceedings of the International Conference Durability of Paper and Writing November 16–19 Ljubljana, Slovenia, 56-58, **2004**

Rowland, S.O., Roberts, E.J., *The nature of accessible surfaces in the microstructure of native cellulose*, J. Polym. Sci., Part A 10, 2447–2461, **1972**

Rychlý, J., Rychlá, L., *Chemiluminescence from polymers* In *Ageing and stabilization of paper*, Eds. Strlič, M., Kolar, J., National and University Library Ljubljana, 65-82, **2005**

Santucci, L., *Report on paper stability. Part 1. Survey of literature, discussion and some experimental contribution* , Bollettino dell'istituto di patologia del libro, 67-104, **1963**

Santucci, L., *Paper deacidification procedures and their effects*, Colloques internationaux du Centre National de la Recherche Scientifique 548, Paris 13-15 sept., 197-212, **1972**

Santucci, L., Plossi Zappalà , M. G., *Invecchiamento della carta in tubo,* Problemi di conservazione, Compositori, Bologna, 501–512, **1975**

Santucci, L., Plossi Zappala, M*., Cellulose Viscometric Oxidometry*, Restaurator, 22 51-65, **2001**

Sawoszczuk, T., Barański, A., Łagan, J. M., Łojewski, T., Zięba, K., *On the use of ASTM closed vessel tests in accelerated ageing research* J Cult Herit 9 (4), 401-411, **2008**

Schult, T., Moe, S. T., Hjerde, T., Christensen, B. E., *Size Exclusion Chromatography of Cellulose dissolved in LiCl/DMAC using Macroporous monodisperse poly(styrene-co divinylbenzene) particles*, J Liq Chromatogr Rel Technol 23, 2277-2288, **2000**

Senvaitiene, J., Beganskiene, A., Kareiva, A.,*Spectroscopic evaluation and characterization of different historical writing inks*, Vib Spectros 37 (1), 61-67, **2005**

Senvaitiene, J., Beganskiene, A., Salickaite-Bunikien, L., Kareiva, A., *Analytical identification of historical writing inks. A new methodological approach,* Lith J Phys, 46 109-115, **2006**

Shahani, C. J., Hengemihle, F. H., E*ffect of some deacidification agents on copper- Catalyzed Degradation of Paper,* Preservation Research and Testing Series No. 9501, **1995**

Shahani, C., Hengemihle, F., *The influence of copper and iron on the permanence of paper* In Historic Textile and Paper Materials, Advances in Chemistry Series, No. 212, Ed. Needles, H. L., Zeronian, S. H. Washington DC, American Chemical Society, 387–410, **1986**

Shahani, C., Lee, S. B., Hengemihle, F. H., Harrison, G., Song, P., Sierra, M. L., Ryan, C. C., Weberg, N., *Accelerated aging of paper: I. Chemical analysis of degradation products. II. Application of Arrhenius relationship. III. Proposal for a new accelerated aging test: ASTM research program into the effect of aging on printing and writing papers* Library of Congress, Washington DC **2001**

Sharples, A., *Degradation of cellulose and its derivatives. A. Acid hydrolysis and alcoholysis*, In Cellulose and cellulose derivatives, Eds. Bikales, N.M., Segal, L., vol V, Pt V, 2nd ed. Wiley-Interscience New York, 991–1006 **1971**

Sharples, A., *The hydrolysis of cellulose part II. Acid sensitive linkages in egyptian cotton*, J Polym Sci 14, 95–104, **1954b**

Sharples, A., *The hydrolysis of cellulose. Part I. The fine structure of Egyptian cotton*, J Polym Sci 13, 393–401, **1954a**

Sjöholm, E., Gustafsson, K., Eriksson, B., Brown, W., Colmsjö, A., *Aggregation of cellulose in lithium chloride/N,N-dimethylacetamide,* Carbohydr Polym 41, 153-161, **2000**

Skubala, W., *Investigation of Ageing of Transformer Insulation With and Without the Effects of an Electric Field*, Prz. Papierniczy 188, 40-58, **1974**

Spitzmueller, P., *Selecting a paper re-sizing agent and its concentration: a look at parchment size and photographic gelati*. in IPC Conference Papers Manchester 1st-4th April 1992, 214-221 **1992**

Stephens, C. H., Whitmore, P. M., Morris, H. R., Bier, M. E., *Hydrolysis of the amorphous cellulose in cotton-based paper*, Biomacromolecules 9, 1093-1099, **2008**

Stijnman, A., *Historical iron-gall ink recipes: art technological source research for InkCor*, Papierrestaurierung 5, 14-17, **2004**

Striegel, A. M., Yau, W. W., Kirkland, J. J., Bly, D. D., *Modern Size-Exclusion Liquid Chromatography- Practice of Gel Permeation and Gel Filtration Chromatography,* Wiley 2nd Edition, **2009**

Striegel, A. M., Timpa, J. D., *Molecular characterization of polysaccharides dissolved in Me 2NAc-LiCl by gel-permeation chromatography*, Carbohyd Res, 267 (2), 271-290, **1995**

Striegel, A., *Theory and applications of DMAC/LICL in the analysis of polysaccharides*, Carbohydr Polym 34, 267-274, **1997**

Strlic, M., Kolar, J., Zigon, M., Pihlar, B., *Evaluation of size-exclusion chromatography and viscometry for the determination of molecular masses of oxidised cellulose*, J Chromatogr A 805, 93-99, **1998**

Strlič, M., Kolar, J., Pihlar, B., Rychly, J., Matisova-Rychla, L., *Chemiluminescence during thermal and thermo-oxidative degradation of cellulose*, Eur Polym J 36, 2351-2358, **2000**

Strlic, M., Kolar, J., *Evaluating and enhancing paper stability - the needs and recent trends* 5th EC Conf. Cultural Herit. Res., Pan-Eur. Challenge, May 16-18, Cracow Poland, 79-86, **2002**

Strlič, M., Kolar, J., Kočar, D., Rychlý, J., *Thermo-oxidative degradation* In Ageing and stabilization of paper, Eds. Strlič, M., Kolar, J., National and University Library Ljubljana, 111-132, **2005a**

Strlič, M.; Rychlý, J.; Haillant, O.; Kočar, D.; Kolar, J. *Chemiluminescence of cellulose and paper* In Ageing and stabilization of paper, Eds. Strlič, M., Kolar, J., National and University Library Ljubljana,121-135, **2005b**

Strlič, M., Menart, E., Cigić, I.K., Kolar, J., de Bruin, G., Cassar, M., *Emission of reactive oxygen species during degradation of iron gall ink*, Polym Degrad Stabil 95, 66–71, **2010**

Strlič, M., Cigić, I.K., Mozir, A., de Bruin, G., Kolar, J., Cassar, M., *The effect of volatile organic compounds and hypoxia on paper degradation*, Polym Degrad Stabil 96, 608-615, **2011**

Strofer-Hua, E., *Experimental measurement: interpreting extrapolation and prediction by accelerating aging*, Restaurator 11, 254-266, **1990**

Sugiyama, J., Harada, H., Fujiyoshi, Y., Uyeda, N., *Observations of Cellulose Microfibrils in Valonia macrophysa by High resolution Electron microscopy*, Mokuzai Gakkaishi, 31 61-67, **1985**

Szczepanowska, H., *Biodeterioration of Art Objects on Paper*, The Paper Conservator 10, 31-39, **1986**

Tang, L. C., *Stabilization of Paper through Sodium Borohydride Treatment in Historic textile and paper materials. Conservation and characterization*, Eds. Needles, H. L., Zeronian, S. H., Advances in Chemistry Series 212, American Chemical Society Washington DC, 411-425, **1986**

Thompson, J. C., *Manuscript Inks* The Caber Press, Portland, Oregon, **1996**

Whitmore, P. M., Bogaard, J., *Determination of the cellulose scission route in the hydrolytic and oxidative degradation of paper*, Restaurator 15, 26–45, **1994**

Whitmore, P. M., Bogaard, J., *The Effect of Oxidation on the Subsequent Oven Aging of Filter Paper*, Restaurator 16, 10-30 **1995**

Williams, J.C., Fowler, C.S., Lyon, M.S., Merrill, T.I., *Metallic Catalysts in the Oxidative Degradation of Paper* in *Preservation of Paper and Textiles of Historic and Artistic Value*, Ed. Williams, J. C., Advances in Chemistry Series 164 American Chemical Society, Washington D.C., **1977**

Wilson, W. K., Parks, E. J., *Historical Survey of Research at the National Bureau of Standards on Materials for Archival Records* Restaurator 5, 191-241, **1983**

Wilson, W. K., Parks, E. J., *An Analysis of the Aging of Paper: Possible Reactions and their Effects on Measurable Properties*, Restaurator 3, 37-61, **1979**

Wunderlich, C. H., Weber, R., Bergerhoff, G., *Über Eisengallustinte,* Z Anorg Allg Chem, 598, 371-376, **1991**

Wunderlich, C.H., *Geschichte und Chemie der Eisengallustinte - Rezepte, Reaktionen und Schadwirkungen*, Restauro 100, 414-421, **1994**

Yachi, T., Hayashi, J., Takai, M., Shimizu, Y., *Supermolecular structure of cellulose: stepwise decrease in LODP and particle size of cellulose hydrolyzed after chemical treatment,* J Appl Polym Sci, Appl Polym Sym 37, 325–343, **1983**

Zerdoun, M., Yehouda, B., *Les encres noires au Moyen Age (jusqu'à 1600)*, Éditions du Centre National de la Recherche Scientifique Paris, **1983**

Zervos, S., *Natural and Accelerated ageing of cellulose and paper: A literature review* in Lejeune, A. and Deprez, T., *"Cellulose: Structure and Properties, Derivatives and Industrial Uses"*, Nova Science Publishers Inc., New York, **2010**

Zervos, S., *Accelerated Ageing Kinetics of Pure Cellulose Paper after Washing, Alkalization and Impregnation with Methylcellulose*, Restaurator 28, 55-69, **2007**

Zervos, S., Moropoulou, A., *Cotton cellulose ageing in sealed vessels. Kinetic model of autocatalytic Depolymerization*, Cellulose 12, 485–496, **2005**

Zou, X., Gurnagul, N., Uesaka, T., Bouchard, J., *Accelerated aging of papers of pure cellulose: mechanism of cellulose degradation and paper embrittlement*, Polym Degrad Stabil 43, 393–402, **1994**

Zou, X., Uesaka, T., Gurnagul, N., *Prediction of paper permanence by accelerated aging. II. Comparison of the predictions with natural aging results*, Cellulose 3, 269-279, **1996b**

Zou, X., Uesaka, T., Gurnagul, N., *Prediction of paper permanence by accelerated aging. I. Kinetic analysis of the aging Process*, Cellulose 3, 243-267, **1996a**

ATTACHMENTS

[1] VISCOMETRY

Viscometry allows the determination of the intrinsic viscosity of a polymer solution. By dissolving polymers in a suitable solvent, an increase in the solution viscosity is generally observed. The evaluated intrinsic viscosity could be then used to characterise the material under investigation as it depends on the molecular weight and the composition of the polymer as well as its loading.

As far as cellulose in pulp is concerned, the methodology consists of dissolving the sample in a diluted solution of Cupriethylenediamine hydroxide[13] (CED) and measuring the flow time a defined volume of the solution passes through the lines of a glass capillary tube viscometer. Indeed, it is assumed that

$$\frac{\eta}{\eta_0} = \frac{t}{t_0}$$

where t, η and t_0, η_0 represent the flow times and the viscosity of a specific volume of polymer solution (no index) and solvent (0 index), respectively.

As defined above, viscometry allows the evaluation of the intrinsic viscosity $[\eta]$ through the increase in the solvent viscosity brought about by the introduction of polymer molecules. However, some preliminary definitions and calculation are necessary in order to determine $[\eta]$.

The *specific viscosity* represents the fractional viscosity increase caused by the solute

$$\eta_{sp} = \frac{\eta - \eta_0}{\eta_0} = \frac{\eta}{\eta_0} - 1 = \eta_r - 1$$

where η_r represents the *relative viscosity* whereas η and η_0 are the viscosity values of the solvent with and without the polymer (solute), respectively. Bearing in mind the relationship between the relative viscosity and the flow time expressed above, the specific viscosity can be defined as

$$\eta_{sp} = \eta_r - 1 = \frac{t - t_0}{t_0}$$

---

[13] Metal ammine complexes (e.g. copper, cadmium, zinc or cobalt, coordination compounds) have been extensively investigated as cellulose solvents (Danilov et al. 1970). Among all, Cadmiumethylenediamine (Cadoxen) and Cupriethylenediamine hydroxide (CED) are considered the best solvents in this group.

By normalising η_{sp} for the polymer concentration, the *reduced viscosity* can be obtained as

$$\eta_{red} = \frac{\eta_r - 1}{c} = \frac{t - t_0}{c \cdot t_0}$$

To avoid the influence of polymer entanglements, the viscosity value to zero concentration can be extrapolate, thus obtaining the sought *intrinsic viscosity* (ml/g):

$$[\eta] = \lim_{c \to 0} \frac{\eta_r - 1}{c}$$

The intrinsic viscosity is related to the viscosity-average degree of polymerization (*DPv*) of the polymer through an empirical relationship known as the Mark-Houwink-Sakurada equation, generally expressed as

$$DP_v = K \, [\eta]^\alpha$$

where K and α are experimental constants. They are also known as the Mark-Houwink parameters and their values are tabulated for many polymer-solvent systems (Mark 1987). The advantage of using an intrinsic-viscosity-dependent relationship is that $[\eta]$ just depends on the molecular mass of the polymer whereas it is independent from the viscosity of the solvent, the concentration of the polymer or the type of viscometer used.

[2] SIZE-EXCLUSION CHROMATOGRAPHY

SEC PRINCIPLES

Size exclusion chromatography (SEC) refers to a liquid chromatographic technique allowing the separation of macromolecules according to their hydrodynamic volume, related to their size in solution. Other interchargeable terms could be also used in reference to such analysis, e.g. Gel Permeation Chromatography (GPC) or Gel Filtration Chromatography (GFC)[14].
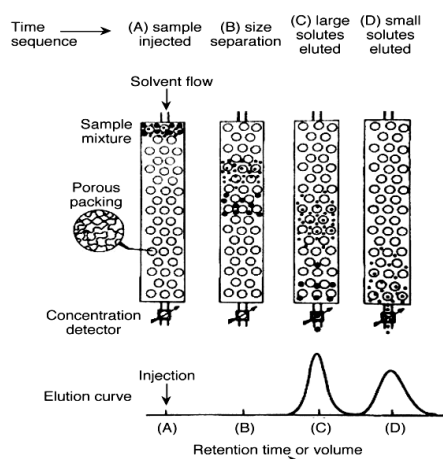
Fig. [3]. 1 – Development and detection of size separation by SEC. Taken from (Striegel et al. 2009).

As depicted in figure [3].1, polymer molecules flow through the column filled with suitable porous materials with defined size. Smaller molecules deeper penetrate the stationary phase being retained for longer time and eluting later (at higher volumes) than bigger molecules (BOCOF's law, '*Big Ones Come Out First'*). At the end of the column, a mass detector encounters molecules of different size then generating a signal proportional to their concentration.

Molecular mass distributions (MMD) has been extensively determined for aged and non aged cellulosic materials. New column packing materials and detection system have been developing, thus improving the cellulose characterisation with SEC (Churms, 1996; Berek, 2000; Schult, 2000; Melander et al., 2001).

---

[14] "Gel" usually refers to the stationary phase used in these techniques (e.g. semi- or non-rigid materials).

As far as this thesis is concerned, some information on the specific analytical setup used at Boku Universität laboratory (Vienna) during the doctoral internship are provided below.

SYSTEM OVERVIEW

A schematic instrumental setup, as used in the present study, is shown in figure [3].2.
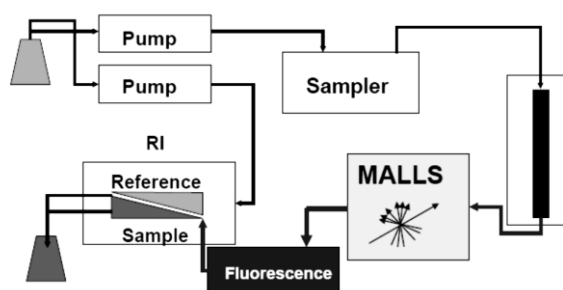
Fig. [3]. 2 – Instrumental setup of the GPC system used (Röhrling et al., 2002c).

SEC detectors

Although different types of detector can be used in SEC, in the present study analyses have been performed with a fluorescence, a refractive index (RI) and a multi-angle laser light scattering detector (MALLS).

Refractive index detector, is a concentration sensitive detector that measures the difference in the refractive index (RI) between the eluant and the eluant plus sample by using a split optical cell. It is consider to be a universal detector as it provides a response for any sample with a significant difference in refractive index as compared to the mobile phase. A drawback of this system is its highly dependence on temperature which required a constant temperature maintenance of columns and injector. Even though the RI response is usually assumed to be equally proportional to polymer concentration in all molecular weight regimes, this is not completely true at low molecular weights. In fact, these fractions has non negligible end-groups portions that change the refractive index compromising the analysis.

Fluorescence detector, is one of the most selective detector and it allows the identification of fluorescent compounds in samples through their emitted fluorescence radiation. The emission intensity depends on excitation and emission wavelength, thus choosing suitable values it is possible to detect specific fluorescent species.

Multi-angle Laser Light Scattering detector (MALLS), is based on the principle that polymer particles in solution cause scattering phenomena to a laser incident beam focused into the sample cell. The scattered light is collected by several photodiodes detectors over a range of angles (i.e. 18 different angles from 5 to 175°) and it is proportional to the size of the scattering particles. It is considered an absolute analytical method as it provides molar mass values without requiring a standard calibration. Molar masses are calculated according to the light scattering theory (Debye 1947) which implies the dependence of scattered light intensity to the polymer concentration.

DMAc/LiCl as SEC SOLVENT FOR CELLULOSE

Cellulose solvents have to be compatible with the column stationary phase in order to perform SEC analyses. Thus, solvents as CED or Cadoxen cannot be used. Nowadays, the most widely used solvent system for cellulose in SEC experiments is lithium chloride/N-N-dimethylacetamide (LiCl/DMAc). Advantages in using DMAc/LiCl solution are numerous:

- It can be either used as cellulose solvent and SEC mobile phase:
- It provides good dissolution of cellulosic materials and solution obtained are stable, with negligible degradation phenomena;
- It is colourless, so that it can be used with light sensitive detectors.
- Several advantages lie behind the choice of DMAc/LiCl as the solvent in SEC analyses:

It is worth noting that cellulose is not directly dissolved in DMAc/LiCl. In fact, a preliminary **activation step** in required in order to make the highly packed crystalline domains accessible to the solvent. The most valuable activation method involved a preliminary water swelling followed by a DMAc exchange:

- *Swelling*. Cellulose has to be firstly activated with water to break down inter- and intra-hydrogen bonding in the material and swell it sufficiently to allow access to the larger and less polar DMAc molecules.

- *DMAc exchange*. Water has to be necessarily removed and exchanged for dry *DMAc* using solvent exchange techniques. This is an essential step of the procedure as water is believed to compete with the hydroxyl groups of the cellulose chain (Potthast et al. 2002a) whereas DMAc exchange hinders the inter- and intra-molecular bonds to form again[15]. Without this step, the DMAc/LiCl solvent cannot complex with the cellulose and dissolution cannot occur.

CELLULOSE FLUORESCENT LABELLING

The reliable and accurate determination of oxidized groups in cellulosic substrates, such as reducing ends, carbonyls and carboxyls, still represents a challenging aspect of cellulose characterization. Oxidized groups can be introduced by a variety of treatments and they affect both physical and optical properties of samples.

Potthast and Rosenau research group (Boku Universität, Vienna) has developed two remarkable fluorescent labelling techniques in order to identify carbonyl (CCOA method) and carboxyl (FDAM method) moieties in cellulosic samples. Moreover, the coupling of fluorescence labelling for the determination of functional groups with GPC measurements of cellulose provides the oxidized group profiles in relation to the molecular weight distribution, together with the average molecular mass of the samples (Mw, Mn, Mz, MMD). These methods are highly sensitive and very small amounts of samples are required. Both methodologies can be performed either in homogeneous or heterogeneous conditions, even though they usually provide analogous results. Nevertheless, if highly ordered domains in cellulose are affected by oxidation, the two approaches give different carbonyl-content values as heterogeneous labelling procedure largely disregards oxidized groups in crystalline areas owing to inaccessibility. Thus, in such cases, the homogeneous approach should be adopted to obtain valuable information on changes occurred in highly-ordered areas.

The two labelling techniques are briefly described below.

---

[15] The interference of water with cellulose dissolution has been verified by Emsley et al. (2000). By adding water to clear solutions of cotton paper prior to dissolution in DMAc/LiCl, a cloudy solution has been formed owing to the cellulose precipitation as a gel. Similar observations have occurred even in previous experiments when some residual water has been unintentionally left in the samples.

CCOA labelling

The method involves the use of the *carbazole-9-carboxylic acid [2-(2-aminooxy-ethoxy)ethoxy]amide* (*Carbazole-Carbonyl-OxyAmine, CCOA*) as carbonyl-selective fluorescence label for cellulose (Röhrling et al., 2001; Röhrling et al., 2002 b, c; Potthast et al. 2003). The labeling molecule is characterised by the carbazole fluorophore, an ethylene glycol spacer and an O-substituted hydroxylammina as anchoring group (Fig. [3].3).
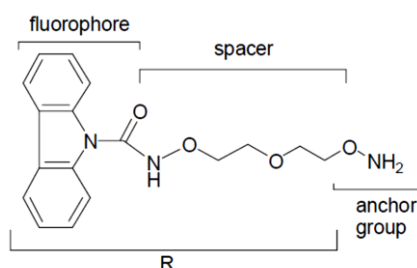

Fig. [3]. 3 – Structure of the fluorescence label carbazole-9-carboxylic acid [2-(2-aminooxy-ethoxy)-ethoxy]-amide (CCOA), abbreviated as R–O–NH2. (Rohrling at al. 2002a)

The labelling procedure involves the quantitative reaction of carbonyl functionalities with the anchoring groups thus leading to the formation of the corresponding oximes (Fig. [3].4).
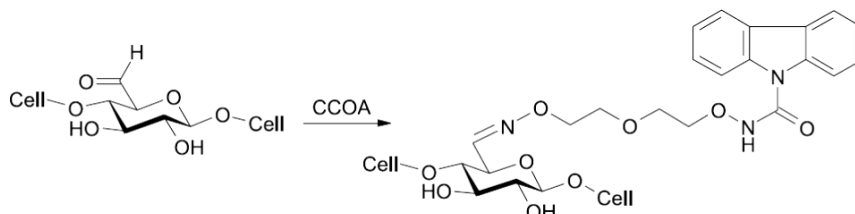
Fig. [3]. 4 – CCOA-labelling of 6-oxycellulose. (Potthast et al. 2006).

FDAM labelling

Several attempts to label carboxyl groups in carbohydrate model compounds have been carried out and reported in literature. Among all, the *9H-fluoren-2-yl-diazomethane* (*Fluorenyl-Di-Azo-Methane, FDAM*) has shown outstanding results on carbohydrate model compounds as well as on real cellulosic samples (Bohrn et al., 2004, 2005, 2006b).

Unlike the previuos method, the FDAM reagent has to be freshly synthesized by first reacting an hydrazine with 9*H*-fluorene-2-carbaldehyde, thus obtaining 9H-Fluorene-2-carbaldehyde hydrazone (Fig. [3].5).
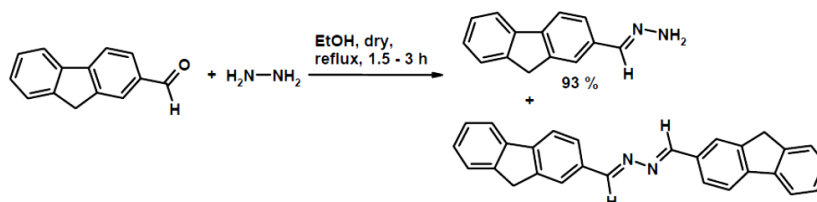
Fig. [3]. 5 – Conversion of 9H-fluorene-2-carbaldeyde with hydrazine to 9H-fluorene-2-carbaldehyde hydrazone and the corresponding dimeric aldazine as byproduct (Bohrn et al. 2004).

A subsequent hydrazone oxidation (with MnO2) leads to the sought diazomethane reagent (Fig. [3].6).
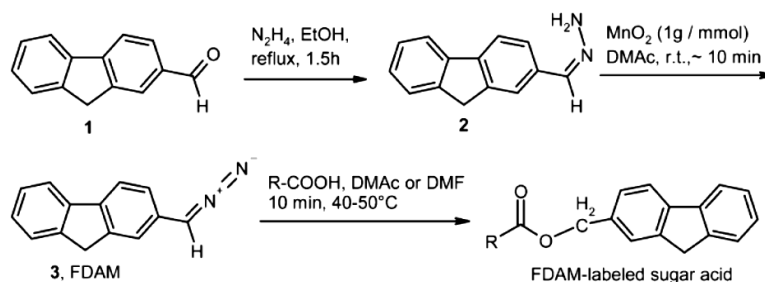
Fig. [3]. 6 – Syntesis of the carboxyl label Fluorenyl-Di-Azo-Methane (FDAM) and its reaction with a general sugar acid (RCOOH). (Bohrn et al., 2006b)

However, according to the reaction mechanism (Fig. [3].7)., the labelling procedure allow to detect only uronic acid moieties (C6-COOH).
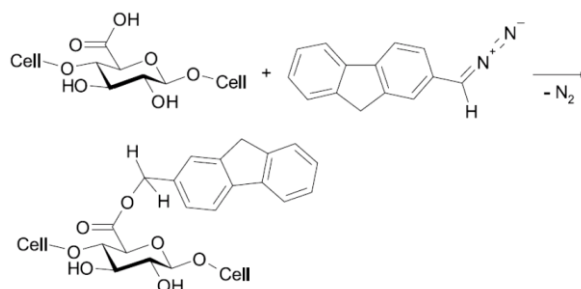
Fig. [3]. 7 – FDAM labelling of cellulose by the example of a C6-carboxylic (glucuronic) acid cellulose. (Potthast et al. 2006).

DATA INTERPRETATION

Molecular mass averages

Generally, polymers are constituted by molecules with different size. Along with the distribution of molar mass (MMD), MALLS detector specifically allow the simultaneous absolute determination of three of the most common molar mass averages (representing three moments of the distributions) and the number n_i of molecules of molar mass M_i in each slice of the resulting chromatogram. This yields to:

- **_number average weight (Mn)_**, which determines the number of particles. It is sensitive to the presence of low-MM components and defined as the total weight of polymer divided by the number of polymer molecules, according to the equation

$$M_n = \frac{\sum n_i M_i}{\sum n_i}$$

- **_weight average weight (Mw)_**, which determines the mass of particles. It reflects changes in the high-MM components, thus the more massive the chain, the more the chain contributes to M_w. It can be defined as

$$M_w = \frac{\sum n_i M_i^2}{\sum n_i M_i}$$

- **_z-average molecular weight (Mz)_**, is measured in some sedimentation equilibrium experiments and it is more sensitive to very high-MM components. It can be calculated by the equation

$$M_z = \frac{\sum n_i M_i^3}{\sum n_i M_i^2}$$

Additionally, another valuable parameter can be defined by the molar mass averages which is the **_polydispersity index_** (PDI). It is expressed as

$$PDI = \frac{M_w}{M_n}$$

and it represent the width of molecular mass distribution. The larger the polydispersity index, the broader the distribution. Thus, a monodisperse polymer characterised by equal chain lengths has a PDI = 1.

Interpretation of a molar mass distribution

The molecular mass distribution (MMD) obtained by SEC analyses is of paramount importance in characterizing polymers. A SEC-characterization of an ideal pure cellulose generally gives a Gaussian unimodal distribution of molar mass (MMD). Depending on parameter plot along the x-axis (retention volumes or logM), a peak maximum at lower retention volumes (or higher logM values) corresponds to cellulose samples with longer chains.

In order to obtain reliable MM values, the distribution of masses across the elution volume should be carefully evaluated. If it is linear, a good separation with no retention phenomena occurred and data obtained are reliable. Otherwise, analytical conditions (e.g. column packing materials) should be suitably changed in order to avoid non-adequate separation.

Carbonyl / Carboxyl content and profiles

The total amount of oxidized functionalities is calculated by integrating RI and fluorescence signals. By combining the fluorescence signal to the molecular weight distribution from MALLS detection, oxidized group profiles can be additionally obtained. Functional group profiles depict the variation in the concentration of such moieties with the molecular weight distribution (DS profiles, 'Degree of substitution'). Generally, carbonyl profiles increase (DS_{CO}) with decreasing Mw as several number of reducing-end groups are formed and can be consequently oxidized. due to the increasing number of reducing end groups available to be oxidized. Conversely, the carboxyl profile (DS_{COOH}) commonly shows a peak treand with decreasing values towards both big and small MW fragments.

IRON-GALL INKS.

A COMPUTATIONAL STUDY

TABLE OF CONTENTS

I

INTRODUCTION and AIM

As described in the first section of the present dissertation (Chap. 4.1), iron-gall inks are one of the most important ancient writing medium. Their widespread usage as well as their highly degrading power toward cellulose have been made them interesting materials to be investigated. Important historical objects in libraries and archives show noticeable degradation phenomena caused by the destructive effects of metallo-gallate inks interacting with cellulose and sizing. Comparable degradation effects are known also for other substrates of interest for cultural heritage (e.g. wool fibres). The chemical phenomenon of corrosion caused by iron gall inks has been intensively studied for many years. Acid hydrolysis and after-effects of Fenton reactions have been blamed (Hey 1981; Banik et al. 1988; Neevel 1995; Wagner and Bulska 2003; Rouchon-Quillet et al. 2004; Kolar and Strlic 2006; Kolar et al. 2006; Jančovičová et al. 2007; Rouchon et al. 2011).

Nonetheless, in spite of the many experimental investigations of iron-gall inks from a conservative point of view, studies by molecular modelling are surprisingly far from numerous (Jurinovich et al. 2012). Scarce information still present in the literature about the chemical structure and electronic features of these molecules makes some degradation pathways still unclear.

The aim of the present study is to improve the knowledge in metallo-gallate inks chemistry. To this end, a computational study has been carried out to ascertain the electronic configuration of the ground and the excited states of iron-gall complexes. This could give an insight into the electronic delocalization and the consequent oxidizing power of these species. This approach may be of paramount interest for the synthesis of new materials and the development of methodologies useful for preservation and restoration of archival holdings.

For these reasons, continuing recent computational studies on the coordination chemistry of group 8 elements (Bordignon and Bortoluzzi 2005; Bortoluzzi et al. 2007, 20011; Albertin et al. 2012), a computational Density Functional Theory (DFT) study on

electronic structures has been carried out. The theoretical research has been performed on

- a 3D model compound (which may represent a model for iron gall inks) by applying periodic boundary conditions combined with plane-waves calculations;

- mono- and tri-nuclear models.

Zaccaron, S., Ganzerla, R., Bortoluzzi, M., *Iron complexes with gallic acid: a computational study on coordination compounds of interest for the preservation of cultural heritage*, J Coord Chem 66, 1709-1719, 2013.

Zaccaron, S., Ganzerla, R., Bortoluzzi, M., *DFT calculations using periodic boundary conditions on an iron gall 3D coordination polymer of interest for cultural heritage conservation*, Sciences at Ca' Foscari 1, 58-62, 2013.

Zaccaron, S., Ganzerla, R., Bortoluzzi, M., *Computational studies on iron-based coordination polymers of interest in cultural heritage*, in conference proceedings of "I Congresso Nazionale della Divisione di Chimica Teorica e Computazionale della Società Chimica Italiana", 22-23 February 2012, Pisa, p 112.

Zaccaron, S., Bortoluzzi, M., Ganzerla, R., *Iron gall inks as 3D coordination polymers. A DFT study using periodic boundary conditions*, in conference proceedings of "II Congresso della Divisione di Chimica Teorica e Computazionale della Società Chimica Italiana", 20-22 February 2013, Padova, p 108.

II

BACKGROUND

Iron-gall inks have been anciently prepared by mixing tannins extracted from plants, vitriol and arabic gum. However, iron gall complexes can be currently synthesized by reacting an iron(II) salt, for example iron sulphate, with gallic acid (3,4,5-trihydroxybenzoic acid) under aerobic conditions in acidulated water. Moreover, iron gall derivatives can be obtained also starting from iron(III) salts, as an example hydrated $FeCl_3$. However, the molecular structures of most of the products of the reaction between tannins and iron salts are still not completely ascertained.

Krekel (1990; 1999) has first hypothesized the formation of **dinuclear complexes** of iron, such as that shown in Figure II.1, where the coordination of a conjugate base of gallic acid (H_4L = gallic acid, 3,4,5-trihydroxybenzoic acid) to formally iron(III) ions occurs through the phenate oxygen atoms. In such a model the ligands behave as chelating-bridging species. Decarboxylation after complexation is a subsequent reaction that is proposed in some cases.
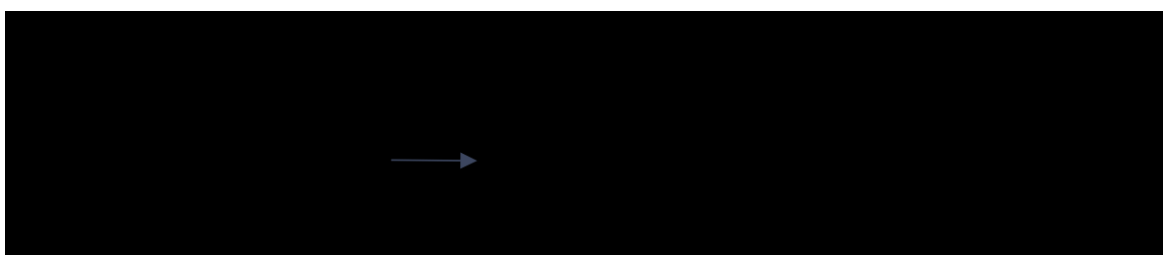
Fig. II. 1 – Example of hypothesized dinuclear structure for iron gall complexes by Krekel (1990).

Despite this hypothesis, experimental analyses have been by Wunderlich and co-workers (1991) performed. Iron-gall ink has been proposed as a coordination polymer where each subunit is characterised by three iron centres (**trinuclear complex**) (Fig. II.2). Single-crystal X-Ray diffraction measurements have been carried out on the

product formed by the reaction of iron(III) chloride and gallic acid. To the best of our knowledge, this compound is the only structurally characterized iron-gall dye.
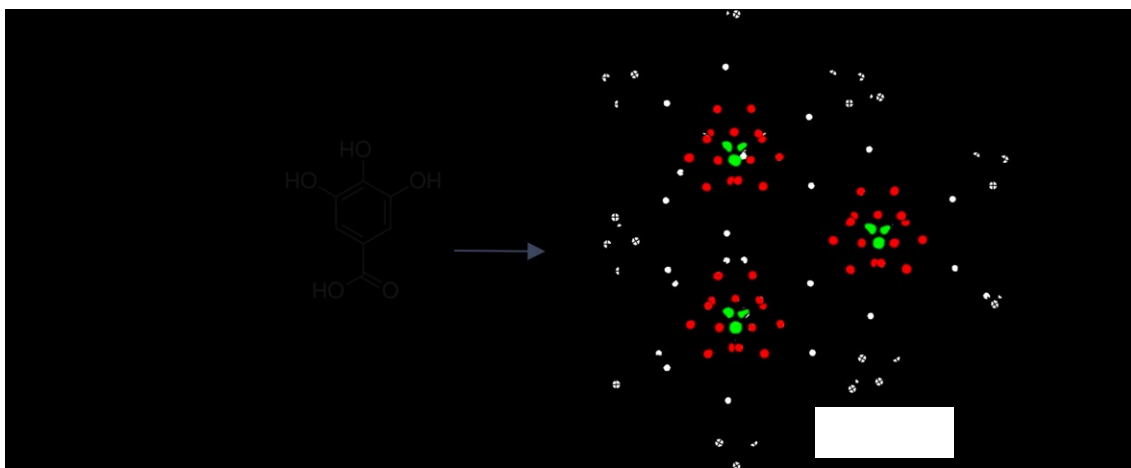

Fig. II. 2 – Molecular structure of the iron-gall complex obtained by Wunderlich et al (1991) through XRD analyses. Colours highlight iron (green) and oxygen atoms (red).

This species is a ***3D polymer*** having formula $[Fe(H_3O)(H_2O)(L)]_n$ and where several iron metal ions are coordinated by the conjugate base (L) of the gallic acid (H_4L). It is characterised by a trigonal space group with a = 8.664 Å, b = 8.664 Å, c = 10.861 Å, α = 90°, β = 90°, γ = 120° (symmetry group $P3_121$) and a cell volume equal to 706.05 Å^3. The excess of negative charge is neutralized by H_3O^+ cations. The iron centres have slightly distorted octahedral geometry with six Fe-O bonds, as shown in Figure II.3.
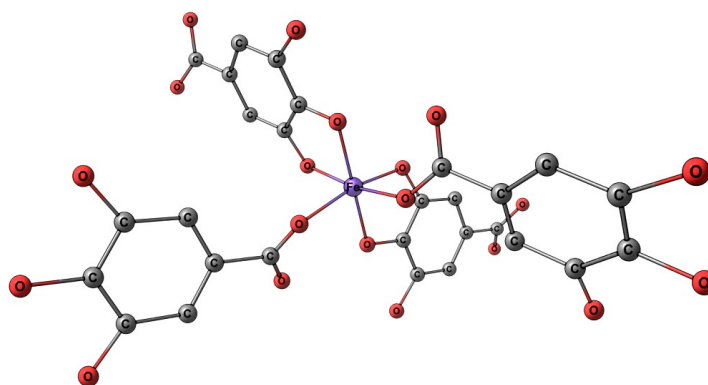
Fig. II. 3 – Octahedral coordination sphere around the iron centre in $[Fe(H_3O)(H_2O)(L)]n$.

Two oxygen atoms mutually in *cis* position belong to two separate carboxylic moieties and the corresponding Fe-O bond lengths are 2.006 Å. Other two L ligands are

mutually *cis* and coordinate the metal ion, each one with two phenate-type oxygen atoms. The corresponding Fe-O bonds are 2.000 Å (oxygen atoms in position 3 and 5) and 2.028 Å (oxygen atoms in position 4). Each carboxylate group behaves as bridging ligand between two iron centres, while the three phenate-type oxygen atoms of every ligand chelate two metal ions. The oxygen atom in *para* position with respect to carboxylate acts as bridging atom, as observable in Figure II.4.
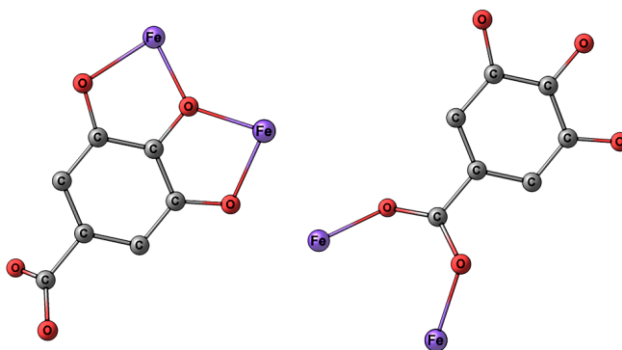

Fig. II. 4 – Coordination modes of the polydentate ligand in [Fe(H₃O)(H₂O)(L)]n. Left: coordination of the phenate oxygen atoms; right: coordination of the carboxylate moiety.

The deep blue colour of iron gall species is probably attributable to a strong electronic delocalisation among the metal ions, but no detailed study is currently present in the literature and real oxidation and spin states of the iron centres are not unambiguously ascertained.

III

3D COORDINATION POLYMER[16]

III. A MODEL STRUCTURE

The three-dimensional model compound $[(Fe_3L_3)_3-]_\infty$ has been built on the basis of the deposited X-Ray data regarding the product of the reaction between iron(III) chloride and gallic acid (Chap II; Wunderlich et al. 1991). Figure III.1 reports the 3D structures of the model under investigation, visualized along the three translation vectors.
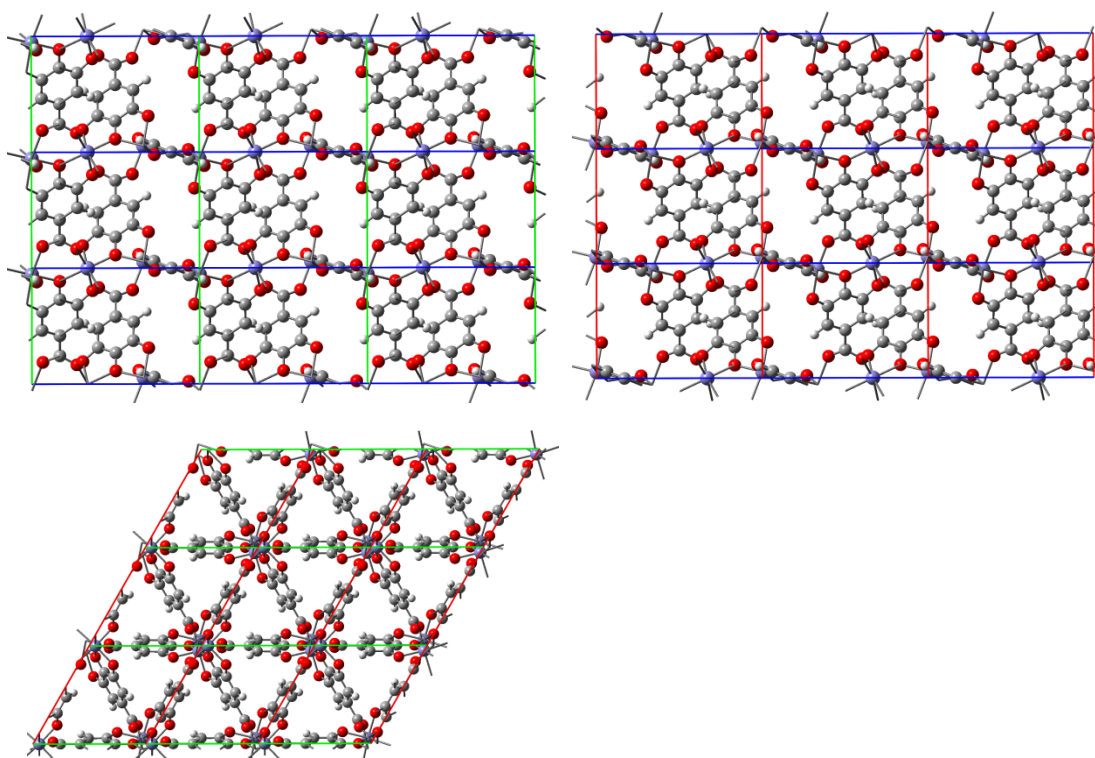

Fig. III. 1 – 3D structure of $[(Fe_3L_3)^{3-}]_\infty$, viewed along vector a (top left), b (top right) and c (bottom left).

[16] Zaccaron, S., Ganzerla, R., Bortoluzzi, M., *DFT calculations using periodic boundary conditions on an iron-gall 3D coordination polymer of interest for cultural heritage conservation*, Sciences at Ca' Foscari 1, 58-62, 2013. Zaccaron, S., Bortoluzzi, M., Ganzerla, R., *Iron gall inks as 3D coordination polymers. A DFT study using periodic boundary conditions*, in conference proceedings of "II Congresso della Divisione di Chimica Teorica e Computazionale della Società Chimica Italiana", 20-22 February 2013, Padova, p 108

The internal coordinates have not been changed with respect to the experimental values. Oxygen atoms present in the cavities of the 3D polymer (corresponding to water molecules or H3O+ cations) have been removed from the original structure. Hydrogen atoms have been added to the carbon atoms in position 2 and 6 of the aromatic rings using the following internal coordinates:

C-H bond lengths = 1.082 Å;
C_1-C-H angle = 120°;
C_{COO}-C_1-C-H dihedral angle = 0°.

The primitive cell has formula $(Fe_3L_3)^{3-}$.

III. B COMPUTATIONAL DETAILS

The periodic boundary conditions used are the same reported among the X-Ray data (i.e. trigonal space group, a = 8.664 Å, b = 8.664 Å, c = 10.861 Å, α = 90°, β = 90°, γ = 120°; cell volume = 706.05 Å3; symmetry group $P3_121$).

Single-point unrestricted DFT calculations have been carried out using the pure GGA functional PBE (Perdew et al. 1996; Cramer 2004) in combination with a plane-waves basis set (energy cutoff = 380 eV) (Young 2001; Jensen 2007). Ultrasoft pseudopotentials have been used to replace the electrons of the inner spheres (Vanderbilt 1990). Initial values of 15, 13, 11 and 9 have been considered for the number of unpaired electrons in the primitive cell of $[(Fe_3L_3)^{3-}]_\infty$.

The optimisation of spin multiplicity during self-consistent field calculations has been allowed and a SCF tolerance of 5.0E-7 eV/atoms has been used. The sampling of the Brillouin zone has been carried out with the scheme of Monkhorst and Pack (shrinking factors: a = 3; b = 3; c = 2, spacing comprised between 0.044 and 0.046 Å-1 in each of the three lattice directions) (Monkhorst and Pack 1976, 1977). Population analyses have been performed using the Mulliken (Mulliken 1955; Segall et al. 19996a, b; Sanchez-Portal et al. 1995) and Hirshfeld (Hirshfeld 1977) distributions.

Two sets of shrinking factors (a = 3; b = 3; c = 2 and a = 6; b = 6; c = 4) have been used for the simulation of the optical properties of the model compound and twelve empty bands have been considered in these last calculations.

The results on the ground-state electronic configuration have been verified by carrying out unrestricted PBE calculations with an atom-centred doubly-numerical

polarized basis set and DFT semi-core pseudopots (Delley, 1990, 2000b). The sampling of the primitive cell in the reciprocal space has been done as described above. SCF tolerance was set equal to 1.0E-6 eV/atoms.

The software used for calculations based on plane-waves is CASTEP (Clark et al. 2005), while DFT PBE calculations with numerical basis set have been carried out with Dmol^3 (Delley 2000a).

III. C RESULTS and DISCUSSION

Total electron density is essentially localized on the atoms and on the C-H, C-C, C-O and Fe-O bonds. No meaningful direct covalent interaction is present among the metal centres.

The most stable electronic configuration corresponds to the higher multiplicity, *i.e.* 15 unpaired electrons in each primitive cell. The comparison of the integral of spin density (7.50 hbar) with the integrated spin density for absolute values of spin states (7.55 hbar) indicates that ferromagnetic interaction is present among the primitive cells.

The energy values of the frontier bands (plane-waves calculations) indicate that the compound can be described as a semiconductor. In fact, the highest-occupied bands range from -0.05 to 0.00 eV (alpha spin) and from -0.30 to -0.29 eV (beta spin), while the lowest-unoccupied bands are comprised between 2.83 and 2.86 eV (alpha spin) and 0.65 and 0.67 eV (beta spin). Therefore, the minimum band gap is 0.65 eV. The same band gap value has been obtained from DFT PBE calculations based on numerical basis set.

Table III.1 reports the Mulliken charge analysis and the Mulliken and Hirshfeld spin distributions. Spin density results essentially localized on the iron centres and, to a lesser extent, on the phenate and carboxylate oxygen atoms, while it is virtually absent on the carbon atoms of the aromatic ring and of the carboxylate moiety. Interestingly, both Mulliken and Hirshfeld distributions agree with a spin density value for the iron centres of about 2 hbar, instead of the 2.5 hbar expected for high-spin iron(III) ions.

Atom type (a)	Mulliken charge	Mulliken spin	Hirshfeld spin
H (6)	0.27	0.00	0.00
C_1 (3)	-0.10	0.01	0.01
$C_2 - C_6$ (6)	-0.37	0.02	0.02
$C_3 - C_5$ (6)	0.17	0.00	0.01
C_4 (3)	0.06	0.02	0.02
C_{COO} (3)	0.56	0.00	0.02
$O_3 - O_5$ (6)	-0.65	0.11	0.10
O_4 (3)	-0.66	0.13	0.13
O_{COO} (6)	-0.62	0.06	0.06
Fe (3)	1.53	1.97 (b)	1.93 (c)

Tab. III. 1 – Mulliken and Hirshfeld charge (a.u.) and spin (hbar) distributions in the primitive cell of $[(Fe_3L_3)^{3-}]_\infty$ (plane-waves basis set). (a) Number of equivalent atoms in parentheses. (b) 2.00 hbar using numerical basis set. (c) 1.93 hbar using numerical basis set.

The computed values indicate the presence of high-spin iron(II) metal ions and this hypothesis is confirmed by the quite low Mulliken charge on the iron atoms. Moreover, a more detailed study of the electronic populations shows that the electronic configuration of the metal ions is essentially d^6, with five up electrons and one down electron. Therefore, the qualitative picture arising from charge and spin distributions corresponds to high-spin iron(II) metal centres (about 4 unpaired electrons) bridged by radical ligands of the type $[L^{3-}]^.$ (about one unpaired electron, delocalised mainly among the oxygen atoms). One of the steps of the formation of the coordination polymer synthesized by Wunderlich appears therefore the one-electron reduction of the iron(III) ions by the gallic acid (Kipton et al. 1982).

The simulation of the optical properties has been carried out in order to validate the model here proposed for the electronic structure of $[(Fe_3L_3)^{3-}]_\infty$. The calculated absorption spectrum, represented in Figure III.2, closely resembles the commonly reported spectra for iron-gall dyes, as shown by the comparison with the experimental spectrum depicted in figure III.3.
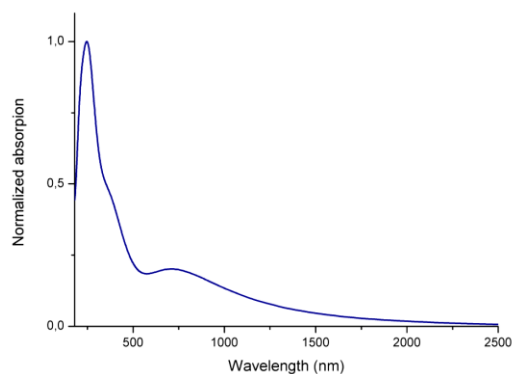
Fig. III. 2 – Simulated absorption spectrum of [(Fe3L3)3-]∞.
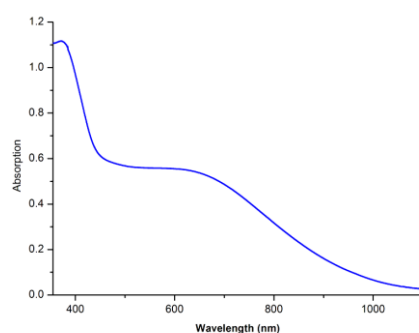

Fig. III. 3 – Experimental absorption spectrum of an iron gall ink.

In particular, besides the usual absorptions centred in the UV range, attributable to transitions inherent the gallic acid electronic structure, a very wide band centred in the red region is predicted, which is the origin of the deep blue colour of this class of compounds. Thus, the good agreement between experimental and theoretical electronic transitions confirms the reliability of the performed computational study about the ground-state electronic configuration of a 3D model for iron gall inks.

IV

MODEL COMPOUNDS[17]

IV. A MODEL STRUCTURES

Accordingly to the deposited X-Ray data (Chap. II; Wunderlich et al. 1991), mono- and tri-nuclear model compounds has been built.

As previously (Chap. III), the internal coordinates concerning the conjugate base of gallic acid (L) and its interactions with the iron centres have not been changed with respect to the experimental values. Hydrogen atoms have been added to the phenyl rings in position 2 and 6 and their coordinates have been optimised using the MMFF94 force field, keeping all the other atoms frozen (Halgren 1996, 1999). Further, hydrogens have been added on phenate and carboxylate oxygens to achieve the desired charge and their positions have been optimized using MMFF94.

Mono-nuclear model

The mono-nuclear structure under investigation is depicted in figure IV.1 and $[FeL_4H_{12}]^-$ and $[FeL_4H_{12}]^{2-}$ represent the two structure computationally studied.

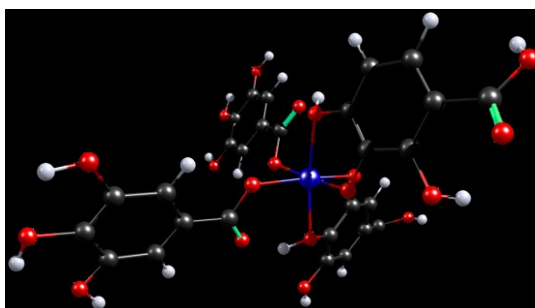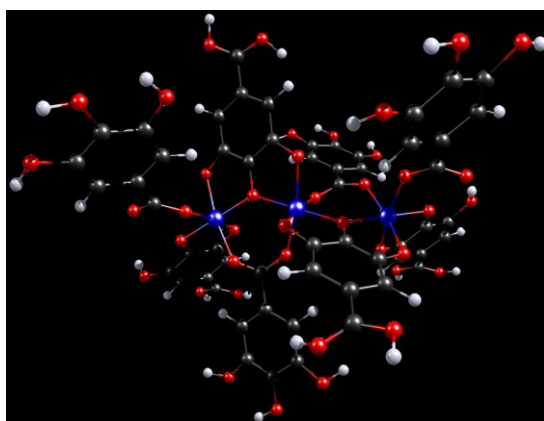*Fig. IV. 1 – Structure of the mono-nuclear models [FeL4H12]n- (n = 1, 2). The structure has been built on the basis of deposited XRD analyses (Wunderlich et al. 1991).*

---

[17] Zaccaron, S., Ganzerla, R., Bortoluzzi, M., *Iron complexes with gallic acid: a computational study on coordination compounds of interest for the preservation of cultural heritage*, J Coord Chem 66, 1709-1719, 2013. Zaccaron, S., Bortoluzzi, M., Ganzerla, R., *Iron gall inks as 3D coordination polymers. A DFT study using periodic boundary conditions*, in conference proceedings of "II Congresso della Divisione di Chimica Teorica e Computazionale della Società Chimica Italiana", 20-22 February 2013, Padova, p 108.

The resulting internal coordinates and the optimised C-H and O-H bond lengths for the mono-nuclear model are:

C-H bond length (average) = 1.086 Å
C_1-C-H angle (average) = 122.5°
C_{COO}-C_1-C-H dihedral angle (average) = 0.0°

O_{Ph}-H bond length (average) = 0.983 Å
O_{COO}-H bond length (average) = 0.985 Å

Tri-nuclear model

$[Fe_3L_8H_{22}]^-$ and $[Fe_3L_8H_{22}]^{2-}$ represent the tri-nuclear structures studied and they are graphically presented in figure III.2.

Fig. IV. 2 – Structure of the tri-nuclear models $[Fe_3L_8H_{22}]^{n-}$ (n = 1, 2). The structure has been built on the basis of deposited XRD analyses (Wunderlich et al. 1991).

The resulting internal coordinates and the optimised C-H and O-H bond lengths for the tri-nuclear model are:

C-H bond length (average) = 1.086 Å
C_1-C-H angle (average) = 123.8°
C_{COO}-C_1-C-H dihedral angle (average) = 0.4°

O_{Ph}-H bond length (average) = 0.975 Å
O_{COO}-H bond length (average) = 0.985 Å.

By considering the formal presence of Fe^{3+} ions and tetra-anionic L ligands, additional hydrogen atoms have been added on phenate and carboxylate oxygen atoms in order to obtain a total charge of -1.

1D periodic model

The mono-dimensional model $[Fe_3L_6H_{15}]_\infty$ is presented in figure IV.3. Periodicity along the translation vector c (10.861 Å) has been maintained with respect to the original structure, together with all the internal coordinates concerning the C-C, C-O and Fe-O bonds.
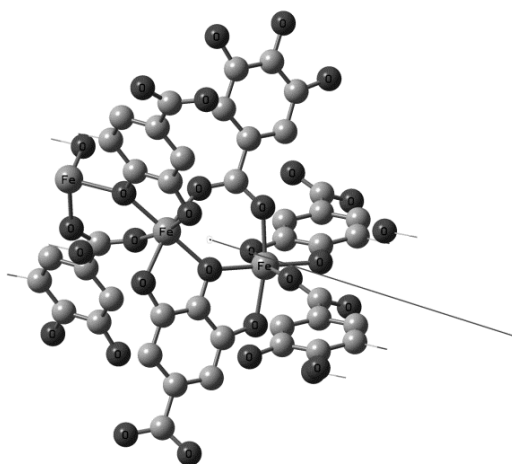

Fig. IV. 3 – Structure of the primitive cell of $[Fe_3L_6H_{15}]_\infty$ and translation vector c. Hydrogen atoms have been omitted for graphical clarity.

Hydrogens have been added on the phenyl rings in positions two and six and on oxygens in order to obtain a neutral primitive cell (owing to the presence of formally Fe^{3+} centres and L^{4-} ligands). A mesh of 62 points has been used for the sampling of the reciprocal space (Monkhorst and Pack 1976, 1977).

IV. B COMPUTATIONAL DETAILS

DFT (Density Functional Theory) calculations have been carried out without symmetry constrains using the PBEPBE pure DFT Generalized Gradient Approximation (GGA) functional (Perdew et al. 1996) and two hybrid DFT functionals, B3PW91 (Becke 1988, 1993; Ziegler 1991; Greelings et al. 2003) and M06 (Zhao and Truhlar 2008).

Split-valence double- and triple-ζ quality basis sets and small-core pseudopotentials for the iron atoms have been used. In particular, double-ζ quality calculations have been performed using the D95V basis set (Dunning 1971; Dunning and Hay 1976) for

carbon, oxygen and hydrogen atoms and the ECP-based SDD basis set for iron atoms (Schwerdtfeger et al. 1989; Bergner et al. 1993). A further refining has been carried out for selected cases using the polarized 6-311G(d,p) basis set on C, O and H (McLean and Chandler 1980) and the polarized ECP-based LANL2TZ(f) basis set on Fe (Hay and Wadt 1985; Roy et al. 2008).

Implicit solvation has been added for non-periodic models by applying the C-PCM model for water, using Universal Force Field atomic radii (Barone and Cossi 1998; Cossi et al. 2003).

The same computational approaches have been applied for the optimisation $[Fe(H_2O)_6]^{n+}$ (n = 2, sextet state; n = 3, quintet state) and $[Fe(EDTA)]^{n-}$ (n = 1, sextet state; n = 2, quintet state; H_4EDTA = Etylenediaminetetraacetic acid), used as comparing structure complexes.

The simulations of the UV-VIS transitions of the radical species $[L\cdot]^{3-}$, $[H_2L\cdot]^-$ and $[H_3L\cdot]$ (doublet state; hydrogen atoms on the phenate oxygen atoms) have been carried out, after geometry optimisation, on the basis of the TD-SCF approach (Cramer 2004). The DFT methods here applied have been verified by comparing the simulated (harmonic approximation) and experimental IR spectra of gallic acid (Cramer 2004).

In all the calculations the unrestricted approach has been used and the absence of meaningful spin contamination has been verified through the comparison of the computed $<S^2>$ values with the theoretical ones (Cramer 2004). Population analyses have been performed on the basis of the Mulliken, Natural and Hirshfeld distributions (Mulliken 1955; Hirshfeld 1977; Reed et al. 1988).

All the calculations based on density functional theory have been carried out with Gaussian 09 (VV.AA 2010). Preliminary MMFF94 optimisations of the positions of the hydrogen atoms have been performed with Spartan 08 (Hehre 2003; Spartan08 2009).

IV.C   RESULTS and DISCUSSION

Electron density

For both mono- and tri-nuclear compounds, the electron density is essentially localized on the non-metal atoms and on the C-H, C-C, C-O and Fe-O bonds. No meaningful direct covalent interaction is present among the metal centres (Fig. IV.4), similarly to the 3D coordination polymer (Chap. III).
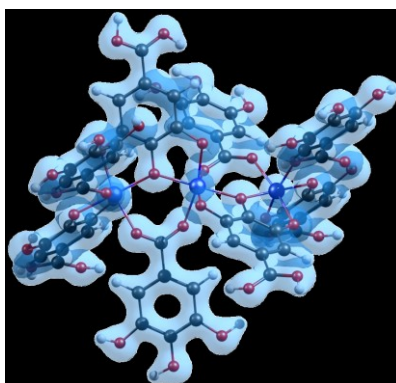
Fig. IV. 4 – Electron density for [Fe$_3$L$_8$H$_{22}$]$^{n-}$ (n = 1, 2). No direct covalent bond among iron centres is present.

Spin multiplicity

Calculations have been carried out with several DFT functionals in order to ascertain the ground-state multiplicity of [FeL$_4$H$_{12}$]$^{n-}$ and [Fe$_3$L$_8$H$_{22}$]$^{n-}$ (n = 1, 2). All the computational models used (PBEPBE, B3PW91 and M06 DFT functionals) have led to comparable results and in all the cases the highest multiplicity corresponds to the most stable ground-state electronic structure. In particular, the energy difference between high-spin (sextet state) and low-spin (doublet state) configurations for [FeL$_4$H$_{12}$]$^-$ is around 60 Kcal mol^{-1}. The high-spin state (quintet) of [FeL$_4$H$_{12}$]$^{2-}$ is more stable by about 50 Kcal mol^{-1} with respect to the singlet configuration. For [Fe$_3$L$_8$H$_{22}$]$^-$ and [Fe$_3$L$_8$H$_{22}$]$^{2-}$ the pairing of two electrons with respect to the highest multiplicities (15 and 14 unpaired electrons, respectively) causes a strong energy rise, more than 30 Kcal mol^{-1} in the first case and about 40 Kcal mol^{-1} for the second complex. Additional electron pairings cause a further growth of the total energy for both the models. The greatest stability of the systems having the maximum number of unpaired electrons is confirmed by DFT PBEPBE calculations carried out on the linear periodic model [Fe$_3$L$_6$H$_{15}$]$_\infty$. Also in this case the most stable electronic configuration corresponds to the maximum multiplicity, *i.e.* 15 unpaired electrons in the primitive cell.

The results about spin multiplicity obtained for [Fe$_3$L$_8$H$_{22}$]$^-$ and [Fe$_3$L$_6$H$_{15}$]$_\infty$ nicely agree with plane-waves GGA DFT calculation results previously described (Chap. III.C).

Spin density

As far as the atomic spin density is concerned, the most stable electronic configuration (*i.e.*, highest multiplicity) has been taken into consideration for [FeL$_4$H$_{12}$]$^{n-}$ and [Fe$_3$L$_8$H$_{22}$]$^{n-}$ (n = 1, 2) models. As shown by values in tables IV.1 and IV.2, the spin density is essentially localized on the iron centres and, to a lesser extent, on

the phenate and carboxylate oxygen atoms bonded to the iron atoms (Fig. IV.5). On the other oxygen atoms as well as on the carbon atoms of the aromatic rings and of the carboxylate moieties the spin density is meaningfully lower whereas it is virtually zero on the hydrogen atoms.

Atom	$[FeL_4H_{12}]^-$		$[FeL_4H_{12}]^{2-}$	
	Mulliken	Hirshfeld[a]	Mulliken	Hirshfeld[a]
Fe[b]	4.1756	4.1166	3.7710	3.6254
O (Fe–O carboxylate)	0.0993	0.1048	0.0132	0.0408
O (Fe-O phenate)	0.1279	0.1319	0.0303	0.0523
O (not coordinated)	0.0019	0.0017	0.0012	0.0013
C (carboxylate)	−0.0005	0.0033	0.0058	0.0051
C (phenate)	0.0038	0.0046	0.0017	0.0019
H(CH)	−0.0004	–	0.0000	–
H(OH)	0.0002	–	0.0001	–

Tab. IV. 1 – Atomic spin densities (M06/C-PCM calculations, a.u. average values) for $[FeL_4H_{12}]^{n-}$ (n = 1, sextet; n = 2, quintet). [a] Hydrogen atoms summed into heavy metals. [b] Natural atomic spin density on Fe for $[FeL_4H_{12}]^- = 3.9860$ a.u.; for $[FeL_4H_{12}]^{2-} = 3.6061$ a.u.

Atom	$[Fe_3L_8H_{22}]^-$		$[Fe_3L_8H_{22}]^{2-}$	
	Mulliken	Hirshfeld[a]	Mulliken	Hirshfeld[a]
Fe[b]	4.1832	4.1393	4.1001	4.0312
O (Fe–O carboxylate)	0.0860	0.0940	0.0666	0.0781
O (Fe-O phenate)	0.1628	0.1615	0.1303	0.1293
O (not coordinated)	0.0021	0.0024	0.0005	0.0000
C (carboxylate)	0.0056	0.0080	−0.0179	−0.0019
C (phenate)	0.0047	0.0058	0.0025	0.0031
H(CH)	−0.0002	–	0.0003	–
H(OH)	0.0001	–	0.0001	–

Tab. IV. 2 – Atomic spin densities (M06/C-PCM calculations, a.u. average values) for $[Fe_3L_8H_{22}]^-$ (15 unpaired electrons) and $[Fe_3L_8H_{22}]^{2-}$ (14 unpaired electrons). [a] Hydrogen atoms summed into heavy metals. [b] Natural atomic spin density on Fe for $[Fe_3L_8H_{22}]^- = 4.0017$ a.u.; for $[Fe_3L_8H_{22}]^{2-} = 3.9206$ a.u.

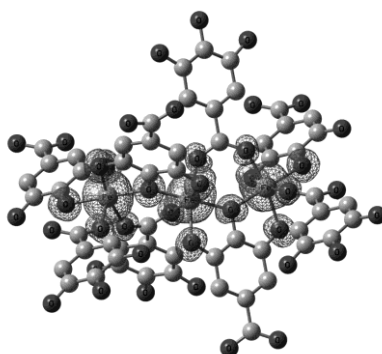*Fig. IV. 5 – Plot of the spin density for $[Fe_3L_8H_{22}]^-$ (15 unpaired electrons, M06/C-PCM). Hydrogen atoms have been omitted for graphical clarity*

The expectable electronic structures for both the mono-nuclear $[FeL_4H_{12}]^-$ and the tri-nuclear $[Fe_3L_8H_{22}]^-$ compounds should be formally iron(III) complexes stabilized by diamagnetic conjugated bases of gallic acid. However, data in Tables IV.1 – IV.2 do not support such an idea. In fact, in all cases spin densities are meaningfully closer to the values expected for high-spin iron(II) metal ions. A more detailed population analysis based on both the Mulliken and the Natural approaches is in agreement with a d^6 configuration of the metal centres, with five up electrons and one down electron. The residual spin density, localised on the coordinated oxygen atoms of the ligands, phenate-type in particular, is probably due to the fact that gallic acid molecules in these compounds behave as radical species, because a formal ligand-to-metal reduction has occurred (Kipton et al. 1982; Carter 2007).

Comparable results have been obtained from PBEPBE calculations on the 1D coordination polymer $[Fe3L6H15]\infty$, where the average spin density on the iron centres of the primitive cell is about 4 a.u. (Mulliken: 4.108 a.u.; Hirshfeld: 4.080 a.u.) and the residual spin densities are mainly on the coordinated phenate (Mulliken: 0.1481 a.u.; Hirshfeld: 0.1787 a.u.) and carboxylate (Mulliken: 0.1083 a.u.; Hirshfeld: 0.1283 a.u.) oxygens.

Regarding the optical behaviour on the investigated species, it is first worth remembering that iron-gall inks are characterised by an intense blue colour. Considering the obtained computational results, this could be attributed to the pseudo-radical electronic structure of the conjugate bases of gallic acid in such complexes. Effectively, simulated UV-VIS spectra of gallic acid radical species (i.e., $[L\cdot]^{3-}$, $[H_2L\cdot]^-$ and $[H_3L\cdot]$) confirm such hypothesis, showing absorption bands centred at the end of the red region or at the beginning of the NIR region. As an example, the simulated UV-Vis spectrum of $[L\cdot]^{3-}$ depicted in Figure IV.6 predicts a low-energy band having wavelength comparable with those commonly reported for iron gall inks (Figure III.3).
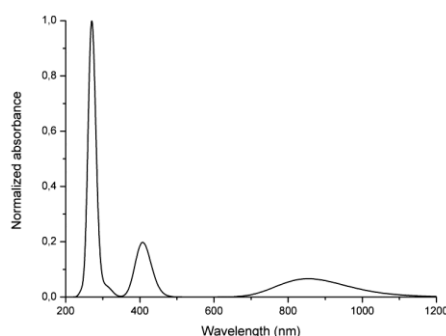

Fig. IV. 6 – Simulated UV-Vis absorption spectrum of [L·]3- (FWHM = 3000 cm-1).

The addition of one electron to $[FeL_4H_{12}]^-$ and $[Fe_3L_8H_{22}]^-$ leads to doubly negative charged systems. Nevertheless, the spin density remains mainly localised on iron and coordinated oxygen atoms as confirmed by data previously reported. In particular, by comparing the two $[Fe_3L_8H_{22}]^{n-}$ systems (n = 1 and 2) the average value for the difference between the spin density on the metal centres is negligible, around 0.08 a.u. by considering the Mulliken and Natural analyses and around 0.11 a.u. using the Hirshfeld population analysis. The addition of one electron to $[Fe_3L_8H_{22}]^-$ leads instead to a reduction of spin density mainly for the sum of the atoms constituting the organic ligands.

The fact that the one-electron reduction has a scarce influence on the electronic configuration of iron ions is confirmed by the comparison of the iron atomic charges between $[Fe_3L_8H_{22}]^-$ and $[Fe_3L_8H_{22}]^{2-}$. In the first case, average values of 0.605 a.u. (Mulliken) and 1.255 (Natural) have been computed (M06/C-PCM calculations) and quite similar average charge have been obtained for the reduced compound, 0.533 a.u. (Mulliken) and 1.181 (Natural). The behaviour towards reduction of $[Fe_3L_8H_{22}]^-$, in particular the apparently scarce role of the metal centres, can be explained from the study of the molecular orbitals of this compound. In particular, the lowest energy unoccupied orbitals are mainly localized on the π-systems of the coordinated ligands and not on the metal centres, as observable for example in Figure IV.7.
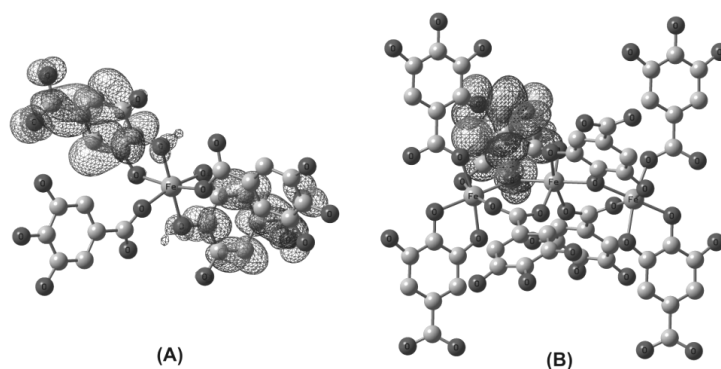

Fig. IV. 7 – Plot of the LUMOs of $[FeL_4H_{12}]^-$ (A) and $[Fe_3L_8H_{22}]^-$ (B)).

Computed data for $[FeL_4H_{12}]^{n-}$ systems allow considerations comparable with those described for the tri-nuclear models. For both the oxidized and the reduced model, spin densities on the metal centre are near the ideal value for free high-spin Fe(II) ions. Moreover, the one-electron reduction leads to a decrease of spin density over the coordinated ligands also for the simpler model $[FeL_4H_{12}]^-$. In fact, as for $[Fe_3L_8H_{22}]^-$, also

for $[FeL_4H_{12}]^-$ the low-energy unoccupied orbitals are localized on the conjugate bases of gallic acid (see Figure IV.7).

Energies ($E+\Delta G_{solv}$) of the mono- and tri-nuclear complexes in oxidized and reduced forms have been used to study the relative oxidizing potentials of these models for iron gall inks (Cossi et al. 2006). Data are collected in Table IV.3, together with those obtained at the same computational level for the systems $[Fe(H_2O)_6]^{n+}$ (n = 2, sextet state; n = 3, quintet state) and $[Fe(EDTA)]^{n-}$ (n = 1, sextet state; n = 2, quintet state), used as references.

Model	Oxidized form	Reduced form
$[FeL_4H_{12}]^{n-}$	-2706.02468	-2706.14008
$[Fe_3L_8H_{22}]^{n-}$	-5534.66343	-5534.77144
$[Fe(H_2O)_6]^{n+}$	-581.90970	-582.13523
$Fe(EDTA)^{n-}$	-1223.16037	-1223.29129

Tab. IV. 3 – *Energy values ($E+\Delta G_{solv}$, M06/C-PCM, a.u.) for the systems $[FeL_4H_{12}]^{n-}$, $[Fe_3L_8H_{22}]^{n-}$ (n = 1, 2), $[Fe(H_2O)_6]^{n+}$ (n = 2, 3) and $[Fe(EDTA)]^{n-}$ (n = 1, 2).*

The energy difference calculable from the data presented in Table IV.3 for the $[Fe(H_2O)_6]^{n+}$ couple is -0.22553 a.u. and corresponds to an experimental reduction potential (vs. NHE) of 0.77 V (Greenwood and Earnshaw 1984). The energy variation from the oxidized to the reduce form of the iron-EDTA complex, -0.13092 a.u., is instead related to an experimental potential value of -0.12 V (Greenwood and Earnshaw 1984). Assuming a liner relationship between experimental and computed data, is it possible to estimate the reduction potentials of $[FeL_4H_{12}]^-$ and $[Fe_3L_8H_{22}]^-$. Both the mono and tri-nuclear models proposed for iron-gall inks have quite negative potentials for the one-electron reduction, about –0.27 V for the mono-nuclear system and –0.34 V for the tri-nuclear complex. Moreover, it is interesting that the most negative potential is the one of the most complex system, *i.e.* that more similar to the experimental structure. The reduction of $[FeL_4H_{12}]^-$ is in fact about 5 Kcal mol^{-1} more favoured than that of $[Fe_3L_8H_{22}]^-$. However, in both cases the estimated potentials indicate a quite scarce oxidizing behaviour of the iron complexes with gallic acid.

V

CONCLUSIONS

The results obtained on 3D periodic models strongly support the idea that a qualitatively correct description of the electronic structures of these compounds could be based on the presence of high-spin Fe(II) metal ions coordinated to partially oxidized conjugate bases of gallic acid. This suggestion has been further corroborated by the computational results reported on simple mono- and tri-nuclear models for iron gall inks. The partially radical character of the oxygen-donor polydentate ligands in these complexes can also explain the absorption properties of these materials.

Regarding the oxidizing power of such species, the computed energy variations associated to one-electron reductions and their comparison with data obtained for other known iron complexes suggests that the direct oxidation of substrates of interest in the field of cultural heritage by iron gall inks is an improbable pathway for the commonly observed corrosive reactions.

VI

REFERENCES

Albertin, G., Albinati, A., Antoniutti, S., Bortoluzzi, M., S. Rizzato, S., *Preparation of half-sandwich ethylenecomplexes of osmium(II)*, J. Organomet. Chem. 702, 45-51, **2012**

Banik, G., Stachelberger, H., Messner, K., *Untersuchung der destruktiven Wirkung von Tinten auf Schriftträgermaterialien*, Restauro 94 (4), 302-308, **1988**

Barone, V., Cossi, M., Quantum Calculation of Molecular Energies and Energy Gradients in Solution by a Conductor Solvent Model, J. Phys. Chem. A 102, 1995-2001, **1998**

Becke, A. D., *Density functional thermochemistry. III. The role of exact Exchange*, J. Chem. Phys. 98, 5648-5652, **1993**

Becke, A. D., *Density-functional exchange-energy approximation with correct asymptotic behavior*, Phys. Rev. A 38, 3098-3100, **1988**

Bergner, A., Dolg, M., Kuechle, W., Stoll, H., Preuss, H., *Ab-initio Energy-Adjusted Pseudopotentials for Elements of Groups 13 - 17* , Mol. Phys. 80, 1431, **1993**

Bordignon, E., Bortoluzzi, M., *Aryldiazenido complexes of ruthenium(II) with tris(pyrazolyl)borate: A DFT study*, Inorg. Chem. Commun. 8, 763-765, **2005**

Bortoluzzi, M., Bordignon, E., Paolucci, G., Pitteri, B., *A computational study on mixed-ligand N2P3 donor-set iron(II) and ruthenium(II) classical and non-classical hydrides*, in Polyhedron 26, 4936-4940, **2007**

Bortouzzi , M., Paolucci, G., Pitteri, B., *Ground-state properties of ruthenium(II) and osmium(II) tin trihydride complexes: a DFT study*, Polyhedron 30, 1524-1529, **2011**

Carter, M. C., *Correlation of electronic transitions and redox potentials measured for pyrocatechol, resorcinol, hydroquinone, pyrogallol, and gallic acid with results of semi-empirical molecular orbital computations – A useful interpretation tool,* J. Mol. Struct. 831, 26-36, **2007**

Clark, S. J., Segall, M. D., Pickard, C. J., Hasnip, P. J., Probert, M. J., Refson, K., Payne, M. C., *First principles methods using CASTEP*, Z. Krist. 220, 567-570, 2005

Cossi, M., Rega, N., Scalmani, G., Barone, V., *Energies, structures, and electronic properties of molecules in solution with the C-PCM solvation model*, J. Comput. Chem. 24, 669-681, **2003**

Cossi, M., Iozzi, M. F., Marrani, A.G., Lavecchia, T., Galloni, P., Zanoni, R., Decker., F., *Measurement and DFT Calculation of Fe(cp)2 Redox Potential in Molecular Monolayers Covalently Bound to H–Si(100)*, J. Phys. Chem. B 110, 22961-965, **2006**

Cramer, C. J., *Essentials of Computational Chemistry, 2nd ed.*, John Wiley and Sons Ed., Chichester, **2004**

Delley, B., *An All-Electron Numerical Method for Solving the Local Density Functional for Polyatomic Molecules*, J. Chem. Phys. 92, 508-517, **1990**

Delley, B., *From molecules to solids with the DMol3 approach*, J. Chem. Phys. 113, 7756-7764, **2000a**

Delley, B., *Hardness conserving semilocal pseudopotentials*, Phys. Rev. B 66, 155125-133, **2002b**

Dunning, T. H., *Gaussian Basis Functions for Use in Molecular Calculations. III. Contraction of (10s6p) Atomic Basis Sets for the First-Row Atoms,* J. Chem. Phys. 55, 716, **1971**

Dunning, T. H., Hay, P. J., in *Modern Theoretical Chemistry Vol. 3*, Ed. H.F. Schafter, Plenum Press, New York, 1–28, **1976**

Gaussian 09, Revision B.01, VV.AA, Gaussian, Inc., Wallingford, CT, **2010**

Greenwood, N.N., Earnshaw, A., *Chemistry of the Elements*, Pergamon Press, Oxford, **1984**

Geerlings, P., De Proft, F., Langenaker, W., *Conceptual density functional theory*, Chem. Rev. 103, 1793-1873, **2003**

Halgren, T. A., *Merck molecular force field*, J. Comput. Chem. 17, 490-641, **1996**

Halgren, T. A., *MMFF VI. MMFF94s option for energy minimization studies*, J. Comput. Chem. 20, 720-729, **1999**

Hay, P. J., Wadt, W. R., *Ab initio effective core potentials for molecular calculations. Potentials for K to Au including the outermost core orbitals*, J. Chem. Phys. 82, 299-310, **1985**

Hehre, W. J., *A Guide to Molecular Mechanics and Quantum Chemical Calculations*, Wavefunction, Inc., Irvine, CA, **2003**

Hey, M., *The Deacidification and Stabilisation of Irongall Inks,* Restaurator 5, 24-44, **1981**

Hirshfeld, F. L., *Bonded-atom fragments for describing molecular charge densities*, Theoret. Chim. Acta 44, 129-138, **1977**

McLean, A. D., Chandler, G. S., *Contracted Gaussian basis sets for molecular calculations. I. Second row atoms, Z=11–18*, J. Chem. Phys. 72, 5639, 1980

Monkhorst, H. J., Pack, J. D., On *Special Points for Brillouin Zone Integrations*, Phys. Rev. B 13, 5188, **1976**

Monkhorst, H. J., Pack, J. D., On *Special Points for Brillouin Zone Integrations*, Phys. Rev. B 16, 1748, **1977**

Mulliken, R., S., *Electronic Population Analysis on LCAOMO Molecular Wave Functions*, J. Chem. Phys. 23, 1833-1840, **1955**

Neevel, J.G., *Phytate: a Potential Conservation Agent for the Treatment of Ink Corrosion Caused by Irongall Inks*, Restaurator 16 (3), 143-160, **1995**

Perdew, J. P., Burke, K., Ernzerhof, M., *Generalized Gradient Approximation Made Simple*, Phys. Rev. Lett. 77, 3865, **1996**

Roy, L. E., Hay, P. J., Martin, R. L., *Revised basis sets for the LANL effective core potentials*, J. Chem. Theory Comput. 4, 1029-1031, **2008**

Rouchon, V., Duranton, M., Burgaud, C., Pellizzi, E., Lavédrine, B., Janssens, K., de Nolf, W., Nuyts, G., Vanmeert, F. K., Hellemans, K., *Room-Temperature Study of Iron Gall Ink Impregnated Paper Degradation under Various Oxygen and Humidity Conditions: Time-Dependent Monitoring by Viscosity and X-ray Absorption Near-Edge Spectrometry Measurements*, Anal Chem 83, 2589-2597, **2011**

Rouchon Quillet, V., Remazeilles, C., Nguyen, T. P., Bleton, J., Tchapla, A., *The impact of gum arabic on iron gall ink corrosion*, Proceedings of the International Conference Durability of Paper and Writing November 16–19 Ljubljana, Slovenia, 56-58, **2004**

Schwerdtfeger, P., Dolg, M., Schwarz, W. H. E., Bowmaker, G. A., Boyd, P. D. W., *Relativistic effects in gold chemistry. I. Diatomic gold compounds,* J. Chem. Phys. 91, 1762-1774, **1989**

Spartan 08, Version 1.1.1, Wavefunction, Inc., Irvine, CA, **2009**

Jančovičová, V., Ćeppan, M., Havlínová, B., Reháková, M., Jakubíková, Z., *Interactions in iron gall inks*, Chem Pap 61, 391-397, **2007**

Jensen, F., *Introduction to Computational Chemistry*, 2nd Ed., John Wiley and Sons, Chichester, **2007**

Jurinovich, S., Degano, I., Mennucci, B., *A Strategy for the Study of the Interactions between Metal-Dyes and Proteins with QM/MM Approaches: the Case of Iron-Gall Dye*, J Phys Chem B 116, 13344-52, **2012**

Kipton, H., Powell, J., Taylor M. C., *Interactions of Iron(II) and Iron(III) with Gallic Acid and its Homologues: a Potentiometric and Spectrophotometric Study*, Aust J Chem 35, 739-756, **1982**

Kolar, J., Strlic., M. Eds., *Iron Gall Inks: On Manufacture, Characterisation, Degradation, And Stabilisation*, National and University Library, Ljubljana, **2006**

Kolar, J., Štolfa, A., Strlič, M., Pompe, M., Pihlar, B., Budnar, M., Simčič, J., Reissland, B., *Historical iron gall ink containing documents - Properties affecting their condition*, Anal Chim Acta 555, 167-174, **2006**

Krekel, C., *Chemische Untersuchungen an Eisengallustinten und Anwendung der Ergebnisse bei der Begutachtung mittelalterlicher Handschriften*, Diplomarbeit, Georg August Göttingen Institut für Anorganische Chemie, **1990**

Krekel, C., *Chemische Struktur historischer Eisengallustinten*, In Tintenfrassschäden und ihre Behandlung, Banik, G., and Weber, H., Ed., W. Kohlhammer GmbH, Stuttgart - Germany, 25-36, **1999**

Reed, A. E., Curtiss, L. A., Weinhold., F., *Intermolecular interactions from a natural bond orbital, donor-acceptor viewpoint* , Chem. Rev. 88, 899-926, **1988**

Sanchez-Portal, D., Artacho, E., Soler, J. M., *Projection of plane-wave calculations into atomic orbitals*, Solid State Commun. 95, 685-690, **1995**

Segall, M. D., Pickard, C. J., Shah, R., Payne, M. C., *Population Analysis in Plane Wave Electronic Structure Calculations*, Mol. Phys. 89, 571-577, **1996a**

Segall, M. D., Shah, R., Pickard, C. J., Payne, M. C., *Population analysis of plane-wave electronic structure calculations of bulk materials*, Phys. Rev. B 54, 16317-16320, **1996b**

Vanderbilt, D., *Soft self-consistent pseudopotentials in a generalized eigenvalue formalism*, Phys. Rev. B 41, 7892-7895, **1990**

Wagner, B., Bulska, E., *Towards a new conservation method for ancient manuscripts by inactivation of iron via complexation and extraction,* Anal Bioanal Chem 375, 1148-1153, **2003**

Wunderlich, C. H., Weber, R., Bergerhoff, G., *Über Eisengallustinte*, Z Anorg Allg Chem 598, 371-376, **1991**

Young, D. C., *Computational Chemistry: A Practical Guide for Applying Techniques to Real-World Problems*, John Wiley and Sons, Chichester, **2001**

Zhao, Y., Truhlar, D. G., *The M06 suite of density functionals for main group thermochemistry, thermochemical kinetics, noncovalent interactions, excited states, and transition elements: two new functionals and systematic testing of four M06-class functionals and 12 other functional*, Theor. Chem. Acc. 120, 215, **2008**

Ziegler, T., *Approximate density functional theory as a practical tool in molecular energetics and dynamics*, Chem. Rev., 91, 651-667, **1991**